UNIVERSIDADE FEDERAL DE LAVRAS

FRANCIELLE ROBERTA DIAS DE LIMA

MERCURY IN TROPICAL SOILS: MODELING AND SPECIATION IN THE AMAZON BIOME AND PHYSIOLOGICAL EFFECTS IN PLANTS

LAVRAS – MG
2021

FRANCIELLE ROBERTA DIAS DE LIMA

MERCURY IN TROPICAL SOILS: MODELING AND SPECIATION IN THE AMAZON BIOME AND PHYSIOLOGICAL EFFECTS IN PLANTS

Tese apresentada à Universidade Federal de Lavras, como parte das exigências do Programa de Pós-Graduação em Ciência do Solo, área de concentração Recursos Ambientais e Uso da Terra da, para à obtenção do título de Doutor.

Prof. Dr. João José Marques
Orientador

Prof. Dr. Luiz Roberto Guimarães Guilherme
Coorientador

LAVRAS – MG
2021

Ficha catalográfica elaborada pelo Sistema de Geração de Ficha Catalográfica da Biblioteca Universitária da UFLA, com dados informados pelo(a) próprio(a) autor(a).

Lima, Francielle Roberta Dias de.
Mercury in Tropical Soils: modeling and speciation in the Amazon biome and physiological effects in plants / Francielle Roberta Dias de Lima. - 2021.
109 p. : il.

Orientador(a): João José Granate de Sá e Melo Marques.
Coorientador(a): Luiz Roberto Guimarães Guilherme.
Tese (doutorado) - Universidade Federal de Lavras, 2021.
Bibliografia.

1. Ciência do Solo. 2. Geoquímica. 3. Fisiologia de Plantas. I. Marques, João José Granate de Sá e Melo. II. Guilherme, Luiz Roberto Guimarães. III. Título.

FRANCIELLE ROBERTA DIAS DE LIMA

MERCURY IN TROPICAL SOILS: MODELING AND SPECIATION IN THE AMAZON BIOME AND PHYSIOLOGICAL EFFECTS IN PLANTS

Tese apresentada à Universidade Federal de Lavras, como parte das exigências do Programa de Pós-Graduação em Ciência do Solo, área de concentração Recursos Ambientais e Uso da Terra da, para à obtenção do título de Doutor.

APROVADA em 03 de fevereiro de 2021.

Dr. Bruno Teixeira Ribeiro	UFLA
Dr. Sérgio Henrique Godinho Silva	UFLA
Dra. Alice Pita Barbosa	UFRGS
Dr. Alberto Vasconcellos Inda Junior	UFRGS

Prof. Dr. João José Granate de Sá e Melo Marques
Orientador

Prof. Dr. Luiz Roberto Guimarães Guilherme
Coorientador

LAVRAS – MG
2021

AGRADECIMENTOS

A Deus, que me concede forças todos os dias para lutar por meus objetivos;

Aos professores João José Marques, Luiz Roberto e Nilton Curi, pelos ensinamentos e incentivo;

Aos professores Alberto Inda, Bruno Ribeiro e Cláudia Carvalhinho, pelo companheirismo e disposição nos respectivos procedimentos laboratoriais;

À coordenação do curso, pelo respeito aos alunos;

A todos os professores, pelos ensinamentos durante o curso;

A todos os funcionários do Departamento de Ciência do Solo da UFLA (DCS – UFLA) pela convivência, amizade e atenção, em especial, Geila, Lívia, Mariene, Bethânia, Alexandre e Dirce;

À CAPES pela concessão da bolsa de doutorado (o presente trabalho foi realizado com apoio da Coordenação de Aperfeiçoamento de Pessoal de Nível Superior – Brasil (CAPES) – Código de Financiamento 001);

À CAPES, CNPq e FAPEMIG pelo auxílio financeiro ao DCS – UFLA;

À equipe “*Mercury girls*” (Isabela, Jakeline e Polyana) pela parceria, conselhos e trabalho duro;

Aos amigos que fiz nessa jornada, pela amizade e momentos de descontração;

Por fim, a minha mãe Maria Inês, pelo excelente exemplo de ser humano e por todo seu incentivo aos estudos dos filhos, essa vitória é nossa!!!

MUITO OBRIGADA!

RESUMO

A poluição por mercúrio (Hg) representa riscos globais. Os solos tropicais, bastante intemperizados e ricos em óxidos de Fe possuem alta capacidade de retenção do Hg e em alguns dos solos do bioma Amazônia são encontradas altas concentrações de Hg, mesmo distante de atividades antropogênicas. O objetivo deste trabalho foi avaliar a geoquímica de diferentes solos do bioma Amazônia, sua relação com as concentrações e espécies de Hg e o uso do algoritmo Random Forest (RF) para a predição das concentrações de Hg em solos. Além disso, busca elucidar as modificações fisiológicas das espécies de *Avena sativa* (aveia) e *Phaseolus vulgaris* (feijão comum) cultivadas em dois Oxisols contaminados por Hg. Amostras de solo de nove locais no bioma Amazônia foram coletadas e a caracterização físico-química e mineralógica foi realizada. A quantificação do Hg total no solo (Hg_{total}) e das espécies de Hg (Hg^0 + Hg^+ e Hg^{2+}) foi realizada através do analisador direto de Hg por termodessorção. Para a análise das modificações fisiológicas em feijão comum e aveia, os experimentos foram realizados em casa de vegetação com um Rhodic Acrudox (RA) e um Typic Hapludox (TH) com concentrações crescentes de $HgCl_2$. Ao final dos experimentos, o impacto do Hg na fotossíntese, estado nutricional e estresse oxidativo foi determinado. Os solos amazônicos apresentaram na fração argila caulinita, goethita, hematita, gibbsita e quartzo, além da presença de mica nos solos do estado do Acre e em um solo do estado do Amazonas e o Hg_{total} nesses solos variou de 21.5 a 208.3 µg kg^{-1} (mediana de 103.9 µg kg^{-1}). O algoritmo RF determinado foi eficaz para a predição do Hg em solos amazônicos e a importância das variáveis é destacada para elevação, teores de nióbio e Al_2O_3 e susceptibilidade magnética. A principal espécie do Hg encontrada nos solos é a Hg^{2+}, quantificado em temperaturas acima de 300 ºC. Para os experimentos com as plantas, o menor conteúdo de argila e matéria orgânica no TH resultou em respostas semelhantes à toxicidade, enquanto respostas semelhantes à aclimatação foram observadas em plantas cultivadas em RA, reforçando como as propriedades físico-químicas do solo interferem na biodisponibilidade do Hg.

Palavras-chave: mercúrio, floresta Amazônica; estresse oxidativo; aprendizagem de máquina.

ABSTRACT

Mercury (Hg) pollution poses global risks. Tropical soils, which are very weathered and rich in Fe oxides, have increased retention capacity of Hg, and high concentrations of Hg are found in some soils of the Amazon biome, even far from anthropogenic activities. The objective of this study was to evaluate the geochemistry of different soils of the Amazon biome, its relationship with the concentrations and species of Hg, and the use of the Random Forest algorithm (RF) to prediction the concentrations of Hg in soils. In addition, this study seeks to elucidate the physiological modifications of the species *Avena sativa* (oat) and *Phaseolus vulgaris* (common bean) cultivated in Oxisols contaminated by Hg. Soil samples from nine sites in the Amazon biome were collected and the physicochemical characterization and mineralogy was determined. The quantification of total Hg in soil (Hg_{total}) and Hg species (Hg^0 + Hg^+ and Hg^{2+}) was performed through direct mercury analyzer by thermosetting. As for the analysis of physiological modifications, the experiments were carried out in greenhouse in a Rhodic Acrudox (RA) and a Typic Hapludox (TH) with increasing concentrations of $HgCl_2$. At the end of the experiment, the impact of Hg on photosynthesis, nutritional status, and oxidative stress was determined. The Amazon soils presented in the clay fraction: kaolinite, goethite, hematite, gibbsite, and quartz, besides mica in the soils of Acre and in a soil of Amazonas. Hg_{total} in the studied soils ranged from 21.5 to 208.3 µg kg^{-1} (median of 103.9 µg kg^{-1}). The RF algorithm determined was effective in the prediction of Hg. The most importance variables to the prediction of Hg were elevation, niobium and Al_2O_3 content, via portable X-ray fluorescence, and magnetic susceptibility. The main Hg species found in soils is Hg^{2+}, quantified at temperatures above 300 ºC. In respect to the experiments with plants, the lower Hg sorption in the TH soil resulted in toxicity-like responses, whereas acclimation-like responses were observed in plants cultivated in the RA, confirming how the physicochemical properties of soils interfere with Hg sorption in tropical soils.

Keywords: mercury, Amazon rainforest; oxidative stress; machine learning.

SUMÁRIO

PRIMEIRA PARTE.. 8
1 INTRODUÇÃO GERAL.. 8
2 REFERENCIAL TEÓRICO.. 9
2.1 Mercúrio.. 9
2.2 Mercúrio no solo.. 10
2.3 Mercúrio e solos do bioma Amazônia.. 11
2.4 Efeitos tóxicos do mercúrio em plantas.. 13
REFERÊNCIAS.. 14
SEGUNDA PARTE – ARTIGOS.. 19
ARTIGO 1 - Mercury in Amazon soils: geochemistry, speciation and modeling by Random Forest algorithm.. 19
ARTIGO 2 - Physiological effects of mercury-contaminated Oxisols on common bean and oat.... 83

PRIMEIRA PARTE

1 INTRODUÇÃO GERAL

O mercúrio (Hg) é considerado um poluente, podendo ser encontrado no ar, água e solo em várias espécies químicas que se diferenciam quanto a origem (atmosférica, material parental ou antropogênica), transporte, toxicidade e bioacumulação (BANK, 2012; WANG et al., 2003). O conhecimento dos níveis e transformações do Hg no ambiente é de fundamental importância para evitar riscos à saúde humana. As consequências da toxicidade do Hg ao longo dos anos aumentaram a compreensão de sua toxicidade, a citar os compostos de metilmercúrio, em que o Hg forma ligação covalente com ao menos um carbono. Estes compostos recebem considerável atenção devido à capacidade de bioacumulação em cadeias alimentares (HORVAT et al., 2003; RICE et al., 2014).

No Brasil, desde os anos 90, são conduzidos diversos estudos relacionados a presença do Hg no ambiente e sua concentração no solo e em seres vivos (LACERDA; SOUZA; RIBEIRO, 2004; LEBEL et al., 1996, 1998; MALM et al., 1995; RHODES et al., 2018; ROULET et al., 1998a). Dentre esses estudos, é notória a discussão sobre a origem (natural ou antropogênica) de altas concentrações de Hg em solos do bioma Amazônia (FADINI e JARDIM, 2001; LECHLER, 2000; ROULET et al., 1998b; WASSERMAN; HACON; WASSERMAN, 2003). O Hg em solos tropicais foi relacionado principalmente a óxidos de Fe (ROULET et al., 1998b), já em solos de ambientes temperados, sua retenção é controlada pelo conteúdo de matéria orgânica do solo (SKYLLBERG et a., 2003).

Os processos que propiciam a erosão e lixiviação dos solos podem aumentar as concentrações de Hg em solos e água dos rios, como o desmatamento e uso da terra para fins agrícolas (BASTOS et al., 2006; CARPI et al., 2014; LACERDA; SOUZA; RIBEIRO, 2004; ROULET et al., 2000; BÉLIVEAU et al., 2017). Grimaldi, Grimaldi e Guedrom (2008) estudando Latossolos e Argissolos, concluíram que o acúmulo do Hg pode ser diretamente relacionado à sua afinidade pelos constituintes do solo, mas também refletem indiretamente processos associados à pedogênese e funcionamento do solo, como funcionamento hídrico. O Latossolo foi considerado um sumidouro do Hg atmosférico, dado o fluxo de água predominantemente vertical, já o Argissolo uma fonte natural de Hg na rede de drenagem, pois este geralmente apresenta maior selamento superficial que o Latossolo (GRIMALDI; GRIMALDI; GUEDROM, 2008).

Em organismos vivos, o nível de dano biológico do Hg depende da sensibilidade do organismo exposto, tempo de exposição e de suas fontes e concentrações. A exposição do Hg às plantas ocasiona estresse oxidativo, danificação do DNA, redução da absorção de nutrientes, interrupção na síntese de clorofila, taxas de fotossíntese e transpiração (ZHANG et al., 2017; MAHBUB et al., 2018). Desse modo, existe o retardo no crescimento devido à interferência do Hg no metabolismo vegetal.

Embora existam muitos estudos com relação ao Hg, há uma escassez de trabalhos com relação a geoquímica e o Hg considerando maior número de áreas no bioma Amazônia. Também é verificada uma escassez de estudos com relação à fitotoxidez de Hg em solos tropicais. Desta forma, esta proposta visa a avaliação da relação da geoquímica dos solos com as concentrações e espécies de Hg e a modelagem do Hg_{total} em 9 locais no bioma Amazônia. Além disso, busca elucidar as modificações fisiológicas das espécies de *Avena sativa* (aveia) e *Phaseolus vulgaris* (feijão) cultivadas em Latossolos contaminados por Hg.

2 REFERENCIAL TEÓRICO

2.1 Mercúrio

O mercúrio (Hg) é um elemento não essencial e altamente tóxico que pode ser encontrado no ambiente na forma de Hg elementar (Hg^0), que é líquido à temperatura ambiente e Hg (I) e Hg (II), em que os átomos perdem um ou dois elétrons, respectivamente, formando o íon mercuroso (Hg^+ ou Hg_2^{2+}) e o íon mercúrico (Hg^{2+}). Dentre os elementos-traço, o Hg é listado em terceira posição como mais perigoso pela *Agency for Toxic Substances and Disease Registry* (ATSDR), com base na análise de frequência, toxicidade e potencial de exposição humana, ficando atrás do arsênio (As) e do chumbo (Pb) (AGENCY FOR TOXIC SUBSTANCES AND DISEASE CONTROL - ATSRD, 2017).

Os teores naturais de Hg na crosta terrestre são em média de 0,07 mg kg^{-1}, sendo que estes valores são menores em rochas ígneas (0,004-0,008 mg kg^{-1}) do que em sedimentares (0,01-0,4 mg kg^{-1}). O Hg pode ser encontrado em mais de vinte minerais na natureza, sendo o cinábrio (HgS) o principal mineral em que o Hg é extraído comercialmente (KABATA PENDIAS e SZTEKE, 2015).

As espécies químicas de Hg podem formar compostos orgânicos e inorgânicos em diversos compartimentos da crosta terrestre, sendo que o íon mercuroso não é estável sob condições ambientais, pois se converte em Hg^0 e Hg^{2+}. O ciclo biogeoquímico do Hg é caracterizado por várias rotas, tendo destaque, pela importância ambiental, sua volatilização do solo e da água e sua deposição no ambiente (BANK, 2012; SCHUSTER, 1991; OBRIST et al, 2018).

Dentre as espécies químicas, destaca-se o metilmercúrio, composto organomercurial produzido na natureza tanto por processos bióticos quanto abióticos. Esse composto pode sofrer biomagnificação nos seres vivos e causar efeitos teratogênicos, carcinogênico e mutagênico dependendo da concentração (DRISCOLL et al., 2013). Os processos bióticos de metilação são mediados por microrganismos, principalmente pela reação com a metilcobalamina, que é capaz de transferir o grupo metil para o íon Hg^{2+} (BISINOTI e JARDIM, 2004). Também é relatado que bactérias resistentes ao Hg, como as redutoras de sulfato e as que reduzem o Fe, podem transformar o Hg inorgânico em formas orgânicas (LEE; LOWRY; HSU-KIM, 2016). Os processos abióticos podem ocorrer por três vias principais: reação de transmetilação; por meio da radiação ultravioleta na presença de compostos orgânicos doadores do grupo metila e por reação com ácidos fúlvicos e húmicos (BISINOTI e JARDIM, 2004). Desse modo, alguns ligantes orgânicos são doadores do grupo metila e, nesse caso, induzem o processo de metilação; enquanto outros não conseguem doar o grupo metila e, nesses casos, inibem o processo de metilação por adsorção específica do Hg (RAVICHANDRAN, 2004).

2.2 Mercúrio no solo

Os fatores de formação do solo, o ciclo biogeoquímico e as atividades antropogênicas regulam os níveis de Hg no solo. A sorção do Hg em solos tropicais é afetada principalmente pelos atributos do solo como pH e teor de argila (SOARES et al., 2015), apresentando destaque para as concentrações de óxidos de Fe (p.ex. hematita, goethita, maghemita, ferrihidrita) como um dos principais fatores na acumulação de Hg (ROULET et al., 1998b), ao contrário de solos de ambientes temperados, onde os níveis de Hg são controlados pelo conteúdo de matéria orgânica do solo (SKYLLBERG et al., 2003). Outros fatores também influenciam sua sorção no solo e suas transformações no ambiente, como matéria orgânica, temperatura, potencial redox, capacidade de troca catiônica, atividade microbiana, concentrações de ferro, enxofre, fósforo e carbono (ALLOWAY, 2013; BISNOTI e JARDIM, 2004; GABRIEL e WILLIAMSON, 2004; KABATA-PENDIAS e SZTEKE, 2015).

Como qualquer outro metal, o Hg no solo pode ocorrer na forma dissolvida (íon livre), adsorvido não especificamente (ligação eletrostática fraca), adsorvido especificamente (ligação covalente), quelado (ligado a compostos orgânicos) ou precipitado na forma mineral (e.g., carbonato, hidróxido, sulfeto) (SCHUSTER, 1991). Geralmente, é fortemente adsorvido pela matéria orgânica (ligação do Hg com grupos funcionais contendo S), óxidos de ferro e minerais de argila (OLIVEIRA et al., 2011; SOARES et al., 2015).

Segundo Alloway (2013), as principais espécies químicas de Hg que participam no ciclo geoquímico deste elemento podem ser classificadas da seguinte forma: a) compostos voláteis: Hg^0; $(CH_3)_2Hg$; b) espécies reativas: Hg^{2+}, HgX_2, HgX_3 e HgX_4^{2-} com X = OH^-, Cl^-ou Br^-; HgO em partículas aerossóis, complexos de Hg^{2+} com ácidos orgânicos; c) espécies não reativas: CH_3Hg^+, CH_3HgCl, CH_3HgOH e outros compostos organomercuriais; $Hg(CN)_2$; HgS; Hg^{2+} ligado ao S em fragmentos de material húmico.

2.3 Mercúrio e solos do bioma Amazônia

O bioma Amazônia é uma extensa região brasileira que apresenta elevada diversidade. Nele estão localizados os Estados do Acre, Amapá, Amazonas, Pará, Rondônia, Roraima e algumas partes do Mato Grosso, Maranhão e Tocantins.

A geologia da Amazônia brasileira é representada pelo cráton amazônico e as sub-bacias sedimentares que formam a bacia sedimentar paleozoica do Amazonas ou bacia intracratônica do Amazonas (SCHAEFER et al., 2017). Dentre as formações sedimentares destaca-se a Formação Solimões, pela forte influência do soerguimento dos Andes, onde os sedimentos depositados são responsáveis pela presença de solos extremamente contrastantes com o resto da Amazônia (solos eutróficos com argila de atividade alta) (DO VALE JÚNIOR et al., 2011). Grande parte da geomorfologia, biogeoquímica e ecologia da Amazônia está relacionada à magnitude e variabilidade da água e dos materiais fornecidos dos Andes (McCLAIN e NAIMAN, 2008).

De modo geral, as características do material de origem, as geoformas e as condições climáticas levam à formação de solos profundos e intemperizados. Dentre as principais classes de solos encontradas na Amazônia, encontram-se os Latossolos e Argissolos (SCHAEFER et al., 2017). Contudo, mesmo com o forte intemperismo, encontram-se as características químicas e mineralógicas dos solos variadas, como áreas de solos eutróficos e estes só existem onde há influência da planície aluvial ou onde afloram rochas de riqueza química maior (calcários e pelíticas carbonáticas em Monte Alegre-Ererê; e basaltos e diabásios em Roraima, Pará e Amapá) (SCHAEFER et al., 2017). A composição mineralógica desses solos é dominada por caulinita, mas ocorrem ainda goethita, gibbsita, hematita, mica, quartzo, além de minerais filossilicatos 2:1 e feldspatos como minerais acessórios ou traços (KITAGAWA e MOLLER, 1979).

Segundo Schaefer et al. (2000), a distribuição das classes de solos amazônicos é marcada pelo controle geomorfológico: geoformas colinosas e residuais aplainados de baixos platôs estão comumente associados a Latossolos Vermelho-Amarelos em áreas de rochas cristalinas ou Latossolos Amarelos nas áreas de sedimentos terciários; nos terços médio e inferior das colinas ou residuais aplainados ocorrem Argissolos, apresentando ou não plintita ou petroplintita, Neossolos Quartzarênicos e Espodossolos. Na planície aluvial (várzea) dos rios de águas brancas, predominam Gleissolos e Neossolos Flúvicos. Plintossolos e solos com caráter plíntico são predominantes nas terras baixas do Alto Amazonas.

No Brasil, a partir da década de 80, o uso do Hg em garimpos de ouro na Amazônia causou sérias consequências para a região (LACERDA, 1997). O impacto real da atividade de mineração de ouro e os níveis de Hg no ambiente passou desde então a ser um tema em debate. Contudo, estudos iniciais negligenciaram os níveis *background* de Hg do solo baseados em características pedológicas e geoquímicas (ROULET et al, 1998b).

Solos da Amazônia apresentam maiores concentrações de Hg em áreas longe de fontes antrópicas (ROULET et al., 1998b; LECHLER et al., 2000; FADINI e JARDIM, 2001). A grande polêmica é que não existe a possibilidade de origem geológica nos locais com maiores concentrações de Hg, já que nenhuma rocha portadora de Hg foi observada na região, assim a maior concentração de Hg nesses solos é atribuída às características que propiciam a acumulação do Hg, como altos teores de óxidos de Fe (ROULET e LUCOTTE, 1995; WASSERMAN; HACON; WASSERMAN, 2003). No entanto, a variabilidade dos teores de Hg entre os solos é expressiva, embora sejam desenvolvidos do mesmo material de origem e recebam a mesma entrada atmosférica. Assim, a classe de solo parece ser um fator determinante (ROULET et al., 1998b; DO VALLE et al., 2005).

Dessa maneira, a acumulação do Hg na superfície do solo na Amazônia constitui um reservatório natural, mas também é resultado da mineração do ouro, desmatamento e uso da terra para fins agrícolas, pois processos que propiciam a erosão e lixiviação dos solos podem aumentar os níveis de Hg no ambiente. A queima da floresta é considerada ainda mais alarmante, dada as altas temperaturas que propiciam a volatilização do Hg do solo e biomassa (BASTOS et al., 2006; CARPI et al., 2014; LACERDA; SOUZA; RIBEIRO, 2004; ROULET et al., 2000). Portanto, práticas que contribuem para a manutenção da integridade do solo e para a redução da mobilidade de Hg devem ser utilizadas, como os sistemas agroflorestais (BÉLIVEAU et al., 2017).

2.4 Efeitos tóxicos do mercúrio em plantas

O mercúrio em plantas ocasiona estresse abiótico e interferência no metabolismo vegetal, sendo o retardo no crescimento a principal consequência da sua presença, com a redução da taxa fotossintética, absorção de água, K, Mg e o acúmulo de Fe (AZEVEDO e RODRIGUEZ, 2012). A diferença no acúmulo de Hg entre as espécies de plantas deve-se a fatores genéticos, que atribuem diferenças como a capacidade de compartimentalização do metal no vacúolo, não interagindo com os processos fisiológicos que ocorrem no citosol e permeabilidade da membrana plasmática (PATRA e SHARMA, 2000). Ainda, a disponibilidade de Hg nas espécies de plantas pode ser influenciada pela presença de ligantes contendo S, e esses, por sua vez, podem aumentar a solubilidade do Hg para absorção pelas plantas (MORENO et al., 2005).

O mercúrio pode induzir estresse oxidativo em plantas, através do desequilíbrio ocasionado entre a geração de espécies reativas de oxigênio (ROS) e a atuação do sistema de defesa antioxidante, com aumento da concentração de ROS: ânion superóxido (O_2^-), o H_2O_2 e radical hidroxila (OH^-). Isso resulta em alteração da atividade das enzimas do sistema e peroxidação lipídica, atribuída a deterioração da membrana plasmática (base lipídica), podendo resultar em extravasamento do conteúdo celular (CALGAROTO et al., 2010).

Estudos feitos por Cargnelutti et al. (2006) com plântulas de pepino em meio nutritivo, demonstram que a presença do Hg (50-250 µmol L^{-1}) acarretou aumento da atividade de enzimas do sistema antioxidante, como a catalase e a ascorbato peroxidase, provando a estimulação do mecanismo de defesa de plântulas de pepino exposta ao Hg. Cho et al. (2000) estudaram a fitotoxicidade por Hg expressa em plantas de tomate e sua relação com o estresse oxidativo, concluindo o acúmulo de H_2O_2 devido à presença de Hg no substrato. No estudo de Cho et al. (2000), as concentrações de Hg causaram estresse oxidativo nas plantas de tomate, comprovado também pela peroxidação lipídica nas folhas, redução da biomassa e da concentração de clorofila, também foi observado o aumento da atividade da superóxido dismutase, catalase e peroxidase, o que proporciona diminuição da concentração de H_2O_2, mas o potencial antioxidante dessas enzimas não seria suficiente para parar o processo de peroxidação lipídica nas plântulas.

De acordo com Foyer e Shigeoka (2011), estresse oxidativo tem sido relacionado como sinônimo de dano oxidativo aos componentes celulares, especialmente nos casos em que a inativação oxidativa ultrapassa a taxa de reparação celular. Com a intensificação das condições estressantes, a taxa de produção de espécies reativas de oxigênio aumenta e o estresse oxidativo e dano irreversível ocorrem. Se este for suficientemente relevante, irá causar a morte celular (MULLINEAUX e BAKER, 2010).

REFERÊNCIAS

AGENCY FOR TOXIC SUBSTANCES AND DISEASE CONTROL - ATSRD. **The priority list of hazardous substances**. Atlanta, 2017. Disponível em: <http://www.atsdr.cdc.gov/spl/>. Acesso em: 22 ago. 2018.

ALLOWAY, B. J. **Heavy metals in soils:** trace metals and metalloids in soils and their bioavailability. Netherlands: Springer Netherlands, 2013. 614 p.

AZEVEDO, R.; RODRIGUEZ, E. Phytotoxicity of mercury in plants: a review. **Journal of Botany**, London, v. 2012, p. 1-6, May. 2012.

BANK, M. S. **Mercury in the environment:** pattern and process. Califórnia: University of Califórnia Press, 2012. 360 p.

BASTOS, W. R. Mercury in the environment and riverside population in the Madeira River Basin, Amazon, Brazil. **Science of the Total Environment**, Amsterdam, v. 368, n. 1, p. 344-351, Sep. 2006.

BÉLIVEAU, A. et al. Reduction of soil erosion and mercury losses in agroforestry systems compared to forests and cultivated fields in the Brazilian Amazon. **Journal of Environmental Management**, Amsterdam, v. 203, p. 522-532, Dec. 2017.

BISINOTI, M. C.; JARDIM, W. F. O comportamento do metilmercúrio (metilHg) no ambiente. **Química Nova**, São Paulo, v. 27, n. 4, p. 593-600, jul./ago. 2004.

CALGAROTO, N. S. et al. Antioxidant system activation by mercury in Pfaffia glomerata plantlets. **Biometals**, London, v. 23, n. 2, p. 295-305, Apr. 2010.

CARGNELUTTI, D. et al. Mercury toxicity induces oxidative stress in growing cucumber seedlings. **Chemosphere**, Oxford, v. 65, p. 999-1006, Nov. 2006.

CARPI, A. Gaseous mercury emissions from soil following forest loss and land use changes: Field experiments in the United States and Brazil. **Atmospheric Environment**, Oxford, v. 96, p. 423-429, Oct. 2014.

CHO, U. H.; PARK, J. O. Mercury-induced oxidative stress in tomato seedlings. **Plant Science**, Clare, v. 156, p. 1-9., July 2000.

DO VALLE, C. M. et al. Speciation and quantification of mercury in Oxisol, Ultisol, and Spodosol from Amazon (Manaus, Brazil). **Chemosphere**, Oxford, v. 58, n. 6, p. 779-792, Feb. 2005.

DO VALE JÚNIOR, J. F.et al. Solos da Amazônia: etnopedologia e desenvolvimento sustentável. **Revista Agro@ mbiente On-line**, Boa Vista, v. 5, n. 2, p. 158-165, Sep. 2011.

DRISCOLL, C. T. et al. Mercury as a global pollutant: sources, pathways, and effects. **Environmental Science & Technology**, Washington, v. 47, n. 10, p. 4967-4983, May 2013.

FADINI, P. S.; JARDIM, W. F. Is the Negro River Basin (Amazon) impacted by naturally occurring mercury? **Science of the Total Environment**, Amsterdam, v. 275, n. 1-3, p. 71-82, July 2001.

FOYER, C. H.; SHIGEOKA, S. Understanding oxidative stress and antioxidant functions to enhance photosynthesis. **Plant Physiology**, Denville, v. 155, p. 93-100, Jan. 2011.

GABRIEL, M. C.; WILLIAMSON, D. G. Principal biogeochemical factors affecting the speciation and transport of mercury through the terrestrial environment. **Environmental Geochemistry and Health**, Dordrecht, v. 26, n. 3-4, p. 421-434, Dec. 2004.

GRIMALDI, C.; GRIMALDI, M.; GUEDRON, S. Mercury distribution in tropical soil profiles related to origin of mercury and soil processes. **Science of the Total Environment**, Amsterdam, v. 401, p. 121-129, Aug. 2008.

HORVAT, M. et al. Total mercury, methylmercury and selenium in mercury polluted areas in the province Guizhou, China. **Science of the Total Environment**, Amsterdam, v. 304, n. 1-3, p. 231-256, Mar. 2003.

KABATA PENDIAS, A.; SZTEKE, B. **Trace elements in Abiotic and Biotic Environments**. New York: CRC Press, 2015. 458 p.

KITAGAWA, Y., MÖLLER, M.R.F. Clay mineralogy of some typical soils in the Brazilian Amazon region. **Pesquisa Agropecuária Brasileira**, Brasília, v. 14, n. 3, p. 201-228, July 1979.

LACERDA, L. D. Contaminação por mercúrio no Brasil: fontes industriais vs garimpo de ouro. **Química Nova**, São Paulo, v. 20, n. 2, p. 196-199, Mar./Apr.1997.

LACERDA, L. D.; SOUZA, M.; RIBEIRO, M. G. The effects of land use change on mercury distribution in soils of Alta Floresta, Southern Amazon. **Environmental Pollution**, Barking, v. 129, n. 2, p. 247-255, May 2004.

LEBEL, J. et al. Evidence of early nervous system dysfunction in Amazonian populations exposed to low-levels of methylmercury. **Neurotoxicology**, Amsterdam, v. 17, n. 1, p. 157-167, 1996.

LEBEL, J. et al. Neurotoxic effects of low-level methylmercury contamination in the Amazonian Basin. **Environmental Research**, New York, v. 79, n. 1, p. 20-32, Oct. 1998.

LECHLER, P. J. et al. Elevated mercury concentrations in soils, sediments, water, and fish of the Madeira River basin, Brazilian Amazon: a function of natural enrichments? **Science of the Total Environment**, Amsterdam, v. 260, n. 1-3, p. 87-96, Oct. 2000.

LEE, S. W.; LOWRY, G. V.; HSU-KIM, H. Biogeochemical transformations of mercury in solid waste landfills and pathways for release. **Environmental Science: processes & impacts**, Easton, v. 18, n. 2, p. 176-189, Dec. 2016.

McClain, M. E.; Naiman, R. J. Andean influences on the biogeochemistry and ecology of the Amazon River. **BioScience**, Washington, v. 58, n. 4, p. 325-338., Apr. 2008.

MAHBUB, K.R., BAHAR, M.M., MEGHARAJ, M., LABBATE, M. Are the existing guideline values adequate to protect soil health from inorganic mercury contamination? **Environment International**, New York, v. 117, p. 10–15, Aug. 2018.

MALM, O. et al. An assessment of Hg pollution in different goldmining areas, Amazon Brazil. **Science of the Total Environment**, Amsterdam, v. 175, n. 2, p. 127-140, Dec. 1995.

MULLINEAUX, P. M.; BAKER, N. R. Oxidative stress: antagonistic signaling for acclimation or cell death? **Plant Physiology**, Denville, v. 154, p. 521-525, Oct. 2010.

MORENO, F. N. et al. Induced plant uptake and transport of mercury in the presence of sulphur containing ligands and humic acid. **New Phytologist**, London, v. 166, n. 2, p. 445-454, May 2005.

OBRIST, D. et al. A review of global environmental mercury processes in response to human and natural perturbations: Changes of emissions, climate, and land use. **Ambio**, Dordrecht, v. 47, n. 2, p. 116-140, Mar. 2018.

OLIVEIRA, L. C. D. et al. Influência das características físico-químicas dos solos no ciclo hidrobiogeoquímico do mercúrio na região do Rio Aracá-AM. **Química Nova**, São Paulo, v. 34, n. 8, p. 1303-1308, June 2011.

PATRA, M.; SHARMA, A. Mercury toxicity in plants. **The Botanical Review**, Oxford, v. 66, n. 3, p. 379-422, Jan. 2000.

RAVICHANDRAN, M. Interactions between mercury and dissolved organic matter: a review. **Chemosphere**, Oxford, v. 55, n. 3, p. 319-51, Apr. 2004.

RHODES, V. P. et al. Speciation and quantification of Hg in sediments contaminated by artisanal gold mining in the Gualaxo do Norte River, Minas Gerais, SE, Brazil. **Environmental Monitoring and Assessment**, Dordrecht, v. 190, n. 1, p. 49, Jan. 2018.

RICE, K. M. et al. Environmental mercury and its toxic effects. **Journal of Preventive Medicine and Public Health**, Seoul, v. 47, n. 2, p. 74, Mar. 2014.

ROULET, M. et al. Distribution and partition of total mercury in waters of the Tapajos River Basin, Brazilian Amazon. **Science of the Total Environment**, Amsterdam, v. 213, n. 1-3, p. 203-211, June 1998a.

ROULET, M. et al. Increase in mercury contamination recorded in lacustrine sediments following deforestation in the central Amazon1. **Chemical Geology**, Amsterdam, v. 165, n. 3-4, p. 243-266, Mar. 2000.

ROULET, M. et al. The geochemistry of mercury in central Amazonian soils developed on the Alter-do-Chão formation of the lower Tapajós River Valley, Pará state, Brazil1. **Science of the Total Environment**, Amsterdam, v. 223, n. 1, p. 1-24, Nov. 1998b.

ROULET, M.; LUCOTTE, M. Geochemistry of mercury in pristine and flooded ferralitic soils of a tropical rain forest in French Guiana, South America. **Water, Air and Soil Pollution**, Dordrecht, v. 80, n. 1-4, p. 1079-1088, Jan. 1995.

Schaefer, C.E.G.R. et al. Solos da região Amazônica. In: Curi, N., Ker, J.C., Novais, R.F., Vidal-Torrado, P., Schaefer, C.E.G.R. (Eds.), **Pedologia: Solos Dos Biomas Brasileiros**. Sociedade Brasileira de Ciência do Solo, Viçosa, pp. 111-175, 2017.

SCHAEFER, C. E. R. et al. Soil use and landscape alterations in Amazonia: scenarios and reflections. **Boletim do Museu Paraense Emilio Goeldi - Ciências da Terra**, Belém, v. 12, p. 63-104, 2000.

SCHUSTER, E. The behavior of mercury in the soil with special emphasis on complexation and adsorption processes-a review of the literature. **Water, Air and Soil Pollution**, Dordrecht, v. 56, n. 1, p. 667-680, Apr. 1991.

SKYLLBERG, U. et al. Distribution of mercury, methyl mercury and organic sulphur species in soil, soil solution and stream of a boreal forest catchment. **Biogeochemistry**, Dordrecht, v. 64, p. 53–76, May 2003.

SOARES, L.S. et al. Mercúrio em Solos da Região Sudeste do Brasil sem Influência Antropogênica e sua Correlação com as Características Químicas e Físicas. **Revista Brasileira de Ciência do Solo**, Viçosa, v. 39, n. 3, p. 903-914, Maio 2015.

WANG, D.; SHI, X.; WEI, S. Accumulation and transformation of atmospheric mercury in soil. **Science of the Total Environment**, Amsterdam, v. 304, p. 209-214, Mar. 2003.

WASSERMAN, J. C.; HACON, S.; WASSERMAN, M. Biogeochemistry of mercury in the Amazonian environment. **Ambio**, Dordrecht, v. 32, n. 5, p. 336-342, Aug. 2003.

ZHANG, T. et al. Mercury induced oxidative stress, DNA damage, and activation of antioxidative system and Hsp 70 induction in duckweed (*Lemna minor*). **Ecotoxicology and Environmental Safety**, Amsterdam, v. 143, p. 46–56, Sep. 2017.

SEGUNDA PARTE – ARTIGOS

ARTIGO 1 - Mercury in Amazon soils: geochemistry, speciation and modeling by Random Forest algorithm

Francielle R.D. Lima [a], Polyana Pereira [a], Ediu C. Silva Júnior [a], Isabela C. F. Vasques [b], Jakeline R. Oliveira [a], Lúcia H. O. Wadt [c], Kátia E. Silva [d], Roberval M. B. Lima [d], Karine D. Batista [e], Marcelino C. Guedes [f], Raimundo C. Oliveira Junior [g], Guilherme Lopes [a], Cláudia M. do Valle[h]; Cláudia C. Windmöller [i], Alberto V. Inda [j], David C. Weindorf [l], Nilton Curi [a], Bruno T. Ribeiro [a], Luiz R. G. Guilherme [a] and João José Marques [a]*

[a] Department of Soil Science, Federal University of Lavras, Lavras, MG, Brazil
[b] Soil and Plant Nutrition Department, Federal University of Viçosa, Viçosa, MG, Brazil
[c] Embrapa Rondônia, Porto Velho, RO, Brazil
[d] Embrapa Amazônia Ocidental, Manaus, AM, Brazil
[e] Embrapa Roraima, Boa Vista, RR, Brazil
[f] Embrapa Amapá, Macapá, AP, Brazil
[g] Embrapa Amazônia Oriental, Belém, PA, Brazil
[h] Federal Institute of Amazonas, Manaus, AM, Brazil
[i] Department of Chemistry, Federal University of Minas Gerais, Belo Horizonte, MG, Brazil
[j] Department of Soils, Federal University of Rio Grande do Sul, Porto Alegre, RS, Brazil
[l] Research and Innovation, Central Michigan University, Mount Pleasant, MI, USA
* Corresponding author: jmarques@ufla.br

Artigo redigido conforme normas do periódico científico *Science of the Total Environment* (ISSN: 0048-9697). Este artigo é uma versão preliminar e, portanto, poderão surgir alterações para adequá-lo.

Abstract

The high toxicity of Hg is the main reason why its investigation in the Amazon biome has been received so much attention from researchers. Research has been intensified after high Hg concentrations have been reported in soil, water and atmosphere. Studying soil attributes that promote higher Hg concentrations and that determine the Hg speciation in different Amazon soils is therefore important. The objective of this study was to evaluate the geochemistry of different soils of Amazon; its relationship with the concentrations and species of Hg; and to estimate Hg content in these soils using in-field easily acquired data. Soil samples from nine sites in the Amazon biome were collected at three depths (0-20, 20-40, and 40-60 cm) in the states of Acre, Amazonas, Amapá, Pará, Mato Grosso, Rondônia, and Roraima. The physicochemical characterization and mineralogy was determined. The Random Forest (RF) algorithm was used as prediction tool for Hg concentration in these soils. Hg_{total} and Hg species (Hg^0, Hg^+ and Hg^{2+}) were quantified through Direct Mercury Analyzer by thermo-desorption coupled to an atomic absorption spectrometer. The clay fraction of Amazon soils was composed of kaolinite, goethite, hematite, gibbsite, and quartz, besides mica in the soils of Acre and in one soil of Amazonas. Hg_{total} in the studied soils ranged from 21.5 to 208.3 µg kg^{-1} (median of 103.9 µg kg^{-1}). Higher Hg_{total} concentrations were found in one of the two locations in Amazonas (median of 160.3 ± 8.8 µg kg^{-1} at the 0-20 cm depth) and in Pará (median of 149.1 ± 12.5 µg kg^{-1} at the 0-20 cm depth) and the lowest concentration were found in Mato Grosso (median of 39.0 ± 3.4 µg kg^{-1}). The most important variables for prediction of the Hg_{total} in soils were elevation, Nb and Al_2O_3 contents and magnetic susceptibility. The main Hg species found in soils was Hg^{2+}. RF is an accurate technique for prediction Hg_{total} in Amazon soils and the use of in-field acquired data (magnetic susceptibility and elemental composition by portable X-ray fluorescence spectrometry) is useful for estimate Hg in soils. Except for MT soils, Hg_{total} concentrations in the studied soils were higher than other sites in Brazil that have established the quality reference values for Hg as 50 µg kg^{-1}. However, no soil studied revealed Hg_{total} concentration greater than the prevention value for Brazilian soils (500 µg kg^{-1}).

Keywords: Amazon rainforest; mercury speciation; Random Forest; proximal sensors.

Highlights

- Hg^{2+} is the predominant form in Amazon soils.
- Hg_{total} content was successfully predicted using pXRF data.
- Nb, Al_2O_3 and magnetic susceptibility were strongly correlated to Hg.

1. Introduction

Given its biological wealth, climate regulation, and biogeochemical cycles, the Amazon Basin has been the focus of several important environmental studies (De Carvalho et al., 2016; Hopkins, 2007; Rödig et al., 2018; Paca et al., 2019). The presence of Hg in the Amazon is one of the most studied topics and investigation started due to with the increase of artisanal mining activities for gold extraction using Hg in the 1970s and 1980s (Lebel et al., 1998; Lacerda and Solomons, 1992; Feitosa-Santana et al., 2018; Pinto et al., 2019). Research has focused on sources of Hg in the soil, whether they are associated with gold mining or with the soil parent material or even with atmospheric deposition (Roulet et al., 1998b; Fadini and Jardim, 2001; Wasserman et al., 2003; Carpi et al., 2014; Figueiredo et al., 2018). High concentrations of Hg in soil have been reported in sites in the Amazon where there never have had mining activities with Hg (Fadini and Jardim, 2001; Oliveira et al., 2011).

Underlying the Amazon biome are Precambrian rocks of the so-called Amazonian Craton and also Paleozoic sedimentary rocks that compose most of the Amazon intracratonic basin (Schaefer et al., 2017). Much of the physiographic features of the Amazon is related to the magnitude and variability of water and material coming from the Andes (McClain and Naim 2008). Ultisols and Oxisols are the most common soil classes in the Amazon, generally with low natural fertility and high saturation of Al^{3+} (Gardi et al., 2015; Schaefer et al., 2017). Eutrophic soils exist on the alluvial plains and where the parent material is naturally rich in plant nutrients (limestone and carbonatic pelites in Monte Alegre-Ererê; and basalts and diabases in Roraima, Pará, and Amapá) (Schaefer et al., 2017). The abundance of Fe and Al oxide/hydroxides in Amazon soils may be a sink for Hg in the environment, due to their adsorption capacity (Roulet et al., 1998; Fadini e Jardim, 2001). However, other soil features may also influence Hg sorption and its transformations in the environment, such as organic matter, temperature, redox potential, cation exchange capacity, microbial activity, Fe, S, P and C contents (Bisnoti and Jardim, 2004; Gabriel and Williamson, 2004; Kabata-Pendias and Szteke, 2015).

Due to the complexity of its geochemistry, the high Hg concentrations found in certain Amazonian regions still need to be better understood. Artaxo et al. (2000) demonstrate the possible atmospheric transport of Hg, related to biomass burning, where high temperatures provide volatilization of Hg, and this association between atmospheric Hg and biomass burning is caused by at least three mechanisms: adsorption of gaseous Hg on existing biomass burning particles; direct release of Hg from vegetation to the atmosphere during fires and evaporation of Hg from soil during forest burning. In tropical regions and where artisanal small-scale gold mining (ASGM) activities are predominant, studies on the transport of atmospheric Hg on a large scale are scarce. The investigation of Hg contamination in gold exploration areas in the Brazilian Amazon is restricted to the Tapajós basin region (Roulet et al., 1998a, 1998b, 2000, 2001; Guimarães et al., 2000; Nevado et al., 2010; Sousa et al., 2010; Béliveau et al., 2017). The smaller number of studies in contaminated sites is mainly due to expensive and time-consuming laboratory preparation of samples (Qu et al., 2019). That is why many studies highlight the importance of adopting faster analytical techniques able to identify areas of Hg contamination, in order to provide subsidies for decision-making, such as the use of thermo-desorption, known by its simplicity, lower costs and faster determination of Hg_{total} and its species in soil (Hg^0 + Hg^{1+} and Hg^{2+}) (Reis et al., 2012, 2016; Mendes et al., 2016; Windmöller et al., 2017).

Currently, portable X-ray fluorescence spectrometry (pXRF) has been used as a fast, low cost, non-destructive technique for analyzing metals in soils (Vanhoof et al., 2004, Weindorf et al., 2013; Wan et al., 2019; Silva et al., 2021). Studying soil contamination in automobile scrap yards, Barbosa et al. (2019) observed that in addition to pXRF, magnetic susceptibility (MS) also proved to be a sensitive technique in detecting metals contamination in these soils. To handle the large amount of data provided by pXRF (quantifies various chemical elements) and MS (quantifies the magnetism) as well as to use such data for prediction purposes, an algorithm that has been extensively used in this context is the Random Forest. It is advantageous due to the accuracy of models prediction and consists of a combination of several predictive trees, suitable both for classification and for regression problems, has been developed to solve the high variance errors typical of a single decision tree (Breiman, 2001). The RF algorithm can handle numerical and categorical data without any assumption of probability distribution, in addition to providing measurements of the most important covariates involved in the model accuracy (Archer et al., 2008; Hueng et al., 2014). Successful use of RF is reported in the prediction of soil parent material (Heung et al., 2014) and for soil classification (Barthold et al., 2013), soil fertility (Andrade et al., 2020; Benedet et al., 2021), among other applications. Thus, in terms of spatial prediction of soil contamination with Hg in locations still unknown, pXRF and MS data can be used combined with statistical modeling techniques to predict Hg content in Amazon soils. The process of defining contaminated areas, quantifying risks to the environment and human health and choosing remediation actions is then more easily done (Kim et al., 2019; Qu et al., 2018; Wan et al., 2019).

Understanding the relationship between concentrations and species of Hg and the physicochemical and mineralogical composition of Amazon soils in different regions is essential for the analysis of Hg accumulation potential. Our objective was to unravel the relationship between soil geochemistry and Hg concentrations and species and to verify if the RF algorithm is useful to modeling and prediction Hg concentrations in soil, being the modeling combined with the use of proximal sensors in the field, reducing costs, time and laboratory waste production.

2. Materials and methods

2.1. Sampling sites

Soil samples were collected at nine sites in the North, South, Central and West regions of the Brazilian Amazon (Fig. 1). Each location was identified by: MT (Itaúba, state of Mato Grosso); RR (Caracaraí, state of Roraima); AP (Laranjal do Jari, state of Amapá); ANO (Anori, state of Amazonas); AR (Aruanã farm in Itacoatiara, state of Amazonas); SM (Sena Madureira, state of Acre); XP (Xapuri, state of Acre); RO (Porto Velho, state of Rondônia) and PA (Santarém, state of Pará). In each site, soil samples were collected in 8 spots, (following the same topography and drainage) at the following depths: 0-20, 20-40 and 40-60 cm, with 216 samples in total. Each sample was collected as a composed sample where samples collected in the North, South, East and West directions at 3 m from the tree trunk of Brazil nut trees were mixed into a single sample at each depth. More details of sampling can be found in Silva Junior et al.

(2017). The soil samples were collected under native Amazon rainforest, except in for AR samples, where were collected in a Brazil nut plantation known as Aruanã Farm. For a more detailed description (mineralogy, specific surface area and Hg speciation) of the samples, the area defined as reference area (RA) were used and this one was collected under the native Amazon rainforest, without the presence of Brazil nut trees. The terrain attributes elevation and slope were extracted from the *Topodata* database (Brazilian geomorphometric database) of the National Institute for Space Research (INPE) (Table 1). The physicochemical composition of the RA samples is not shown in the present study, because they agree with the values found for the other soil samples (Tables 2 and 3).

2.1. Soil classes

Oxisols and Utisols were the soils studied (Soil Survey Staff, 2014). These were classified in soil suborders according to the Brazilian Soil Classification System (SiBCS) (Santos et al., 2018): Red Latosol (LV), Red-Yellow Latosol (LVA), Yellow Latosol (LA) and Red-Yellow Argisol (PVA). This classification corresponds to Anionic Acrudox, Typic Hapludox, Xanthic Hapludox and Typic Hapludult according to Soil Taxonomy, respectively (Soil Survey Staff, 2014). The fourth categorical level (subgroups) for soil classification according to SiBCS was also used (Table 1): LV, LVA and LVA presented the classification typical dystrophic (d); PVA presented the classifications plintic alitic (alf) and plintosolytic dystrophic (df).

2.2 Characterization of soil samples

2.2.1 Soil Mineralogical

The clay fraction (<0.002 mm) was characterized mineralogically by using X-ray diffractometry (XRD). An amount of 50 g of the sample was dispersed with 1 mol L^{-1} of NaOH maintaining the 1: 50 soil / solution ratio for adequate dispersion and the process was carried out by slow stirring for 16 h. The sand fraction was separated using a 0.053 mm sieve, and the clay fraction separated from the silt + clay suspension according to Stokes' law. Minerals identification and characterization was carried out by X-ray diffraction on Brunker equipment, model D2 Phaser with Cu Kα radiation filter (λ = 1.54 Å), voltage 30 kV and Lynxe detector. The blades for the XRD were done with an amount of 0.6 g of the sample, using powder material, not oriented. The X-ray diffractograms and their peaks were interpreted according to Chen (1977) and Brindley and Brown (1980).

2.2.2 Soil physical

The physical characterization was carried out in the air-dried fine earth fraction, <2 mm (ADFE). The particle size distribution (clay, silt and sand) was performed according to the methodology of "Bouyoucos" (Teixeira et al., 2017).

Magnetic susceptibility (MS) was measured using a Bartington MS2 susceptibility sensor at the 0.47 KHz frequency (low frequency - LF) (Dearing, 1999). The equipment was calibrated to use 10 g of sample (ADFE) and its calibration was performed with equipment reference standards. MS was calculated by the equation: MS = sample (g) / determination in the LF. This system is based on the application of a magnetic field in a non-magnetized sample and depending on the magnetic characteristic of the sample (ferrimagnetic, paramagnetic, antiferrimagnetic or diamagnetic) it will be more or less magnetized (Poggere et al., 2018).

Specific surface area (SSA) was estimated from its water adsorption capacity (Quirk, 1955). Approximately 1 g of the sample (ADFE) was weighed and placed in a desiccator containing phosphorus pentoxide (P_2O_5) under an atmosphere of 0% relative humidity for 12 days before weighing. Then, each sample was placed in the desiccator, containing potassium acetate (KCH_3COO) at a relative humidity of 20% for additional 12 days before weighing. SSA was calculated from the following formula under the assumption that one water molecule spanned an area of 0.108 nm^2: SSA (m^2 g^{-1}) = (6.02214 × 1023 molecules H_2O / 18 g H_2O) × (0.108 × 10-18 m^2/ molecule of H_2O) × (g H_2O / g sample).

2.2.3 Soil chemical

The chemical characterization was carried out in ADFE. The pH (in H_2O) was measured by using 1: 2.5 soil / solution ratio, the soil organic matter content (SOM) was determined according to Carter and Gregorich (2006), sulfur ($S\text{-}SO_4^{2-}$) extracted as sulfate by monocalcium phosphate with acetic acid and the result was converted to S. The cation exchange capacity (CEC) at pH 7 was calculated based on the results of the chemical analysis and corresponds to the sum of bases (SB) + Al + H at pH 7.

The Fe and Al in pedogenic Fe oxides (Fe_{DCB} and Al_{DCB}) were extracted with dithionite-citrate-bicarbonate at 80 ºC (Mehra and Jackson, 1960). The Fe and Al in forms of low crystallinity (basically ferrihydrite - Fe_{ox}, and aluminum polymers - Al_{ox}) were extracted using 0.2 mol L^{-1} ammonium oxalate at pH 3.0 in darkness (Schwertmann, 1964). The contents of dissolved Fe and Al were determined by inductively coupled plasma optical emission spectrometry (ICP-OES).

The total elemental composition of soil samples was performed using portable X-ray fluorescence spectrometry (pXRF) following the technical recommendations described by Weindorf and Chakraborty (2016) and USEPA 6200 method (USEPA, 2007). Soil samples (ADFE) were scanned using a Vanta Analyzer M-series (Olympus, Waltham, MA, USA) pXRF unit. Under laboratory conditions, the X-ray source and detector aperture (~ 2 cm) was totally covered by Prolene® thin-film (Chemplex, Industries, INC) (63.5 mm diameter). Approximately 10 g of soil was massed over the Prolene® thin-film ensuring at least 10 mm thickness as recommended by Padilla et al. (2019). The analysis was performed at the following operational features: i) Li ion batteries; ii) Rh X-ray tube (8–50 kV) as the primary X-ray excitation source; iii) silicon drift detector (SDD); iv) line power 115 VAC; v) two beans (dwell time of 30 s per beam); vi) operation in Geochem(2) mode. For quality assurance and control of pXRF analysis the internal calibration (cal-check) was perfomed using an Olympus® 316 stainless steel calibration. Also, blank sample (pure SiO_2) and certified reference materials 2710a and 2711a from the National Institute of Standards and Technology (NIST) were analyzed. The recovery percentage for the elements identified are as follows (2710a / 2711a) (0 value indicates no reference value in the certified materials or no elemental detection by pXRF): Al (71/73), Si (57/64), P (63/72), K (88/82), Ca (75/90), Ti (92/91), V (0/0), Cr (0/90), Mn (85/93), Fe (94/96), Co (0/738), Ni (0/129), Cu (105/100), Zn (100/102), As (122/151), Sr (97/94), Zr (0/0), Nb (0/0), Ba (90/97), Pb (93/97). The limits of detection (LOD) reported by the manufacturer are as follow (mg kg^{-1}): 400 for Al and Si; 50 for P; 25 for K, Ca, Ti and V; 10 for Cr; 5 for Mn, Fe, Co, Ni, Cu, Zn, As, Sr, Zr, Nb, Ba and Pb.

2.3 Speciation and total determination of Hg

The quantification of total Hg in soil (Hg_{total}) and its speciation (Hg^0 + Hg_2^{2+} and Hg^{2+}) using stepwise heating were performed on the ADFE samples using the thermo-desorption coupled to the atomic absorption spectrometry (AAS) at Direct Mercury

Analyzer (DMA-80, Milestone, Sorisole, Italy). The DMA system is based on sample pyrolysis and subsequent capture of the Hg gas phase with oxygen flow in a gold amalgamator. The Hg / Au amalgam is then heated and the detection of Hg concentration is performed in the AAS, at a wavelength of 253.7 nm. In the first heating step, the oxygen flow that helps the thermal decomposition is 165 mL min^{-1}. The analytical curves were prepared with an appropriate dilution of a 1,000 mg L^{-1} standard solution (Merck, Darmstadt, Germany). The certified material NIST 2710a Montana Soil I was used in triplicates to evaluate the accuracy of Hg_{total} results. LOD and limit of quantitation (LOQ) were determined using the mean concentration of ten blank samples plus three and 10 times the standard deviation of the blank samples, respectively (Windmöller et al., 2017). The LOD and LOQ were 0.88 and 1.42 µg kg^{-1}, respectively. The recovery in the certified Montana Soil I sample was 91 ± 3%.

In addition to the heating steps that already exist in the DMA, the equipment can also be programmed to detect Hg at different temperatures. In doing so, it can differentiate Hg oxidation states, highlighting the great potential to distinguish Hg^0 from other Hg^{2+} (Windmöller et al. 2017). Thus, Hg speciation was determined by 10 temperatures: 50, 100, 150, 200, 250, 300, 400, 500, 600 and 700 °C. After each heating step, the detection occurred as the Hg-Au amalgam was heated to 750ºC and Hg was detected by AAS. The results were compared with patterns of known Hg species (Hg^0, $HgCl_2$, Hg_2Cl_2, and $HgSO_4$) analyzed under the same conditions of the samples by Windmöller et al. (2017).

2.4 Statistical analysis

Statistical analysis was carried out using the R programming language (R Core Team, 2020), version 4.0.3. Hg_{total} values of sites and depths were compared using Tukey’s HSD test with the emmeans v1.4 package (Length, 2020) after verifying the significance in the variance analysis ($P < 0.05$).

Random Forest (RF) algorithm (Breiman, 2001) was tested to prediction of Hg_{total} in Amazon soils. RF algorithm is a non-parametric technique, developed by Breiman (2001), to improve the accuracy of model prediction, which consists of a combination of several predictive trees and is suitable both for classification and for regression problems, has been developed to solve the high variance errors typical of a single decision tree. Analyses were performed using the “caret” (Kuhn, 2012) and "ranger" (with default settings) (Wright and Ziegler, 2017) R packages for RF model. External validation was used to verify the performance of each RF model, in which the soil samples were randomly separated, 70% (n = 151, considering the all depths) of the samples were chosen for model training and the remaining 30% (n = 65, considering the all depths) for model validation. Elemental contents lower than the limit of detection (<LOD) of the pXRF were considered being LOD/2.

The modeling of Hg_{total} in Amazon soils was performed with the data set: (1) all attributes measured, (2) soil texture, MS and pXRF, (3) MS and pXRF and (4) pXRF. Besides that, the models were created for four conditions: using only 0-20 cm data (72 samples), only 20-40 cm data (72 samples), only 40-60 cm data (72 samples), and using all depths data combined (216 samples). To compare the performance of different modeling approaches, coefficient of determination (R^2), root mean square error (RMSE) and mean absolute error (MAE) were used for evaluating the quality of RF models. However, the accuracy of the models was compared using their respective RMSE values. The lower the RMSE, greater the accuracy of the prediction models. RF also provides the importance of variables for the model, i.e. it shows the most important variables for the modelling that when removed, the prediction error increases (Breiman, 2001).

Principal component analysis (PCA) was performed to show the order of importance of the in soil attributes in explaining Hg_{total} in Amazon soils by using the vegan v2.5-6 package (Oksanen et al., 2016).

3. Results

3.1 Characterization of soil samples

3.1.1 Soil Mineralogical

Clay mineralogical composition was evaluated in the reference area samples and is composed by kaolinite, gibbsite, goethite, hematite, mica and quartz (Fig. 2). The soils of SM, AP, ANO, AR and PA are kaolinitic, with no gibbsite detection; XP, RO and RR soils are kaolinitic with lower proportions of gibbsite; and MT soil is kaolinitic-gibbysitic. The presence of mica was observed in SM, XP and ANO. These samples have a common characteristic: they belong to the Solimões Formation geological unit (Table 1). ANO is one of the most recent sedimentary deposits (Quaternary) in the

Amazon, followed by SM and XP (Tertiary) (Fig. 1). The occurrence of 2:1 clay minerals (mica) in SM, XP and ANO is also confirmed by their higher contents of K_2O (Table 3).

3.1.2 Soil physical

SSA was performed on RA samples, likewise XRD analysis. SSA reflects the textural composition of the soil samples and the sites that showed the highest values of SSA: AR (29.6 m2 g^{-1}), PA (23.9 m^2 g^{-1}) and RO (33.4 m^2 g^{-1}) had the highest clay contents (Table 2). These three sites before mentioned had the highest steepness in the relief, and were the only ones characterized as clayey soils (Table 1). The MT and SM samples had the lowest SSA values; 10.9 m^2 g^{-1} and 9.1 m^2 g^{-1}, respectively, both classified as sandy clay loam for their texture.

The soil samples with the highest MS values were MT and RO, with 19.3 ± 2.3 and 19.1 ± 13.2 10^{-7} m^3 kg^{-1} as respective median values at 0-20 cm. A high variability in the results of MS in RO was observed. The results for other locations did not exceed 10.6 10^{-7} m^3 kg^{-1}, with the exception of a sample in SM that had median values for MS of 26.2, 38.2 and 42.1 10^{-7} m^3 kg^{-1}, at depths 0-20, 20 -40 and 40-60, respectively. The median values in SM for MS, considering all SM samples, were 2.4, 4.2 and 4.6, at depths 0-20, 20-40 and 40-60, respectively.

3.1.3 Soil chemical

The soils were acidic (pH less than 6.0), with pH values (in H_2O) reaching 3.7 (± 0.2) for RO samples (Table 2). Another chemical property that is characteristic of highly weathered soils in the tropics, like the acidic pH, is the low CEC and this fact deserves to be highlighted, as contrasting values were found. ANO had a median of 21.8 ± 8.7 3 $cmol_c$ kg^{-1} for CEC, but for other sites this value was 5.3 ± 1.9 $cmol_c$ kg^{-1}. Low contents of SOM (1.2 ± 0.5%) was also observed. Sulphur contents showed a high variation between the studied sites (9.8 ± 8.1 mg kg^{-1}). The highest concentrations of S were found at AR and RO (Table 2), with an increase in S concentration with increasing depth and this behavior is also verified for other locations (Table S2). At a depth of 40-60 cm, the S has concentrations of 34.1 ± 14.2 and 46.3 ± 6.0 mg kg^{-1} for AR and RO, respectively.

The contents of Fe and Al relative to the total pedogenic Fe oxides (Fe_{DCB} and

Al_{DCB}), and the low crystallinity forms (Fe_{ox} and Al_{ox}) were quantified in the fraction ADFE (<2 mm) and these are mainly related to the clay fraction of the soils. The highest values for Fe_{DCB} and Al_{DCB} were found in RO and RR. At 0-20 cm the values for Fe_{DCB} had a median of 42.3 (± 16.1) and 34.3 ± 8.4 g kg^{-1}, for RO and RR, respectively. Also at this same depth, Al_{DCB} had medians 7.0 (± 1.2) and 4.7 (± 0.9) g kg^{-1} for RO and RR, respectively. The Fe_{DCB} and Al_{DCB} values for the other samples had a median below 14.4 and 2.2 g kg^{-1}, respectively. According to the Fe_{ox}/Fe_{DCB} ratio, the highest proportions of crystalline Fe oxides (hematite, goethite, maghemite) occur in RR and RO soils (ratio < or = 0.05), while the highest proportions of low crystallinity forms (ferrihydrite) occur in AR and ANO soils (ratio > 0.20). Likewise, the proportion of Al in low crystallinity polymers in relation to Al in the Fe oxide structure, expressed by the Al_{ox}/Al_{DCB} ratio, was the lowest in RR and RO soils (ratio < or = 0.25) and the greatest in AR soils. and ANO (ratio > or = 0.69).

The contents of the 20 elements measured via pXRF in the ADFE fraction (<2 mm) are shown in Table 3 (0-20 cm). Major elements are expressed as oxides due to convention as the results do not imply chemical speciation. The main constituent of soils is Si, followed by Al and Fe. AR and PA had the highest concentrations of Al_2O_3 (197 g kg^{-1}) and RO had the highest concentration of Fe_2O_3 (109.2 ± 28.1 g kg^{-1}) and the lowest of SiO_2 (192.3 ± 40.1 g kg^{-1}). It is worth mentioning the greatest concentration of K_2O for ANO (6.5 ± 0.9 g kg^{-1}), SM (6.3 ± 1.3 g kg^{-1}) and XP (6.8 ± 1.4 g kg^{-1}), while the other samples that had K_2O values above LOD, they were no greater than 0.3 g kg^{-1}. In 0-20 cm, RO showed high values for Co (112 mg kg^{-1}), As (17.5 mg kg^{-1}), Ba (58.5 mg kg^{-1}), Zr (1167 mg kg^{-1}) and Nb (48.0 mg kg^{-1}). SM showed the highest concentrations of As (17.3 mg kg^{-1}) and Ba (200.5 mg kg^{-1}).

3.2 Speciation and quantification of Hg_{total}

The Hg_{total} varied from 21.5 to 208.3 µg kg^{-1} with a median of 103.9 µg kg^{-1} (Fig. 3). In the upper layer, Hg_{total} was higher for AR (median 160.3 ± 8.8 µg kg^{-1}) and PA (median 149.1 ± 12.5 µg kg^{-1}) and lower for MT (median 39.0 ± 3.4 µg kg^{-1}). AR and PA showed higher values for Hg_{total} at the three depths evaluated. With the increase in depth, Hg_{total} showed a 41% decrease in MT and 29% increase in AP.

Fig. 4 shows the concentration of Hg in soils in each temperature. The temperature range from 50 to 150 ºC corresponds to the release of reduced species (Hg^0

and Hg^{1+}). Oxidized species (Hg^{2+}) are released above 200 ºC. But strongly absorbed Hg^{2+} may be released only above 300 ºC (Windmöller et al., 2017). Using this technique in our samples, Hg was detected mainly at 300 ºC. Some sites showed detection of Hg at even higher temperatures, confirming the strong adsorption of Hg. The XP sample, at 20-40 cm, revealed the highest concentration of Hg at 300 ºC (185 µg kg^{-1}). In general, LAd showed the highest concentrations of Hg above 300 ºC (400, 500 and 600 ºC).

3.3 RF modeling and prediction of Hg_{total}

The RF predictive models were built using using 47 variables for 16 data sets referring to physicochemical and terrain attributes for Amazon soils. The predictive models were for: (1) all attributes measured, (2) soil texture, MS and pXRF, (3) MS and pXRF and (4) pXRF at each depth (0-20, 20-40, 40-60 cm) and considering the three depths. Our results demonstrate that RF is a powerful tool to prediction of Hg_{total} in Amazon soils, stating the effectiveness of RF prediction models (Fig. 5).

The effectiveness of the use of proximal sensors, magnetic susceptibility and pXRF in prediction Hg_{total} in Amazon soils was verified with the analysis of these proposed models. The highest R^2 (87.16) and lower RMSE (15.57) was found using the data set from the soil texture, MS and pXRF (Fig. 5b). The use of the data set pXRF of the sampled soils also resulted in a good explanation of the Hg_{total} predicted versus observed values (R^2 = 83.39, RMSE = 19.10 and MAE = 14.38) (Fig. 5d).

The relative importance of variables (soil attributes) for RF models is shown in Fig. 6. Elevation, concentration of Nb and Al_2O_3 via pXRF and MS were the main variables that can interfere in the lower accuracy of RF models. Thus, these variables have an important relationship with Hg_{total} in Amazon soils even if causation is not always clear.

Informations from various soil attributes are combined in the PCA (Fig. 7). PC1 could distinguish the size of soil particles, where clay contents, Fe_{DCB}, Al_{DCB}, Al_2O_3-pXRF, Fe_2O_3-pXRF, TiO_2, Nb, Zr and S are associated and Hg_{total} belongs to this group, and soils are highly weathered (LAd and LVAd). The PVAalf soil, found in SM and PVAd found in ANO and XP are grouped in PC2 and are related to the properties of less weathered soils, and therefore, with attributes such as K_2O, SiO_2 and CEC concentrations.

4. Discussion

4.1 Soil geochemistry

Oxisols and Utisols are the main soil classes found in the Amazon biome and are characterized with very deep soil profiles, highly weathered and with low-fertility (Schaefer, Lima, and Teixeira 2017). As confirmed by the Oxisols and Utisols samples of the present study, kaolinite predominates in the clay fraction of Amazon soils, followed by goethite, hematite, gibbsite and quartz, with a lower content of 2:1 clay minerals (Kitagawa and Moller, 1979; Chauvel, 1981; Schaefer et al., 2017). The lower degree of pedogenetic development, which is indicated by the occurrence of mica in the clay fraction in ANO, SM and XP, is related to the most recent formation (Solimões Formation) with its sedimentation associated with the Andean orogeny (Bernini et al., 2013). AR (LAd), PA (LAd), RO (PVAdf) and MT (LVd) samples represent the most weathered soils, these had the highest concentrations of Al_2O_3 and Fe_2O_3 and the lowest concentration of SiO_2.

Fe oxides can be classified according to MS and this is related to the concentration of magnetic minerals present in the soil, such as magnetite and maghemite (ferrimagnetic minerals) which have a strong magnetic character in response to the application of an external magnetic field. Also, it must be mentioned that hematite and goethite (antiferromagnetic minerals) have a low magnetic moment (Thompson and Oldfield, 1986; Poggere et al., 2018). The MS in the soil samples studied, mainly in MT and RO, is explained by possible presence of maghemite in the ADFE fraction. In the ADFE fraction of the studied soils, MS varied between 0.7 and 19.3 10^{-7} m^3 kg^{-1} (Table 2). The highest values were found in RO and MT soils, developed from detritic-lateritic covers from Pleistocene although the AR soil, developed from the same material, had the lowest MS value. These MS values are low and are in agreement with the low contents of Fe_2O_3 in the ADFE and also in agreement with the parent materials that are sediments from the Amazon region, unlike soils developed from itabirites, basalts, tuffites and gabbros, these ones having MS values ranging between 350 and 1600 10^{-7} m^3 kg^{-1} (Poggere et al., 2020). Thus, further studies concerning Hg and soils with high MS are needed. MS has been widely applied as a method for estimating contaminated areas (Bourliva et al., 2017 Rachwał et al., 2017), and references have been showing significant correlations between magnetic parameters and high concentrations of trace elements (Rachwał et al., 2017; Yang et al., 2012; Szuszkiewicz et al., 2016). Similar results were observed by Gao et al. (2020), who found a high correlation between total Hg contents with hematite after evaluating the magnetic characteristics of sediments. In addition, at this latter study, the SSA of hematite was associated with the Hg adsorption capacity.

The highest contents of Hg_{total} were determined in the AR, PA and RO soil samples (Figure 3). These three soils showed the highest clay content, associated with the highest Al_2O_3 content in AR and PA, and Fe_2O_3 and Fe_{DCB} in RO. In tropical soils, this strong association of Hg with clay contents and Fe oxides is documented (Roulet et al., 1998b; Oliveira et al., 2020). The higher adsorption and lower bioavailability of Hg in tropical soils is related to the higher proportion of clay and Fe and Al oxide content (Lima et al., 2019; Oliveira et al., 2020). The Fe contents in pedogenic Fe oxides can be expressed in their entirety (hematite, goethite, maghemite, ferrihydrite, lepidocrocite), when extracted by sodium dithionite-citrate-bicarbonate (Fe_{DCB}), as well as the Al contents that replace Fe isomorphically (Al_{DCB}). The contents of Fe and Al in low crystallinity forms (ferrihydrite and lepidocrocyte; and aluminum polymers) are selectively extracted by ammonium oxalate (Fe_{ox} and Al_{ox}) (Inda and Kämpf, 2003). The aluminum oxide, i.e. gibbsite, has been determined by XRD and thermal analysis. The relationship between pedogenic oxides (Fe_{DCB} and Al_{DCB}) and Hg_{total} contents in Amazon soils was studied by Roulet et al. (1998b), where they observed a greater influence of the Fe oxides with high substitution for Al (Al_{DCB}) in the great contents of Hg_{total} in the soils of the Tapajós region. Our study aimed to elucidate the relationship between Fe_{DCB} and Al_{DCB}, as Roulet et al. (1998b), and Fe_{ox} and Al_{ox} with Hg_{total} levels in Amazon soils with more sampling spots. The highest concentrations of Hg_{total} were found in sites with higher levels of Al_{ox}, indicating greater participation of low crystallinity Al polymers. It is known that Fe oxides and Al polymers that are not crystalline have a higher SSA than the crystalline ones (Borggaard, 1982), which increases the surface area for bonds with Hg. In addition, the surface areas of crystalline Fe oxides such as hematite and goethite are slightly smaller than the average according to the results of Bigham et al. (1978).

Mercury in soils of the present study can also be associated with the topographic position, where lower areas in the landscape have higher concentrations of Hg. The phenomenon is promoted by the intense movement of clay particles and of their aggregated clay minerals through drainage. Thus, these processes increase the adsorptive area of mineral surfaces and a consequent increase in the adsorption of metals, such as Hg. In addition to the soil properties that promote Hg retention, which is similar to other sites in tropical environments, several studies try to clarify the sources of Hg in the soils of the Amazon biome, whether they are natural (from parent material and volcanic eruptions), atmospheric or anthropogenic sources (Roulet et al., 1998b; Fadini e Jardim, 2001; Wasserman et al., 2003; Carpi et al., 2014; Ermolim et al., 2018; Figueiredo et al., 2018). The Hg_{total} concentrations (21.5 to 208.3 µg kg^{-1}) found in the present study are in agreement with some locations in the Amazon biome that are not close to mining areas. Fadini and Jardim (2001) found an average Hg value of 172 µg kg^{-1} when studying soil samples from the Rio Negro basin. Oliveira et al. (2011) revealed soil concentrations of Hg from 97.4 to 964.4 µg kg^{-1} in the Middle and Upper Rio Negro region. Horbe et al. (2007) reported Hg contents between 14 and 171 µg kg^{-1} in soil profiles in the Solimões Formation (geomorphological unit) and observed that the highest levels of Hg were in the soil with the lowest concentrations of other trace elements. Souza et al. (2018) also find very high contents of Hg in the soil (median of 8.1 mg kg^{-1}) in the Solimões Formation. High variation in Hg concentrations in soils is observed, which is expected due to the considerable area and heterogeneity of pedogeoclimatic conditions of this biome. In Brazil, this is particularly important, making it difficult to establish soil quality reference values (QRV) (Souza et al., 2015). There is no national reference value for Hg concentration in Brazil. The States of Minas Gerais (COPAM, 2011) and São Paulo (CETESB, 2016) proposed QRV of 50 µg kg^{-1} and Paraíba of 40 µg kg^{-1} (da Silva et al., 2015), respectively. Fernandes et al. (2018) proposed a QRV for Hg in the Pará State (Eastern Amazon) of 330 µg kg^{-1} (90th percentile). The critical value for Hg in soils in Brazil is 500 µg kg^{-1} (CONAMA, 2009) and above this concentration, soil functions are compromised.

4.2 Hg speciation

In order to have a simpler, cheaper and faster identification of Hg species in the soil, thermo-desorption speciation has emerged as an alternative to chemical extraction. In addition, this technique allows less losses of volatile Hg compounds, as it requires little preparation of the sample (Reis et al., 2016; Windmöller et al., 2017). The determination of Hg species is performed with the quantification of Hg at different temperature levels. The process is based on the principle that different species of Hg are released from a matrix at different temperature ranges (Windmöller et al., 2017). With the temperature increase, the Hg species are released in the following order: $HgCl_2$ = Hg associated with Fe_2O_3 <Hg associated with humic acids <HgS <HgO, having an overlap of $HgCl_2$ and Hg associated with iron oxides (Reis et al., 2015).

Hg^{2+} species are released above 200 ºC and those that are most retained by soil matrix (organo-mineral components) are released above 300 ºC (do Valle et al., 2005; Mendes et al., 2016). Hg^0 and Hg_2^{2+} are released at temperatures above 150 ºC (Windmöller et al., 2017). Thus, the main species of Hg in the studied samples is Hg^{2+}, the species of greatest occurrence in soils, since Hg_2^{2+} is highly instable and Hg^0 is highly volatile and susceptible to oxidation (do Valle, 2005, 2006; Windmöller et al., 2017). Hg^0 concentrations are almost zero in the studied soils. The oxidation of Hg^0 to Hg^{2+} in the soil can occur by sorption onto soil minerals (Fe, Mn and Al oxides) or SOM and this process was even verified after 50 years of using Hg^0 in the artisanal gold mining in the State of Minas Geras, Brazil (Durão et al., 2009). The oxidation process of Hg^0 to Hg^{2+} in tropical soils (pH between 5.6–5.8 and 1.6–2.7% SOM) was also studied by Windmöller et al. (2015) and a large percentage of Hg^0 was oxidized to Hg^{2+} (~ 36–88%).

The overlap of Hg species occurs at certain temperatures, but higher temperatures, from 250 to 430 ºC, are related to Hg bound to humic acids (do Valle et al., 2005). Humic acids offer more than one reactive site to which Hg^{2+} can bind (Reis et al., 2015). The Hg released at higher temperatures (400 ºC), may be related, in addition to SOM, to the existence of cinnabar (HgS) in the soil (Palmieri et al., 2006; do Valle, 2005). Palmieri et al. (2006) observed the Hg desorption peaks in natural and synthetic cinnabar above 400 ºC. The temperature variation at Hg release changes according to the crystallinity and cinnabar grain size (Biester et al., 2000; Palmieri et al., 2006; Windmöller et al., 2007). Rhodes et al. (2018) and Windmöller et al. (2017) also observed that there was a release of Hg at temperatures of 400 and 600 °C and attributed such desorption to the $HgSO_4$ and HgS species. The occurrence of this mineral in soils is due to its low solubility which leads to resistance to weathering processes (Rytuba, 2003).

The Hg compounds in soil depend on the contents and composition of SOM, clay minerals (such as Fe and Al oxides), presence of chemical elements in their reduced state (such as S^{2-}), and soil pH and redox conditions (O'Connor et al., 2019). The studied samples revealed an association of Hg with S in soil (AR and RO), however, SOM was not an important variable to determine Hg_{total} concentrations in soils. In part, the relationship of Hg_{total} and S in soils can be explained by covalent bonds with any available reduced S active sites (Reis et al., 2015). The low or absent correlation between Hg and SOM can be explained in part by the absence of sulfhydryl groups (-SH) in SOM (Ravichandran, 2004; He et al., 2019).

4.3 RF modeling and prediction of Hg_{total}

The use of proximal sensors, such as pXRF, in order to determine Hg is still difficult due to high LOD (Miller et al., 2013). However, the use of this sensor can facilitate the prediction of the Hg retention capacity in soils through the evaluation of other soil properties, mainly in the Amazon biome. The use of pXRF combined with machine learning to accurately predict soil properties, such as fertility and soil texture (Santana et al. 2018; 2019; Andrade et al., 2020; de Faria et al., 2020; Benedet et al., 2021) is confirmed in tropical soils. In addition, as confirmed in the present study, RF algorithm can also be of great use in the modeling and prediction of Hg_{total}. RF is used with accurate to estimate several attributes, such as soil fertility properties (Benedet et al., 2021) and oxides by sulfuric acid digestion analyses, mainly Fe_2O_3 (Silva et al., 2020). In addition to pXRF, sensors for quantification of MS can be used to characterize relationships between elements occurring in soil and magnetic minerals (Rachwał et al., 2017).

Among the sensors used, the MS also showed an advantage when associated with the pXRF. The accurate of RF models confirmed the pXRF in the prediction of soil properties that govern Hg_{total} in Amazon soils and are therefore, effective in the present study. pXRF is useful for determining elemental contents expressed as oxides (Santana et al., 2018), and these are umbiquitious in tropical soils. Gómez-Armesto et al. (2020) modelling the Hg_{total} found higher concentrations related to well-humified soil organic C and Al-humus complexes, whereas Fe-humus complexes showed a minor influence, reinforcing that the Hg geochemistry is dominated by interactions between SOM, metal-humus complexes and Fe and Al oxyhydroxides. The fact that Nb was the most important variable for prediction of Hg in soils, can be explained by its low mobility in soil, which can be used in studies to evaluate the distribution of Hg in soil, as presented by Grimaldi et al. (2008) where lithogenic Hg is derived from weathering of the parental material and atmospheric Hg after surface entry is transferred into the soil. According to Grimaldi et al. (2008), Hg and Nb do not have soil affinity. However, further studies are needed in order to reveal the relationship of Nb deposits with Hg concentrations in Amazon soils.

The modeling and prediction of Hg in soils of the Amazon biome is important and can be performed from soil attributes. Given the high concentrations found in some sites, the present study can help with risk management. It is known that the forest conversion into agricultural land (including slash-and-burn agriculture) contributes to the release of Hg from soil to the the aquatic ecosystem in the Amazon biome (Roulet et al., 2000; Lacerda et al., 2004; Bastos et al., 2006; Béliveau et al., 2009; Carpi et al., 2014). With deforestation and inappropriate land use, there is a direct impact of rainwater and greater runoff on the soil surface, promoting leaching and erosion of fine particles, together with the Hg associated with the mineral phase. Thus, soil practices that contribute to maintaining soil integrity and reducing Hg mobility should be chosen (Béliveau et al., 2017). The higher temperatures during fires and the absence of soil cover promote the loss of Hg in both the forest and the soil, contributing to the acceleration of biogeochemical cycle of Hg and increasing its concentration in the atmosphere. Globally, average Hg emissions from the soil are estimated to be about 1 ng m^{-2} h^{-1} (O'Connor et al., 2019). Thus, environmental pollution by Hg is a global concern and more research is needed to verify its behavior in different environments.

5. Conclusions

In the studied sites of the Amazon Biome, Hg^{2+} is the predominant form in soils. Its occurrence and concentration are strongly correlated to the geomorphological condition and soil attributes. The main attributes of Amazon soils that influence Hg_{total} levels were the concentrations of Al_2O_3 and Nb, elevation and magnetic susceptibility.

Except for MT soils (median of 39.0 µg kg^{-1}), Hg_{total} concentrations in the studied soils (median of 103.9 µg kg^{-1}) were higher than other sites in Brazil that have established the quality reference values for Hg as 50 µg kg^{-1}. However, no soil studied revealed Hg_{total} concentration greater than the prevention value for Brazilian soils (500 µg kg^{-1}).

The total elemental composition obtained via pXRF combined or not to other soil attributes and magnetic susceptibility was an excellent proxy for Hg_{total} prediction in Amazon soils. Further studies and the in-field investigation of Hg-contaminated areas will be greatly benefited by using proximal sensors like pXRF and magnetic susceptibility.

Acknowledgments

The authors would like to thank the National Council of Technology and Scientific Development (CNPq), the Coordination for the Improvement of Higher Education Personnel (CAPES), and the Foundation for Research Support of the State of Minas Gerais (FAPEMIG) for financial support for this study. This study was financed in part by the Coordenação de Aperfeiçoamento de Pessoal de Nível Superior – Brasil (CAPES) – Finance Code 001.

References

Andrade, R., Faria, W.M., Silva, S.H.G., Chakraborty, S., Weindorf, D.C., Mesquita, L.F., Guilherme, L.R.G., Curi, N., 2020. Prediction of soil fertility via portable X-ray fluorescence (pXRF) spectrometry and soil texture in the Brazilian Coastal Plains. Geoderma 357, 113960. https://doi.org/10.1016/j.geoderma.2019.113960

Archer, K.J., Kimes, R. V., 2008. Empirical characterization of Random Forest variable importance measures. Comput. Stat. Data Anal. 52, 2249–2260. https://doi.org/10.1016/j.csda.2007.08.015

Artaxo, P., Calixto De Campos, R., Fernandes, E.T., Martins, J. V., Xiao, Z., Lindqvist, O., Fernández-Jiménez, M.T., Maenhaut, W., 2000. Large scale mercury and trace element measurements in the Amazon basin. Atmos. Environ. 34, 4085–4096. https://doi.org/10.1016/S1352-2310(00)00106-0

Barbosa, J.Z., Poggere, G.C., Teixeira, W.W.R., Motta, A.C.V., Prior, S.A., Curi, N., 2020. Assessing soil contamination in automobile scrap yards by portable X-ray fluorescence spectrometry and magnetic susceptibility. Environ. Monit. Assess. 192, 1–10. https://doi.org/10.1007/s10661-019-8025-8

Barthold, F.K., Wiesmeier, M., Breuer, L., Frede, H.G., Wu, J., Blank, F.B., 2013. Land use and climate control the spatial distribution of soil types in the grasslands of Inner Mongolia. J. Arid Environ. 88, 194–205. https://doi.org/10.1016/j.jaridenv.2012.08.004

Bastos, W.R., Gomes, J.P.O., Oliveira, R.C., Almeida, R., Nascimento, E.L., Bernardi, J.V.E., de Lacerda, L.D., da Silveira, E.G., Pfeiffer, W.C., 2006. Mercury in the environment and riverside population in the Madeira River Basin, Amazon, Brazil. Sci. Total Environ. 368, 344–351. https://doi.org/10.1016/j.scitotenv.2005.09.048

Béliveau, A., Lucotte, M., Davidson, R., do Canto Lopes, L.O., Paquet, S., 2009. Early Hg mobility in cultivated tropical soils one year after slash-and-burn of the primary forest, in the Brazilian Amazon. Sci. Total Environ. 407, 4480–4489. https://doi.org/10.1016/j.scitotenv.2009.04.012

Béliveau, A., Lucotte, M., Davidson, R., Paquet, S., Mertens, F., Passos, C.J., Romana, C.A., 2017. Reduction of soil erosion and mercury losses in agroforestry systems compared to forests and cultivated fields in the Brazilian Amazon. J. Environ. Manage. 203, 522–532. https://doi.org/10.1016/j.jenvman.2017.07.037

Benedet, L., Acuña-Guzman, S.F., Faria, W.M., Silva, S.H.G., Mancini, M., Teixeira, A.F. dos S., Pierangeli, L.M.P., Acerbi Júnior, F.W., Gomide, L.R., Pádua Júnior, A.L., Souza, I.A. de, de Menezes, M.D., Marques, J.J., Guilherme, L.R.G., Curi, N., 2021. Rapid soil fertility prediction using X-ray fluorescence data and machine learning algorithms. Catena 197, 105003. https://doi.org/10.1016/j.catena.2020.105003

Biester, H., Gosar, M., Covelli, S., 2000. Mercury speciation in sediments affected by dumped mining residues in the drainage area of the Idrija mercury mine, Slovenia. Environ. Sci. Technol. 34, 3330–3336. https://doi.org/10.1021/es991334v

Bigham, J.M., Golden, D.C., Buol, S.W., Weed, S.B., Bowen, L.H., 1978. Iron Oxide

Mineralogy of Well-drained Ultisols and Oxisols: II. Influence on Color, Surface Area, and Phosphate Retention. Soil Sci. Soc. Am. J. 42, 825–830. https://doi.org/10.2136/sssaj1978.03615995004200050034x

Bisinoti, M.C., Jardim, W.F., 2004. O comportamento do metilmercúrio (MetilHg) no ambiente, Quimica Nova. SBQ, 593–600. https://doi.org/10.1590/s0100-40422004000400014

Borggaard, O.K., 1982. The influence of iron oxides on the surface area of soil. J. Soil Sci. 33, 443–449. https://doi.org/10.1111/j.1365-2389.1982.tb01779.x

Bourliva, A., Papadopoulou, L., Aidona, E., Giouri, K., 2017. Magnetic signature, geochemistry, and oral bioaccessibility of “technogenic” metals in contaminated industrial soils from Sindos Industrial Area, Northern Greece. Environ. Sci. Pollut. Res. 24, 17041–17055. https://doi.org/10.1007/s11356-017-9355-0

Breiman, L., 2001. Random Forests. Mach. Learn. 45, 5–32. https://doi.org/10.1023/A:1010933404324

Brown, G., Brindley, G.W., 1980. X-ray diffraction procedures for clay mineral identification, in: Brindley, G.W., Brown, G. (Eds.), Crystal structures of clays minerals and their X-ray identification. Mineralogical Society, London, pp. 305–360

Carpi, A., Fostier, A.H., Orta, O.R., dos Santos, J.C., Gittings, M., 2014. Gaseous mercury emissions from soil following forest loss and land use changes: Field experiments in the United States and Brazil. Atmos. Environ. 96, 423–429. https://doi.org/10.1016/j.atmosenv.2014.08.004

Carter, M. R., & Gregorich, E. G. (Eds.). (2006). Soil sampling and methods of analysis. CRC press. 1224p.

CETESB. Relatório de estabelecimento de valores orientadores para solos e águas subterrâneas no Estado de São Paulo: Decisão de Diretoria Nº 256/2016/E. (2016).

Diário Oficial do Estado de São Paulo, Poder Executivo, São Paulo, Brasil.

Chauvel, A., 1981. Contribuição para o estudo da evolução dos latossolos amarelos, distróficos, argilosos na borda do platô, na região de Manaus: mecanismos da gibbsitização (). Acta Amaz. 11, 227–245. https://doi.org/10.1590/1809-43921981112227

Chen, P. Y. (1977). Table of key lines in X-ray powder diffraction patterns ofminerals in clays and associated rocks. Department of Natural Resources. Geological Survey, Bloomington.

CONAMA, C.N.D.M.A., 2009. Resolução CONAMA Nº 420, Diário Oficial da União no 249. Ministério do Meio Ambiente, Brasilia, Brasil.

COPAM. Deliberação Normativa COPAM nº 166, de 29 de junho de 2011. Altera o Anexo I da Deliberação Normativa Conjunta COPAM CERH nº 2 de 6 de setembro de 2010, estabelecendo os Valores de Referência de Qualidade dos Solos. (2011). Belo Horizonte, Brasil.

Da Silva, Yuri Jacques Agra Bezerra, do Nascimento, C.W.A., Cantalice, J.R.B., da Silva, Ygor Jacques Agra Bezerra, Cruz, C.M.C.A., 2015. Watershed-scale assessment of background concentrations and guidance values for heavy metals in soils from a semiarid and coastal zone of Brazil. Environ. Monit. Assess. 187, 1–10. https://doi.org/10.1007/s10661-015-4782-1

De Carvalho, T.S., Da Conceição Jesus, E., Barlow, J., Gardner, T.A., Soares, I.C., Tiedje, J.M., De Souza Moreira, F.M., 2016. Land use intensification in the humid tropics increased both alpha and beta diversity of soil bacteria. Ecology 97, 2760–2771. https://doi.org/10.1002/ecy.1513

Dearing J. A. 1999 Environmental magnetic susceptibility, using the Bartington MS2 System. Chi Publishers, Kenilworth, UK.

Do Valle, C.M., Santana, G.P., Augusti, R., Egreja Filho, F.B., Windmöller, C.C., 2005. Speciation and quantification of mercury in Oxisol, Ultisol, and Spodosol from Amazon (Manaus, Brazil). Chemosphere 58, 779–792. https://doi.org/10.1016/j.chemosphere.2004.09.005

Do Valle, C.M., Santana, G.P., Windmöller, C.C., 2006. Mercury conversion processes in Amazon soils evaluated by thermodesorption analysis. Chemosphere 65, 1966–1975. https://doi.org/10.1016/j.chemosphere.2006.07.001

Durão Júnior, W.A., Palmieri, H.E.L., Trindade, M.C., De Aquino Branco, O.E., Filho, C.A.C., Fleming, P.M., Da Silva, J.B.B., Windmöller, C.C., 2009. Speciation, distribution, and transport of mercury in contaminated soils from Descoberto, Minas Gerais, Brazil. J. Environ. Monit. 11, 1056–1063. https://doi.org/10.1039/b813997k

Ermolin, M.S., Fedotov, P.S., Malik, N.A., Karandashev, V.K., 2018. Nanoparticles of volcanic ash as a carrier for toxic elements on the global scale. Chemosphere 200, 16–22. https://doi.org/10.1016/j.chemosphere.2018.02.089

Fadini, P.S., Jardim, W.F., 2001. Is the Negro River Basin (Amazon) impacted by naturally occurring mercury? Sci. Total Environ. 275, 71–82. https://doi.org/10.1016/S0048-9697(00)00855-X

Faria, Á.J.G. De, Silva, S.H.G., Melo, L.C.A., Andrade, R., Mancini, M., Mesquita, L.F., Teixeira, A.F.D.S., Guilherme, L.R.G., Curi, N., 2020. Soils of the Brazilian Coastal Plains biome: Prediction of chemical attributes via portable X-ray fluorescence (pXRF) spectrometry and robust prediction models. Soil Res. 58, 683–695. https://doi.org/10.1071/SR20136

Feitosa-Santana, C., Souza, G. da S., Sirius, E.V.P., Rodrigues, A.R., Cortes, M.I.T., Silveira, L.C. de L., Ventura, D.F., 2018. Color vision impairment with low-level methylmercury exposure of an Amazonian population – Brazil. Neurotoxicology 66, 179–184. https://doi.org/10.1016/j.neuro.2018.01.010

Fernandes, A.R., Souza, E.S. de, de Souza Braz, A.M., Birani, S.M., Alleoni, L.R.F., 2018. Quality reference values and background concentrations of potentially toxic elements in soils from the Eastern Amazon, Brazil. J. Geochemical Explor. 190, 453–463. https://doi.org/10.1016/j.gexplo.2018.04.012

Figueiredo, B.R., De Campos, A.B., Da Silva, R., Hoffman, N.C., 2018. Mercury sink in Amazon rainforest: soil geochemical data from the Tapajos National Forest, Brazil. Environ. Earth Sci. 77, 1–7. https://doi.org/10.1007/s12665-018-7471-x

Gabriel, M.C., Williamson, D.G., 2004. Principal biogeochemical factors affecting the speciation and transport of mercury through the terrestrial environment. Environ. Geochem. Health. https://doi.org/10.1007/s10653-004-1308-0

Gao, X., Kang, S., Liu, Q., Chen, P., Duan, Z., 2020. Magnetic characteristics of lake sediments in Qiangyong Co Lake, southern Tibetan Plateau and their application to the evaluation of mercury deposition. J. Geogr. Sci. 30, 1481–1494. https://doi.org/10.1007/s11442-020-1794-8

Gardi, C., Angelini, M., Barceló, S., Comerma, J., Gaistardo, C. C., Rojas, A. E., ... & da Silva, M. R. (Eds.). (2015). Soil atlas of Latin America and the Caribbean. Publications Office.

Gómez-Armesto, A., Martínez-Cortizas, A., Ferro-Vázquez, C., Méndez-López, M., Arias-Estévez, M., Nóvoa-Muñoz, J.C., 2020. Modelling Hg mobility in podzols: Role of soil components and environmental implications. Environ. Pollut. 260, 114040. https://doi.org/10.1016/j.envpol.2020.114040

Grimaldi, C., Grimaldi, M., Guedron, S., 2008. Mercury distribution in tropical soil profiles related to origin of mercury and soil processes. Sci. Total Environ. 401, 121–129. https://doi.org/10.1016/j.scitotenv.2008.04.001

Guimarães, J.R.D., Meili, M., Hylander, L.D., Silva, E.D.C.E., Roulet, M., Mauro, J.B.N., De Lemos, R.A., 2000. Mercury net methylation in five tropical flood plain regions of Brazil: High in the root zone of floating macrophyte mats but low in surface sediments and flooded soils. Sci. Total Environ. 261, 99–107. https://doi.org/10.1016/S0048-9697(00)00628-8

He, M., Tian, L., Braaten, H.F.V., Wu, Q., Luo, J., Cai, L.M., Meng, J.H., Lin, Y., 2019. Mercury–Organic Matter Interactions in Soils and Sediments: Angel or Devil? Bull. Environ. Contam. Toxicol. https://doi.org/10.1007/s00128-018-2523-1

Heung, B., Bulmer, C.E., Schmidt, M.G., 2014. Predictive soil parent material mapping at a regional-scale: A Random Forest approach. Geoderma 214–215, 141–154. https://doi.org/10.1016/j.geoderma.2013.09.016

Hopkins, M.J.G., 2007. Modelling the known and unknown plant biodiversity of the Amazon Basin. J. Biogeogr. 34, 1400–1411. https://doi.org/10.1111/j.1365-2699.2007.01737.x

Horbe, A.M.C., De Paiva, M.R.P., Motta, M.B., Horbe, A., 2007. Mineralogy and geochemistry of Neogene and Quaternary sediment profiles from the Solimões Basin in the region of Coari, Amazonas. Acta Amaz. 37, 81–89. https://doi.org/10.1590/s0044-59672007000100009

Inda Junior, A. V., Kämpf, N., 2003. Avaliação de procedimentos de extração dos óxidos de ferro pedogênicos com ditionito-citrato-bicarbonato de sódio. Rev. Bras. Ciência do Solo 27, 1139–1147. https://doi.org/10.1590/s0100-06832003000600018

Inda, A.V., Kämpf, N., 2005. Goethite and hematite variability via reductive dissolution in soils from tropical and subtropical regions. Rev. Bras. Cienc. do Solo 29, 851–866. https://doi.org/10.1590/s0100-06832005000600003

Kabata-Pendias, A., Szteke, B., 2015. Trace elements in abiotic and biotic environments. Taylor & Francis, Boca Raton, FL.

Kim, H.R., Kim, K.H., Yu, S., Moniruzzaman, M., Hwang, S. Il, Lee, G.T., Yun, S.T.,

2019. Better assessment of the distribution of As and Pb in soils in a former smelting area, using ordinary co-kriging and sequential Gaussian co-simulation of portable X-ray fluorescence (PXRF) and ICP-AES data. Geoderma 341, 26–38. https://doi.org/10.1016/j.geoderma.2019.01.031

Kitagawa, V., Moller, M.R.F., 1979. Clay mineralogy of some typical soils in the Brazilian Amazon region. Pesqui. Agropecuária Bras. 14, 201–228.

Kuhn, M., 2012. Variable importance using the caret package. J. Stat. Softw. 1–6.

Lacerda, L.D. De, Solomons, W., 1992. Mercúrio na Amazonia: uma bomba relógio química? CETEM/CNPq, Rio de Janeiro.

Lebel, J., Mergler, D., Branches, F., Lucotte, M., Amorim, M., Larribe, F., Dolbec, J., 1998. Neurotoxic effects of low-level methylmercury contamination in the Amazonian basin. Environ. Res. 79, 20–32. https://doi.org/10.1006/enrs.1998.3846

Lenth, R. V., Buerkner, P., Herve, M., Love, J., Riebl, H. and Singmann, H. 2020. Estimated Marginal Means, aka Least-Squares Means. R package version 1.5.3.

Lima, F.R.D., Martins, G.C., Silva, A.O., Vasques, I.C.F., Engelhardt, M.M., Cândido, G.S., Pereira, P., Reis, R.H.C.L., Carvalho, G.S., Windmöller, C.C., Moreira, F.M.S., Guilherme, L.R.G., Marques, J.J., 2019. Critical mercury concentration in tropical soils: Impact on plants and soil biological attributes. Sci. Total Environ. 666, 472–479. https://doi.org/10.1016/j.scitotenv.2019.02.216

McClain, M.E., Naiman, R.J., 2008. Andean influences on the biogeochemistry and ecology of the Amazon River. Bioscience 58, 325–338. https://doi.org/10.1641/B580408

Mehra, O.P., Jackson, M.L., 1960. Iron oxide removal from soils and clays by a dithionite-citrate system buffered with sodium bicarbonate. Clays Clay Miner. 317–327. https://doi.org/10.1016/b978-0-08-009235-5.50026-7

Mendes, L.A., de Lena, J.C., do Valle, C.M., Fleming, P.M., Windmöller, C.C., 2016. Quantification of methylmercury and geochemistry of mercury in sediments from a contaminated area of Descoberto (MG), Brazil. Appl. Geochemistry 75, 32–43. https://doi.org/10.1016/j.apgeochem.2016.10.011

Miller, C.L., Watson, D.B., Lester, B.P., Lowe, K.A., Pierce, E.M., Liang, L., 2013. Characterization of soils from an industrial complex contaminated with elemental mercury. Environ. Res. 125, 20–29. https://doi.org/10.1016/j.envres.2013.03.013

Montoya, A.J., Lena, J.C., Windmöller, C.C., 2019. Adsorption of gaseous elemental mercury on soils: Influence of chemical and/or mineralogical characteristics. Ecotoxicol. Environ. Saf. 170, 98–106. https://doi.org/10.1016/j.ecoenv.2018.11.054

Nevado, J.J.B., Rodríguez Martín-Doimeadios, R.C., Guzmán Bernardo, F.J., Jiménez Moreno, M., Herculano, A.M., do Nascimento, J.L.M., Crespo-López, M.E., 2010. Mercury in the Tapajós River basin, Brazilian Amazon: A review. Environ. Int. 36, 593–608. https://doi.org/10.1016/j.envint.2010.03.011

O'Connor, D., Hou, D., Ok, Y.S., Mulder, J., Duan, L., Wu, Q., Wang, S., Tack, F.M.G., Rinklebe, J., 2019. Mercury speciation, transformation, and transportation in soils, atmospheric flux, and implications for risk management: A critical review. Environ. Int. 126, 747–761. https://doi.org/10.1016/j.envint.2019.03.019

Oksanen, J., Blanchet, F.G., Friendly, M., Kindt, R., Legendre, P., McGlinn, D., Minchin, P.R., O'Hara, R.B., Simpson, G.L., Solymos, P., Henry, M., Stevens, H., Szoecs, E., Wagner, H., 2016. Vegan: Community Ecology Package. Ordination methods, diversity analysis and other functions for community and vegetation ecologists.

Oliveira, L.C. de, Botero, W.G., Santos, A. dos, Cordovil, M.C. de O., Rocha, J.C., Silva, H.C. da, 2011. Influência das características físico-químicas dos solos no ciclo hidrobiogeoquímico do mercúrio na região do Rio Aracá - AM. Quim. Nova 34, 1303–

1308. https://doi.org/10.1590/s0100-40422011000800002

Oliveira, J.R., Vasques, I.C.F., Lima, F.R.D., Carvalho, G.S., Job, M.T.P., de Oliveira, T.S., Marques, J.J., 2020. Mercury adsorption in tropical soils and zeolite: characterization by Fourier-transform infrared spectroscopy. Arch. Agron. Soil Sci. https://doi.org/10.1080/03650340.2020.1845318

Paca, V.H. da M., Espinoza-Dávalos, G.E., Hessels, T.M., Moreira, D.M., Comair, G.F., Bastiaanssen, W.G.M., 2019. The spatial variability of actual evapotranspiration across the Amazon River Basin based on remote sensing products validated with flux towers. Ecol. Process. 8, 1–20. https://doi.org/10.1186/s13717-019-0158-8

Padilla, J.T., Hormes, J., Magdi Selim, H., 2019. Use of portable XRF: Effect of thickness and antecedent moisture of soils on measured concentration of trace elements. Geoderma 337, 143–149. https://doi.org/10.1016/j.geoderma.2018.09.022

Palmieri, H.E.L., Nalini, H.A., Leonel, L. V., Windmöller, C.C., Santos, R.C., de Brito, W., 2006. Quantification and speciation of mercury in soils from the Tripuí Ecological Station, Minas Gerais, Brazil. Sci. Total Environ. 368, 69–78. https://doi.org/10.1016/j.scitotenv.2005.09.085

Pinto, L. de C.M., Dórea, J.G., Bernardi, J.V.E., Gomes, L.F., 2019. Mapping the evolution of mercury (Hg) research in the amazon (1991-2017): A scientometric analysis. Int. J. Environ. Res. Public Health 16, 1111. https://doi.org/10.3390/ijerph16071111

Poggere, G.C., Barrón, V., Inda, A.V., Barbosa, J.Z., Brito, A.D.B., Curi, N., 2020. Linking phosphorus sorption and magnetic susceptibility in clays and tropical soils. Soil Res. 58, 430-440. https://doi.org/10.1071/SR20099

Poggere, G.C., Inda, A.V., Barrón, V., Kämpf, N., de Brito, A.D.B., Barbosa, J.Z., Curi, N., 2018. Maghemite quantification and magnetic signature of Brazilian soils with contrasting parent materials. Appl. Clay Sci. 161, 385-394.

https://doi.org/10.1016/j.clay.2018.05.014

Qu, M., Chen, J., Li, W., Zhang, C., Wan, M., Huang, B., Zhao, Y., 2019. Correction of in-situ portable X-ray fluorescence (PXRF) data of soil heavy metal for enhancing spatial prediction. Environ. Pollut. 254, 112993. https://doi.org/10.1016/j.envpol.2019.112993

Qu, M., Wang, Y., Huang, B., & Zhao, Y., 2018. Spatial uncertainty assessment of the environmental risk of soil copper using auxiliary portable X-ray fluorescence spectrometry data and soil pH. Environ. Pollut. 240, 184-190. https://doi.org/10.1016/j.envpol.2018.04.118

Quirk, J.P., 1955. Significance of surface areas calculated from water vapor sorption isotherms by use of the BET equation. Soil Sci. 80, 423-430. https://doi.org/10.1097/00010694-195512000-00001

R Development Core Team, 2020. R: A Language and Environment for Statistical Computing. R Foundation for Statistical Computing, Vienna, Austria (Version 4.0.3).

Rachwał, M., Kardel, K., Magiera, T., Bens, O., 2017. Application of magnetic susceptibility in assessment of heavy metal contamination of Saxonian soil (Germany) caused by industrial dust deposition. Geoderma 295, 10-21. https://doi.org/10.1016/j.geoderma.2017.02.007

Ravichandran, M., 2004. Interactions between mercury and dissolved organic matter—a review. Chemosphere 55, 319-331. https://doi.org/10.1016/j.chemosphere.2003.11.011

Reis, A.T., Coelho, J.P., Rodrigues, S.M., Rocha, R., Davidson, C.M., Duarte, A.C., Pereira, E., 2012. Development and validation of a simple thermo-desorption technique for mercury speciation in soils and sediments. Talanta 99, 363-368. https://doi.org/10.1016/j.talanta.2012.05.065

Reis, A.T., Coelho, J.P., Rucandio, I., Davidson, C.M., Duarte, A.C., Pereira, E., 2015.

Thermo-desorption: a valid tool for mercury speciation in soils and sediments?. Geoderma 237, 98-104. https://doi.org/10.1016/j.geoderma.2014.08.019

Reis, A.T., Davidson, C.M., Vale, C., Pereira, E., 2016. Overview and challenges of mercury fractionation and speciation in soils. Trends Analyt. Chem. 82, 109-117. https://doi.org/10.1016/j.trac.2016.05.008

Rocha, J.C., Junior, É.S., Zara, L.F., Rosa, A.H., dos Santos, A., Burba, P., 2000. Reduction of mercury (II) by tropical river humic substances (Rio Negro)—a possible process of the mercury cycle in Brazil. Talanta 53, 551-559. https://doi.org/10.1016/S0039-9140(00)00532-4

Rhodes, V.P. de, de Lena, J.C., Santolin, C.V.A., Pinto, T. da S., Mendes, L.A., Windmöller, C.C., 2018. Speciation and quantification of Hg in sediments contaminated by artisanal gold mining in the Gualaxo do Norte River, Minas Gerais, SE, Brazil. Environ. Monit. Assess. 190: 49. https://doi.org/ 10.1007/s10661-017-6394-4

Rödig, E., Cuntz, M., Rammig, A., Fischer, R., Taubert, F., Huth, A., 2018. The importance of forest structure for carbon fluxes of the Amazon rainforest. Environ. Res. Lett. 13, 054013. https://doi.org/10.1088/1748-9326/aabc61

Roulet, M., Lucotte, M., Canuel, R., Farella, N., De Freitos Goch, Y. G., Peleja, J.R.P. J. R., Guimarães, J.R.D., Mergler, D., Amorim, M., 2001. Spatio-temporal geochemistry of mercury in waters of the Tapajós and Amazon rivers, Brazil. Limnol. Oceanogr. 46, 1141-1157. https://doi.org/10.4319/lo.2001.46.5.1141

Roulet, M., Lucotte, M., Canuel, R., Rheault, I., Tran, S., Gog, Y. D. F. Farella, N., Vale, R.S. do, Passos, C.J.S., Silva, E. de J., Mergler D., Amorim, M., 1998a. Distribution and partition of total mercury in waters of the Tapajós River Basin, Brazilian Amazon. Sci. Total Environ. 213, 203-211. https://doi.org/10.1016/S0048-9697(98)00093-X

Roulet, M., Lucotte, M., Guimarães, J.R.D., Rheault, I., 2000. Methylmercury in water, seston, and epiphyton of an Amazonian river and its floodplain, Tapajos River, Brazil. Sci. Total Environ. 261, 43-59. https://doi.org/10.1016/S0048-9697(00)00594-5

Roulet, M., Lucotte, M., Saint-Aubin, A., Tran, S., Rheault, I., Farella, N., Silva, E. de J., Dezencourt, J., Passos, C.J.S., Soares, G.S., Guimarães, J.R.D., Mergler, D., Amorim, M., 1998b. The geochemistry of mercury in central Amazonian soils developed on the Alter-do-Chao formation of the lower Tapajos River Valley, Para state, Brazil. Sci. Total Environ 223, 1-24. https://doi.org/10.1016/S0048-9697(98)00265-4

Rytuba, J.J., 2003. Mercury from mineral deposits and potential environmental impact. Env. Geol. 43, 326-338. https://doi.org/10.1007/s00254-002-0629-5

Santana, M.L.T., Carvalho, G.S., Guilherme, L.R.G., Curi, N., Ribeiro, B.T., 2019. Elemental concentration via portable x-ray fluorescence spectrometry: Assessing the impact of water content. Ciênc. agrotec. 43. https://doi.org/10.1590/1413-7054201943029218

Santana, M.L.T., Ribeiro, B.T., Silva, S.H.G., Poggere, G.C., Guilherme, L.R.G., Curi, N., 2018. Conditions affecting oxide quantification in unknown tropical soils via handheld X-ray fluorescence spectrometer. Soil Res. 56, 648-655. https://doi.org/10.1071/SR18099

Santos, H.G., Jacomine, P.K.T., dos Anjos, L.H.C., de Oliveira, V.Á., Lumbreras, J.F., Coelho, M.R., de Almeida, J.A., Cunha, T.J.F., de Oliveira, J.B., 2018. Sistema brasileiro de classificação de solos 5ª edição revista e ampliada. Sistema brasileiro de classificação de solos. https://doi.org/10.1007/s10608-010-9295-1

Schaefer, C.E.G.R., Lima, H.N., Teixeira, W.G., Vale Junior, J.F., Souza, K.W., Corrêia, G.R., de Mendonça, B.A.F., Amaral, E.F., Campos, M.C.C., Ruivo, M.L.P., 2017. Solos da região Amazônica. In: Curi, N., Ker, J.C., Novais, R.F., Vidal-Torrado, P., Schaefer, C.E.G.R. (Eds.), Pedologia: Solos Dos Biomas Brasileiros. Sociedade Brasileira de Ciência do Solo, Viçosa, pp. 111-175

Silva, S.H.G., Ribeiro, B.T, Guerra, M.B.B., Carvalho, H.W.P., Lopes, G., Carvalho, G.S., Guilherme, L.R.G., Resende, M., Mancini, M., Curi, N., Rafael, R.B.A., Cardelli, V., Cocco, S., Corti, G, Chakraborty, S, Li, B., Weindorf, D., 2021. pXRF in tropical soils: Methodology, applications, achievements and challenges. Adv. Agron. https://doi.org/10.1016/bs.agron.2020.12.001

Silva, S.H.G., Silva, E.A., Poggere, G.C., Pádua Junior, A.L., Gonçalves, M.G.M., Guilherme, L.R.G., Curi, N., 2020. Modeling and prediction of sulfuric acid digestion analyses data from pXRF spectrometry in tropical soils. Sci. agric. 77. https://doi.org/10.1590/1678-992x-2018-0132

Silva Junior, E.C., Wadt, L.H.O., Silva, K.E., Lima, R.M.B., Batista, K.D., Guedes, M.C., Carvalho, G.S., Carvalho, T.S., Reis, A.R., Lopes, G., Guilherme, L.R.G., 2017. Natural variation of selenium in Brazil nuts and soils from the Amazon region. Chemosphere 188, 650–658. https://doi.org/10.1016/j.chemosphere.2017.08.158

Soil Survey Staff. 2014. Keys to Soil Taxonomy, 12th ed. USDA-Natural Resources Conservation Service, Washington, DC.

Sousa, R., Veiga, N., Klein, M.M., Telmer, B., Gunson, K. A. J., Bernaudat, L., 2010. Strategies for reducing the environmental impact of reprocessing mercury-contaminated tailings in the artisanal and small-scale gold mining sector: insights from Tapajos River Basin, Brazil. J. Cleaner Produc. 18, 1757-1766. https://doi.org/10.1016/j.jclepro.2010.06.016

Souza, J.J.L.L., Abrahão, W.A.P., de Mello, J.W.V., da Silva, J., da Costa, L. M., Oliveira, T.S., 2015. Geochemistry and spatial variability of metal (loid) concentrations in soils of the state of Minas Gerais, Brazil. Sci. Total Environ. 505, 338-349. https://doi.org/10.1016/j.scitotenv.2014.09.098

Souza, J.J.L.L., Fontes, M.P.F., Gilkes, R., Costa, L.M.D., Oliveira, T.S., 2018. Geochemical signature of Amazon tropical rainforest soils. Rev. Bras. Ciênc. Solo. 42, e0170192. https://doi.org/10.1590/18069657rbcs20170192

Schwertmann, U. 1964. Differentiation of soil iron oxides by extraction with ammonium oxalate-solution. Zeitschrift für Pflanzenernährung Düngung und Bodenkunde. 105, 194–202
(in German).

Szuszkiewicz, M., Łukasik, A., Magiera, T., Mendakiewicz, M., 2016. Combination of geo-pedo-and technogenic magnetic and geochemical signals in soil profiles–diversification and its interpretation: a new approach. Environ. Pollution, 214, 464-477. https://doi.org/10.1016/j.envpol.2016.04.044

Teixeira, P.C., Donagemma, G.K., Fontana, A., Teixeira, W.G., 2017. Manual de métodos de análise de solo, terceira edição. Rio de Janeiro, Embrapa. pp. 573.

Thompson, R., Oldfield, F., 1986. Environmental Magnetism. Allen and Unwin, London, pp. 227.

US Environmental Protection Agency Method 6200—Field Portable X-Ray Fluorescence Spectrometry for the Determination of Elemental Concentrations in Soil and Sediment Available online at: https://www.epa.gov/hw-sw846/sw-846-test-method-6200-field-portable-x-ray-fluorescence-spectrometry-determination (verified 24 Jan. 2021).

Vanhoof, C., Corthouts, V., Tirez, K., 2004. Energy-dispersive X-ray fluorescence systems as analytical tool for assessment of contaminated soils. J. Environ. Monit. 6, 344-350. https://doi.org/10.1039/b312781h

Wan, M., Hu, W., Qu, M., Tian, K., Zhang, H., Wang, Y., Huang, B., 2019. Application of arc emission spectrometry and portable X-ray fluorescence spectrometry to rapid risk assessment of heavy metals in agricultural soils. Ecologic. Indicators. 101, 583-594. https://doi.org/10.1016/j.ecolind.2019.01.069

Wasserman, J.C., Hacon, S., Wasserman, M.A., 2003. Biogeochemistry of mercury in the Amazonian environment. Ambio: A J. Human Environ. 32, 336-342. https://doi.org/10.1579/0044-7447-32.5.336

Weindorf, D.C., Somsubhra, C., 2016. Portable X-ray fluorescence spectrometry analysis of soils. In: Hirmas, D. (Ed.), Methods of Soil Analysis. Soil Science Society America, Madison, 1 (1).

Weindorf, D.C., Paulette, L., Man, T., 2013. In-situ assessment of metal contamination via portable X-ray fluorescence spectroscopy: Zlatna, Romania. Environ. Pollution. 182, 92-100. https://doi.org/10.1016/j.envpol.2013.07.008

Windmöller, C.C., Júnior, W.A.D., Oliveira, A., do Valle, C.M., 2015. The redox processes in Hg-contaminated soils from Descoberto (Minas Gerais, Brazil): implications for the mercury cycle. Ecotoxic. Environ. Safety. 112, 201-211. https://doi.org/10.1016/j.ecoenv.2014.11.009

Windmöller, C.C., Silva, N.C., Andrade, P.H.M., Mendes, L.A., do Valle, C.M., 2017. Use of a direct mercury analyzer® for mercury speciation in different matrices without sample preparation. Analyt. Methods. 9, 2159-2167. https://doi.org/10.1039/c6ay03041f

Wright, M.N., Ziegler, A., 2017. Ranger: a fast implementation of Random Forests for high dimensional data in C++ and R. J. Stat. Softw. 77, 1–17. https://doi.org/10.18637/jss.v077.i01

Yang, T., Liu, Q., Zeng, Q., Chan, L., 2012. Relationship between magnetic properties and heavy metals of urban soils with different soil types and environmental settings: implications for magnetic mapping. Environ. Earth Scie. 66, 409-420. https://doi.org/10.1007/s12665-011-1248-9

List of Figures

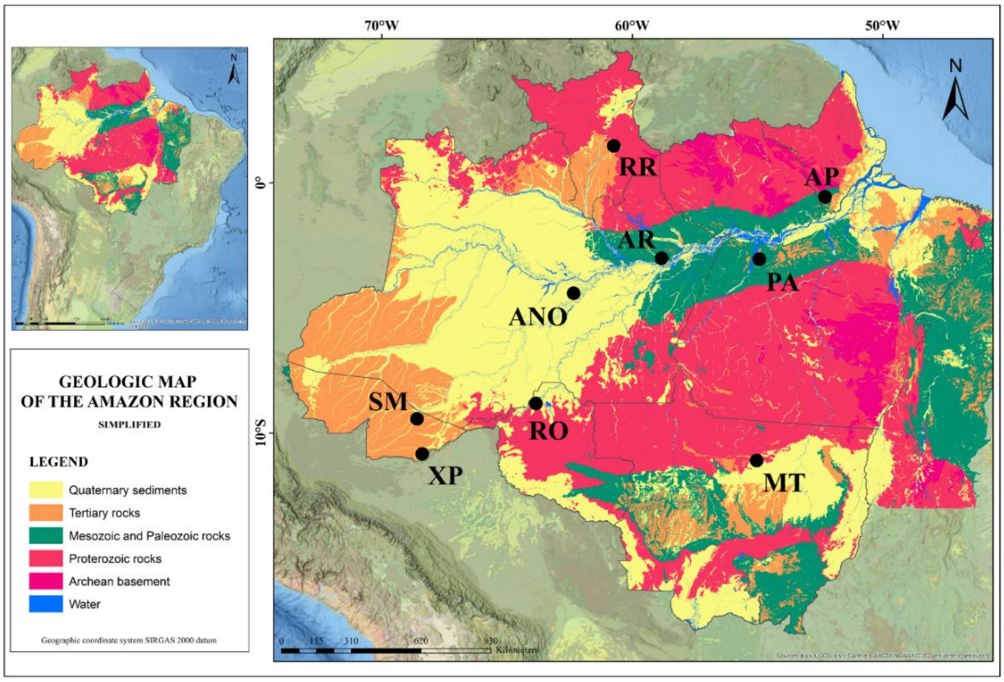

Fig. 1. Simplified geologic map of the soil samples collected in the Amazon region. The sites are identified as: ANO - Anori, state of Amazonas; AP - Laranjal do Jari, state of Amapá; AR - Aruanã farm in Itacoatiara, state of Amazonas; MT - Itaúba, state of Mato Grosso; PA - Santarém, state of Pará; RO - Porto Velho, state of Rondônia; RR - Caracaraí, state of Roraima; SM - Sena Madureira, state of Acre and XP - Xapuri, state of Acre

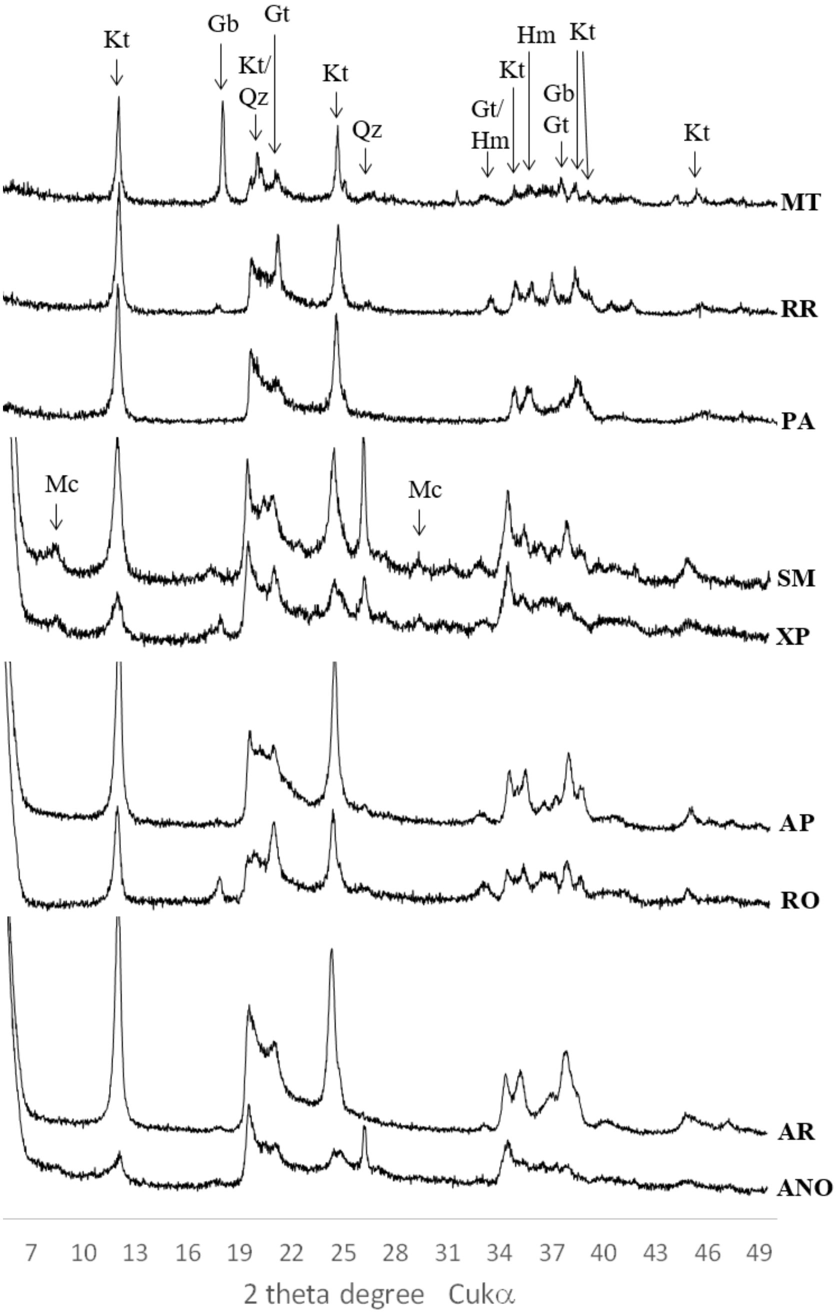

Fig. 2. X-ray diffractometry patterns of the clay size fraction (< 2 µm) for the soil samples collected (0-20 cm) in different sites of the Amazon region. The terms are identified as: Gt - geothite, Hm - hematite, Gb - gibbsite, Kt - kaolinite, Qz - quartz, Mc - mica; ANO - Anori, state of Amazonas; AP - Laranjal do Jari, state of Amapá; AR - Aruanã farm in Itacoatiara, state of Amazonas; MT - Itaúba, state of Mato Grosso; PA - Santarém, state of Pará; RO - Porto Velho, state of Rondônia; RR - Caracaraí, state of Roraima; SM - Sena Madureira, state of Acre and XP - Xapuri, state of Acre

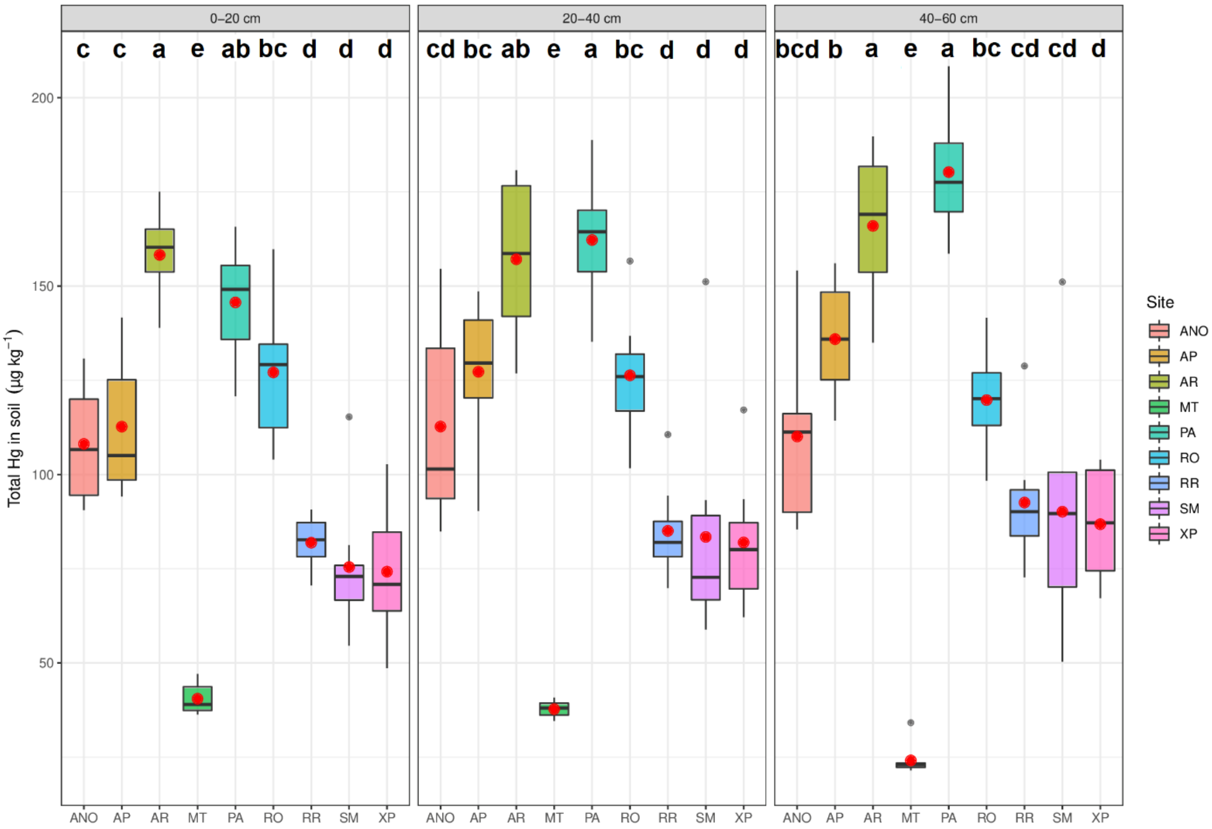

Fig. 3. Total mercury results for the soil samples collected in the depths 0-20, 20-40 and 40-60 cm in different sites of the Amazon region. The sites are identified as: ANO - Anori, state of Amazonas; AP - Laranjal do Jari, state of Amapá; AR - Aruanã farm in Itacoatiara, state of Amazonas; MT - Itaúba, state of Mato Grosso; PA - Santarém, state of Pará; RO - Porto Velho, state of Rondônia; RR - Caracaraí, state of Roraima; SM - Sena Madureira, state of Acre and XP - Xapuri, state of Acre. Lowercase letters compare sites ($P < 0.05$). Red points on each boxplot are the mean of the 8 samples from each site and depth

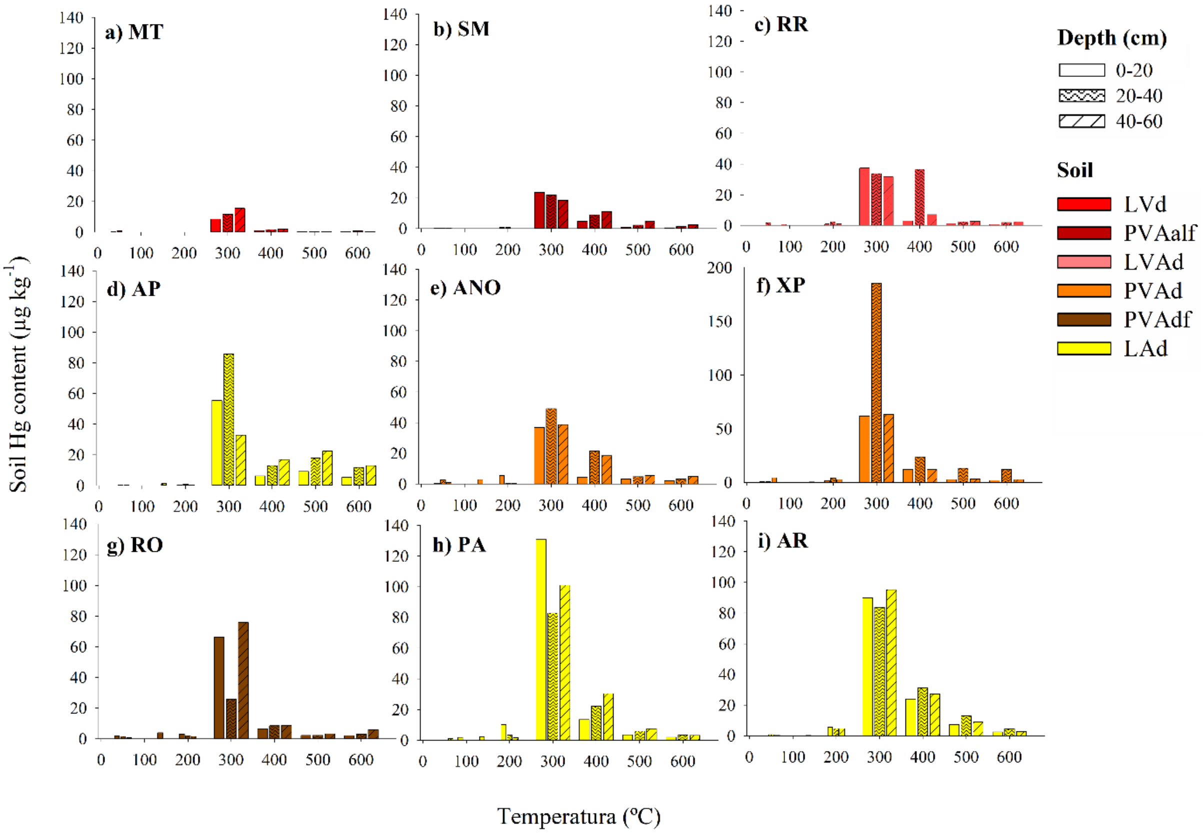

Fig. 4. Soil mercury content using stepwise heating with Direct Mercury Analyzer (DMA-80) for the soil samples collected in the depths 0-20, 20-40 and 40-60 cm in different sites of the Amazon region. The terms are identified as: MT - Itaúba, state of Mato Grosso (a); SM - Sena Madureira, state of Acre (b); RR - Caracaraí, state of Roraima (c); AP - Laranjal do Jari, state of Amapá (d); ANO - Anori, state of Amazonas (e); XP - Xapuri, state of Acre (f); RO - Porto Velho, state of Rondônia (g); PA - Santarém, state of Pará (h); AR - Aruanã farm in Itacoatiara, state of Amazonas (i); LVd - Dystrophic Red Latosol; PVAalf - Plinthic Allitic Yellow-Red Argisol; LVAd - Dystrophic Yellow-Red Latosol; PVAd - Dystrophic Yellow-Red Argisol; PVAdf - Plinthosolic Dystrophic Yellow-Red Argisol and LAd - Dystrophic Yellow Latosol

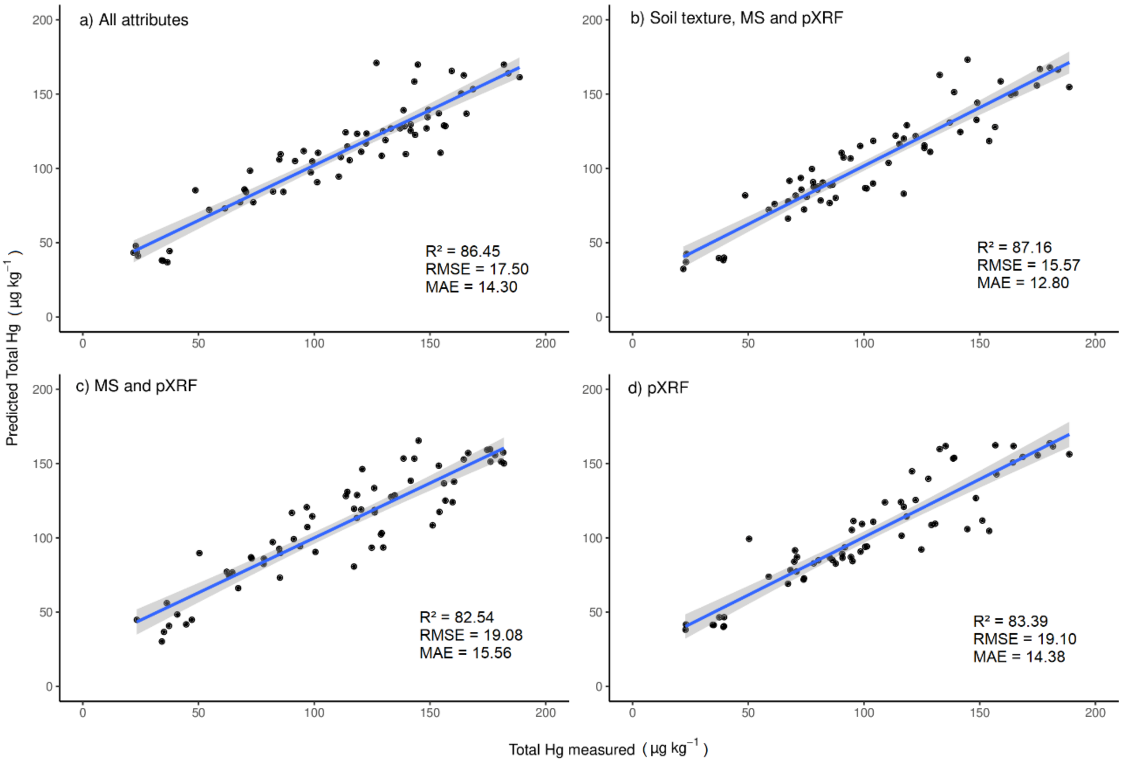

Fig. 5. Plots showing measured soil total Hg vs. soil all physicochemical attributes (a), soil texture, magnetic susceptibility (MS), portable X-ray fluorescence spectrometry (pXRF) (b) and pXRF (c) via Random Forest algorithm using 0-20, 20-40 and 40-60 depths data combined obtained from soil samples collected in different sites of the Amazon region. The line is fitted using the geom_smooth command in ggplot2 within R

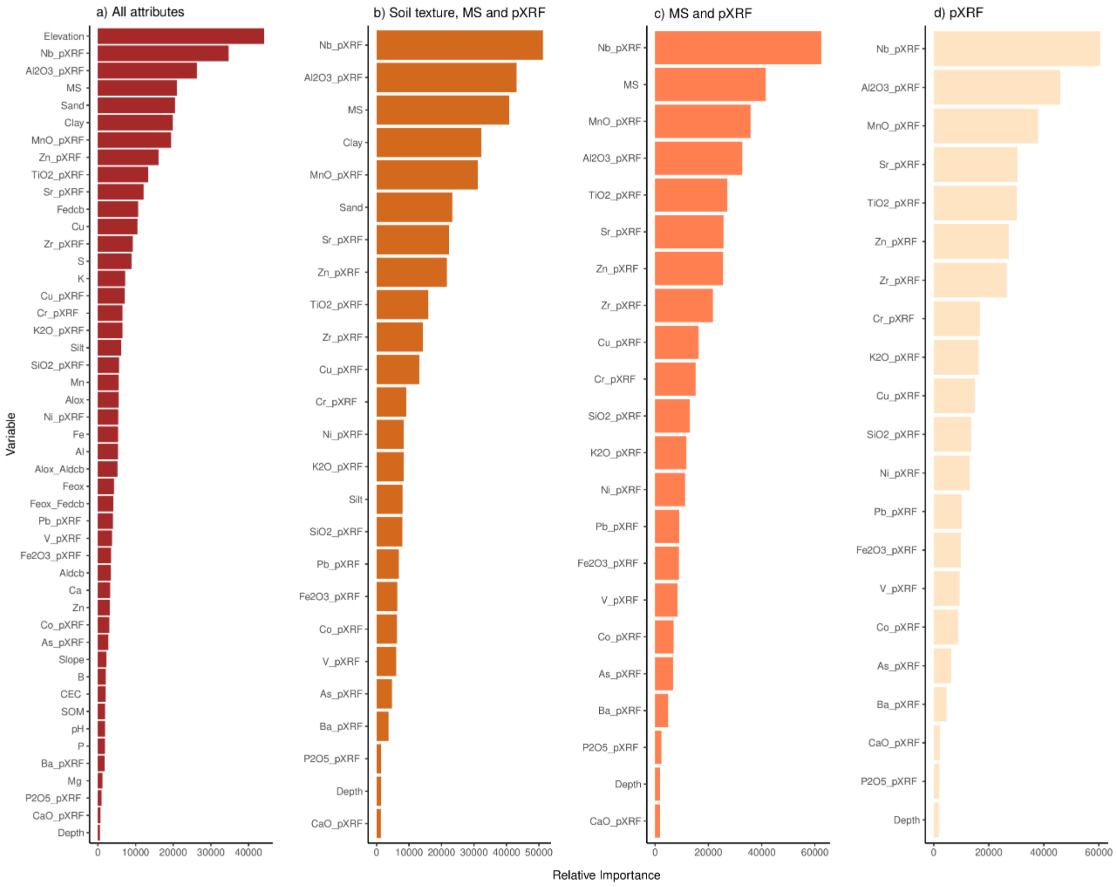

Fig. 6. Variables importance in decreasing order based on prediction results for total Hg (all attributes (a), soil texture, magnetic susceptibility (MS), portable X-ray fluorescence spectrometry (pXRF) (b), MS and pXRF (c) and pXRF (d)) via Random Forest algorithm using 0-20, 20-40 and 40-60 depths data combined obtained from soil samples collected in different sites of the Amazon region. The terms are identified as: MS - Magnetic Susceptibility; SOM - Soil Organic Matter; CEC - cation exchange capacity; OX - extracted with ammonium acid oxalate solution and DCB - extracted with sodium dithionite-citrate-bicarbonate solution

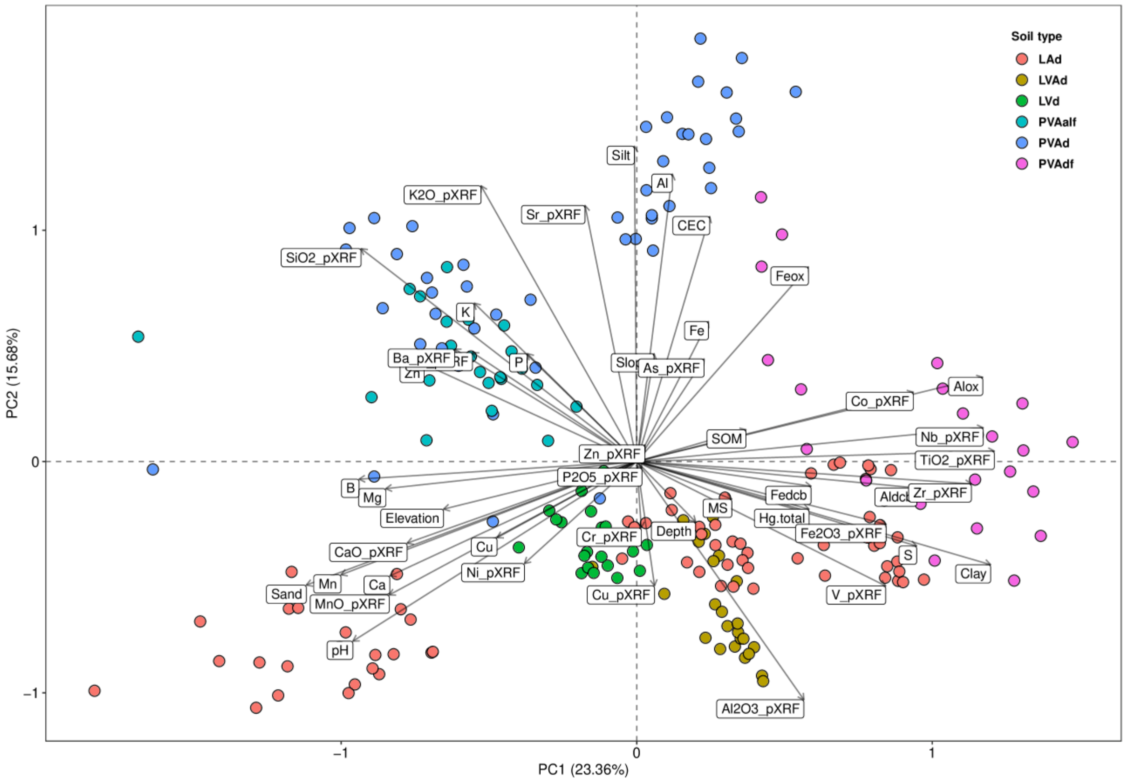

Fig. 7. Principal component analysis between total Hg (THg), elements by portable X-ray fluorescence data, physicochemical properties, elevation and slope for the soil samples collected in the depths 0-20, 20-40 and 40-60 cm in Amazon region. The terms are identified as: ANO - Anori, state of Amazonas; AP - Laranjal do Jari, state of Amapá; AR - Aruanã farm in Itacoatiara, state of Amazonas; MT - Itaúba, state of Mato Grosso; PA - Santarém, state of Pará; RO - Porto Velho, state of Rondônia; RR - Caracaraí, state of Roraima; SM - Sena Madureira, state of Acre and XP - Xapuri, state of Acre; SSA - Specific Surface Área; MS - Magnetic Susceptibility; SOM - Soil Organic Matter; CEC - cation exchange capacity; OX - extracted with ammonium acid oxalate solution and DCB - extracted with sodium dithionite-citrate-bicarbonate solution

List of Tables

Table 1. Classifications of soil samples collected in in different sites of the Amazon region

Site[a]	Geological unit[c]	SiBCS classification[b]	SSA[d]	Elevation[e]	Slope[f]	Climate[g]
ANO	Solimões Formation	PVAd	22.03	53	3.28	Af
AP	Barreiras Group	LAd	10.92	150	4.90	Am
AR	Paleogenic Detrito-Lateritic Coverage	LAd	29.56	93	15.0	Af
MT	Pleistocene Detrito-Lateritic Coverage	LVd	10.90	386	1.80	Am
PA	Alter do Chão Formation	LAd	23.86	89	7.23	Am
RO	Pleistocene Detrito-Lateritic Coverage	PVAdf	33.44	105	14.85	Am
RR	Serra da Lua Gneisses	LVAd	14.66	107	4.12	Am
SM	Soilimões Formation	PVAalf	9.07	243	2.50	Am
XP	Solimões Formation	PVAd	16.50	259	3.61	Am

[a] The sites are identified as: ANO - Anori, state of Amazonas; AP - Laranjal do Jari, state of Amapá; AR - Aruanã farm in Itacoatiara, state of Amazonas; MT - Itaúba, state of Mato Grosso; PA - Santarém, state of Pará; RO - Porto Velho, state of Rondônia; RR - Caracaraí, state of Roraima; SM - Sena Madureira, state of Acre and XP - Xapuri, state of Acre;

[b] LVd - Dystrophic Red Latosol; PVAalf - Plinthic Allitic Yellow-Red Argisol; LVAd - Dystrophic Yellow-Red Latosol; PVAd - Dystrophic Yellow-Red Argisol; PVAdf - Plinthosolic Dystrophic Yellow-Red Argisol and LAd - Dystrophic Yellow Latosol according to Brazilian Soil Classification System (SiBCS) (dos Santos et al., 2018);

[c] Source: INDE – Infraestrutura Nacional de Dados Especiais. Fratura Geológica da Amazônia Legal 1:250.000. http://www.visualizador.inde.gov.br;

[d] SSA - specific surface area in $m^2 g^{-1}$ for samples in 0-20 cm. SSA was derived from one sample and the analysis was performed in duplicate;

[e] Elevation in meters;

[f] Slope in meters, source: INPE - Instituto Nacional de Pesquisas Espaciais. Topodata: banco de dados geomorfométricos do Brasil. Variáveis geomorfométricas locais. http://www.dsr.inpe.br/topodata/;

[g] Köppen class: Af - tropical rainforest climate and Am - tropical monsoon climate.

Table 2. Physicochemical properties for the soil samples collected (0-20 cm) in different sites of the Amazon region

Properties	*n*	Site								
		ANO	AP	AR	MT	PA	RO	RR	SM	XP
pH (H_2O)	8	4.20 (0.23)	5.40 (0.30)	4.20 (0.07)	4.20 (0.06)	4.35 (0.23)	3.75 (0.18)	4.45 (0.15)	4.50 (0.30)	4.50 (0.24)
SOM (%)	8	1.82 (0.65)	1.18 (0.26)	2.55 (0.19)	2.17 (0.43)	2.04 (0.22)	2.21 (0.31)	2.61 (0.29)	1.47 (0.27)	1.52 (0.51)
CEC ($cmol_c$ dm^3)	8	19.60 (6.51)	4.08 (0.53)	7.73 (1.56)	6.63 (1.48)	8.14 (1.38)	11.17 (2.54)	5.50 (0.57)	6.29 (0.88)	6.04 (1.40)
S (mg dm^3)	8	8.85 (4.42)	9.70 (1.14)	17.43 (6.28)	7.82 (0.98)	9.69 (2.37)	17.02 (7.70)	9.70 (1.79)	4.94 (0.98)	5.50 (2.32)
Clay content (%)	8	29.50 (4.53)	19.00 (2.25)	79.00 (3.09)	19.00 (1.47)	53.00	55.00 (7.88)	43.50 (2.06)	18.50 (3.75)	18.00 (4.00)
MS^b (10^{-7} m^3 kg^{-1})	8	1.06 (0.11)	1.75 (0.26)	0.70 (0.11)	19.30 (2.29)	0.79 (0.24)	19.05 (13.23)	3.80 (0.65)	2.35 (5.21)	3.95 (2.23)
Fe_{DCB} (g kg^{-1})	8	14.36 (2.33)	6.70 (0.66)	6.55 (0.58)	14.04 (1.90)	8.65 (2.70)	42.26 (16.15)	34.35 (8.37)	12.54 (5.81)	11.86 (2.63)
Fe_{ox} (g kg^{-1})	8	3.03 (0.55)	1.08 (0.26)	1.75 (0.19)	1.67 (0.18)	1.14 (0.08)	2.36 (0.41)	1.02 (0.13)	1.06 (0.20)	1.07 (0.20)
Al_{DCB} (g kg^{-1})	8	2.20 (0.34)	0.69 (0.09)	1.79 (0.11)	2.23 (0.23)	1.69 (0.55)	6.96 (1.19)	4.68 (0.87)	1.12 (0.38)	1.29 (0.36)
Al_{ox} (g kg^{-1})	8	1.58 (0.23)	0.40 (0.11)	1.67 (0.18)	1.14 (0.16)	0.85 (0.12)	1.74 (0.23)	0.73 (0.13)	0.43 (0.06)	0.52 (0.12)
Fe_{ox} / Fe_{DCB}	8	0.21 (0.02)	0.15 (0.04)	0.26 (0.03)	0.11 (0.01)	0.12 (0.05)	0.05 (0.10)	0.03 (0.01)	0.12 (0.04)	0.08 (0.05)
Al_{ox} / Al_{DCB}	8	0.69 (0.09)	0.60 (0.11)	0.93 (0.07)	0.53 (0.04)	0.52 (0.11)	0.25 (0.06)	0.17 (0.03)	0.45 (0.13)	0.35 (0.10)

The terms are identified as: ANO - Anori, state of Amazonas; AP - Laranjal do Jari, state of Amapá; AR - Aruanã farm in Itacoatiara, state of Amazonas; MT - Itaúba, state of Mato Grosso; PA - Santarém, state of Pará; RO - Porto Velho, state of Rondônia; RR - Caracaraí, state of Roraima; SM - Sena Madureira, state of Acre and XP - Xapuri, state of Acre; MS - Magnetic Susceptibility; pH - pH in water (1: 2.5 soil / solution); CEC - Cation exchange capacity at pH 7.0; SOM - Soil Organic Matter; S - Sulfur extracted as sulfate by monocalcium phosphate with acetic acid and the result was converted to S; ox - extracted by ammonium oxalate acid; DCB - extracted by sodium dithionite-citrate-bicarbonate; Clay content in PA was derived from one single analysis performed by a composite sample resulted of subsamples from 5 spots in the site; Values represent medians and mean absolute deviations (in parenthesis).

Table 3. Chemical composition determined by portable X-ray fluorescence for the soil samples collected (0-20 cm) in different sites of the Amazon region

Element/oxide	*n*	Site								
(g kg^{-1})		ANO	AP	AR	MT	PA	RO	RR	SM	XP
Al_2O_3	8	84.3 (5.8)	140.5 (8.9)	197.5 (7.2)	133.8 (6.8)	197.0 (3.9)	139.7 (14.7)	139.4 (2.3)	96.7 (15.9)	91.5 (20.7)
Fe_2O_3	8	34.5 (5.0)	26.7 (1.8)	38.9 (3.7)	40.3 (6.2)	32.5 (5.1)	109.2 (28.1)	79.0 (6.2)	25.6 (15.0)	24.5 (4.8)
SiO_2	8	432.7 (23.5)	330.9 (15.1)	228.9 (12.8)	287.1 (14.8)	276.3 (5.5)	192.3 (40.1)	232.7 (10.7)	477.9 (62.9)	595.9 (64.87)
MnO	8	0.1 (0.01)	2.5 (0.9)	0.04 (0.02)	0.1 (0.02)	0.05 (0.02)	0.2 (0.04)	0.4 (0.1)	0.2 (0.3)	0.1 (0.12)
CaO	8	< LOD	1.1 (0.6)	< LOD	0.1 (0.2)	0.2 (0.2)	< LOD	< LOD	0.1 (0.2)	0.1 (0.8)
TiO_2	8	5.3 (0.6)	3.1 (0.3)	6.8 (0.4)	3.4 (0.2)	5.8 (0.1)	5.8 (0.31)	6.3 (0.2)	4.0 (0.28)	3.6 (0.29)
P_2O_5	8	0.1 (0.1)	0.2 (0.1)	< LOD	0.3 (0.1)	< LOD	0.2 (0.1)	0.2 (0.07)	0.3 (0.2)	< LOD
K_2O	8	6.5 (0.9)	0.1 (0.1)	< LOD	0.3 (0.2)	< LOD	0.3 (1.1)	< LOD	6.3 (1.27)	6.8 (1.4)
Trace-elements (mg kg^{-1})										
Cu	8	16.5 (4.4)	36.0 (5.0)	8.0 (3.4)	11.0 (4.2)	10.0 (2.4)	32.5 (13.4)	43.5 (7.0)	10.4 (2.9)	13.6 (2.4)
Zn	8	24.5 (4.9)	24.5 (6.2)	7.5 (2.1)	8.0 (2.0)	8.5 (1.1)	29.5 (7.0)	41.0 (2.6)	16.6 (7.9)	16.8 (2.2)
Ni	8	14.0 (5.1)	23.5 (6.5)	< LOD	< LOD	< LOD	7.0 (8.2)	33.0 (4.2)	9.0 (6.6)	10.5 (6.7)
Pb	8	12.0 (2.5)	15.5 (1.7)	8.0 (1.0)	5.5 (1.0)	6.0 (0.8)	7.5 (4.0)	5.5 (1.2)	12.3 (2.5)	7.7 (1.5)
Cr	8	42.0 (16.7)	49.0 (11.2)	43.0 (11.3)	71.5 (12.2)	38.5 (8.7)	53.0 (31.7)	56.0 (22.2)	36.5 (14.6)	39.3 (20.7)
Co	8	61.0 (26.2)	< LOD	28.0 (30.9)	< LOD	< LOD	112.0 (28.0)	< LOD	< LOD	< LOD
As	8	6.0 (0.7)	< LOD	9.0 (0.6)	< LOD	< LOD	17.5 (6.9)	< LOD	17.2 (3.3)	7.3 (1.8)
Ba	8	0 (125.6)	66.0 (17.2)	< LOD	< LOD	0 (8.7)	58.5 (24.1)	0 (11.8)	200.5 (352.3)	666.1 (414.8)
Sr	8	43.5 (10.1)	20.0 (4.7)	12.5 (0.7)	8.5 (1.4)	13.0 (2.5)	22.5 (9.4)	20.0 (5.4)	20.5 (5.2)	29.9 (4.4)
V	8	109.0 (54.0)	0 (40.3)	140.5 (18.5)	147.0 (23.6)	101.0 (27.1)	107.0 (49.6)	206.5 (17.1)	< LOD	< LOD
Zr	8	607.5 (37.4)	218.5 (20.1)	1657.0 (181.4)	298.5 (36.7)	676.5 (42.4)	1167.0 (360.8)	806.5 (66.9)	375.3 (31.5)	487.2 (58.4)
Nb	8	24.5 (5.0)	8.0 (1.0)	47.0 (3.6)	13.5 (0.9)	27.0 (0.5)	48.0 (18.9)	14.5 (1.2)	15.2 (1.3)	15.0 (1.5)

The sites are identified as: ANO - Anori, state of Amazonas; AP - Laranjal do Jari, state of Amapá; AR - Aruanã farm in Itacoatiara, state of Amazonas; MT - Itaúba, state of Mato Grosso; PA - Santarém, state of Pará; RO - Porto Velho, state of Rondônia; RR - Caracaraí, state of Roraima; SM - Sena Madureira, state of Acre and XP - Xapuri, state of Acre; Values represent medians and mean absolute deviations (in parenthesis); LOD - Limit of detection.

Supplementary material

Table S1. Description of the sampled areas in different sites of the Amazon region

Site[a]	GPS coordinates	
ANO	62°20'34"W	4°24'52"S
AP	52°18'23"W	0°33'49"S
AR	58°49'42"W	3°01'04"S
MT	55°02'11"W	11°05'56"S
PA	54°55'42"W	3°03'18"S
RO	63°50'50"W	8°48'46"S
RR	60°44'16"W	1°28'15"N
SM	68°35'44"W	9°26'04"S
XP	68°23'11"W	10°49'52"S

[a] The sites are identified as: ANO - Anori, state of Amazonas; AP - Laranjal do Jari, state of Amapá; AR - Aruanã farm in Itacoatiara, state of Amazonas; MT - Itaúba, state of Mato Grosso; PA - Santarém, state of Pará; RO - Porto Velho, state of Rondônia; RR - Caracaraí, state of Roraima; SM - Sena Madureira, state of Acre and XP - Xapuri, state of Acre.

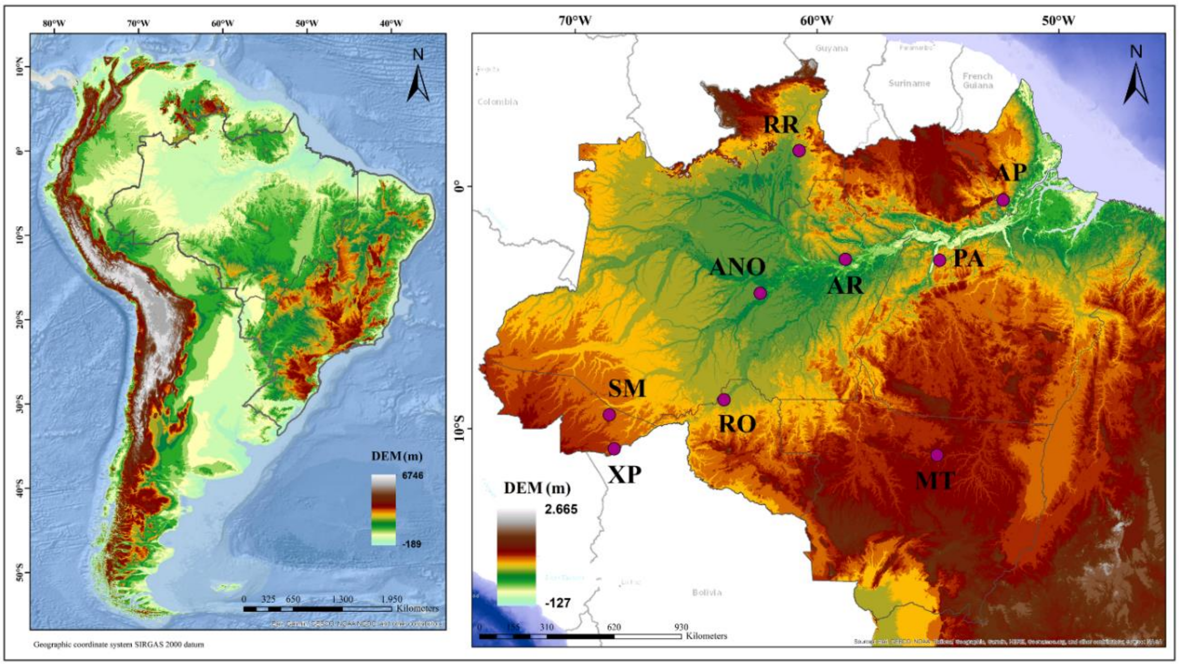

Fig. S1. Map of digital elevation model (DEM) the soil samples collected in in different sites of the Amazon region. Each site is identified by: MT - Itaúba, state of Mato Grosso; SM - Sena Madureira, state of Acre; RR - Caracaraí, state of Roraima; AP - Laranjal do Jari, state of Amapá; ANO - Anori, state of Amazonas; XP - Xapuri, state of Acre; RO - Porto Velho, state of Rondônia; PA - Santarém, state of Pará and AR - Aruanã farm in Itacoatiara, state of Amazonas

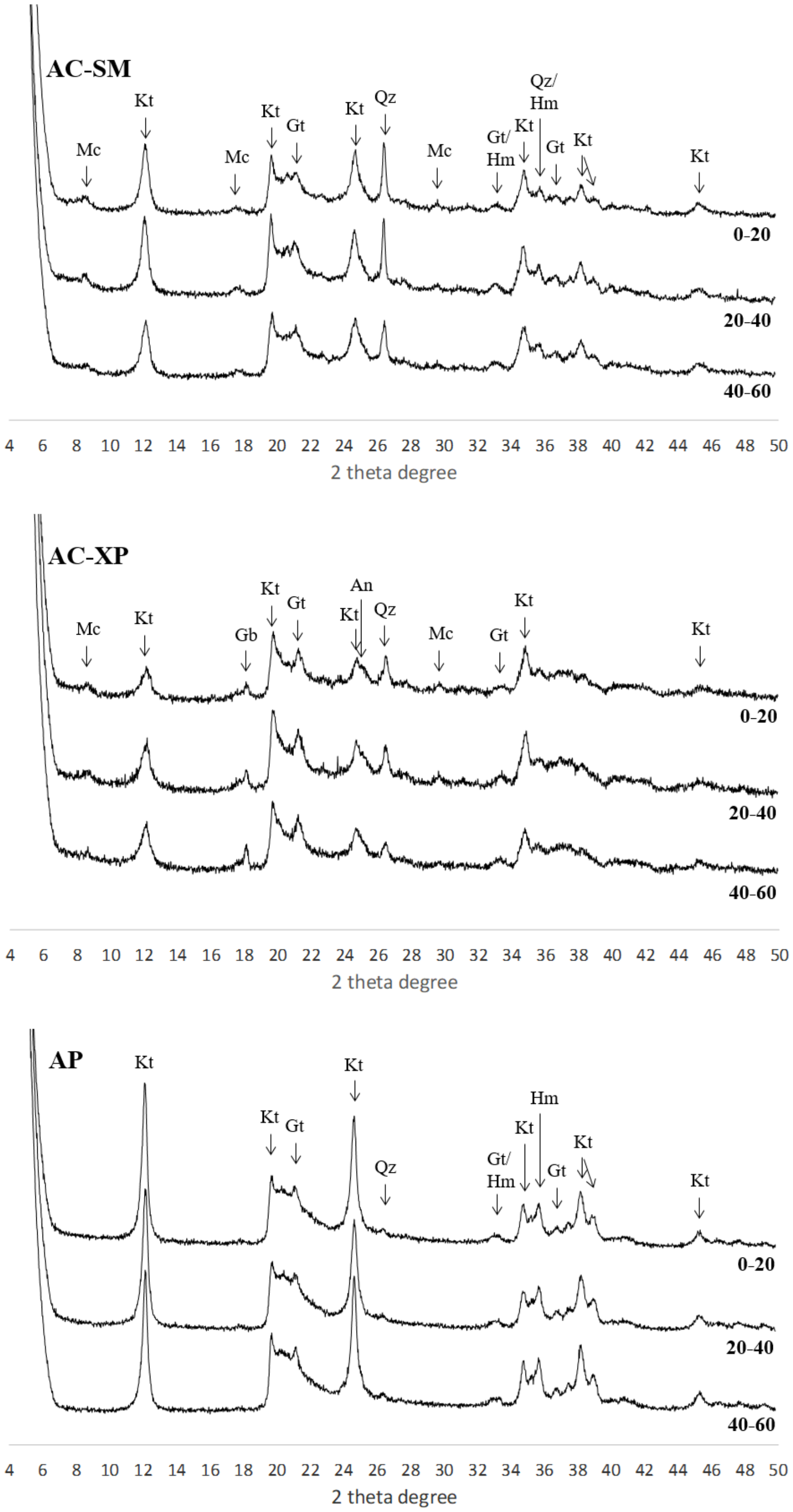

Fig. S2. X-ray diffractometry patterns of the clay size fraction (< 2 μm) for the soil samples collected in the depths 0-20, 20-40 and 40-60 cm in different sites of the Amazon region. The terms are identified as: Gt - geothite; Hm - hematite; Gb - gibbsite; Kt - kaolinite; Qz - quartz; Mc - mica; AP - Laranjal do Jari, state of Amapá; AC-XP - Xapuri, state of Acre and AC-SM - Sena Madureira, state of Acre

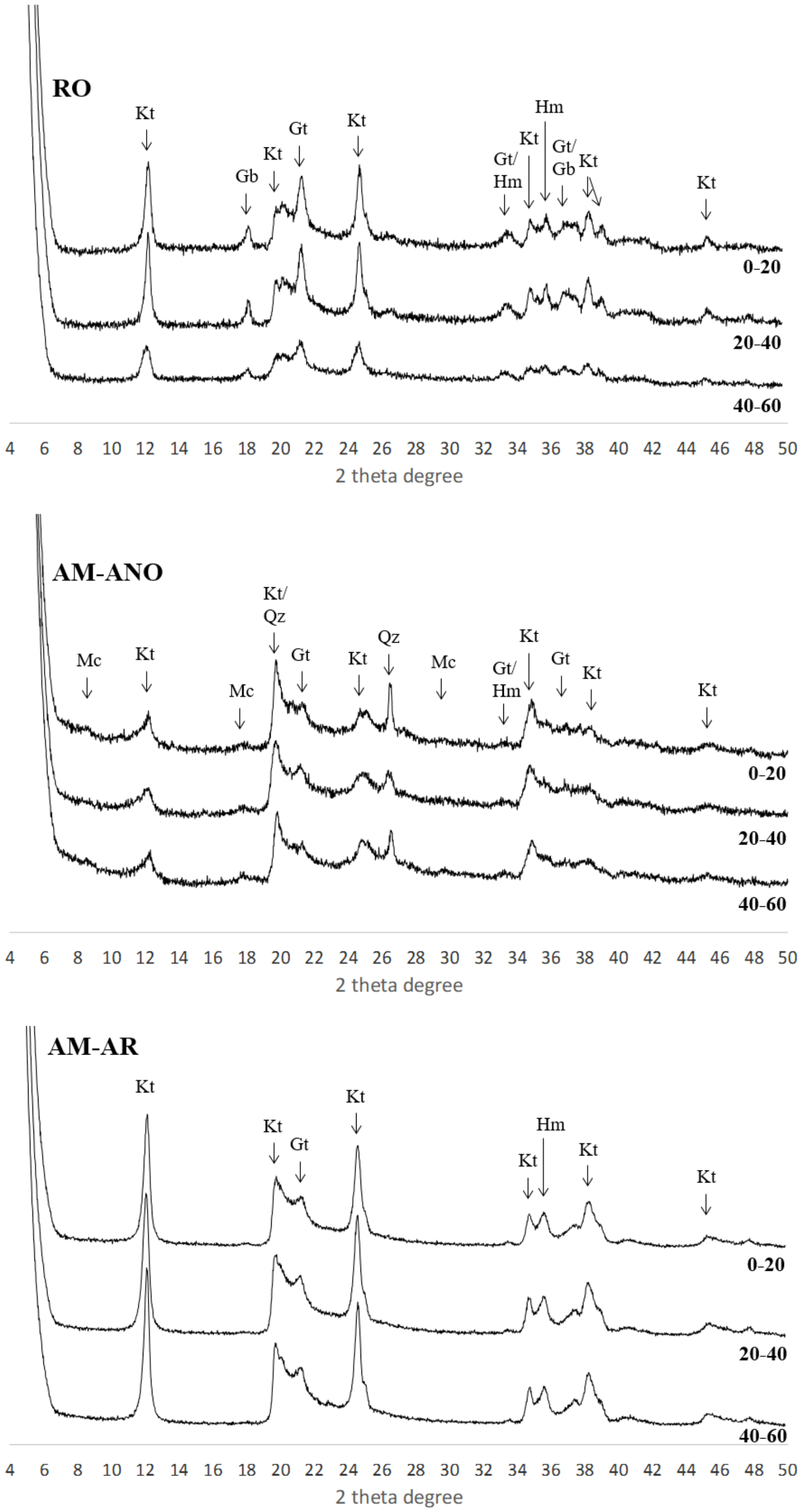

Fig. S3. X-ray diffractometry patterns of the clay size fraction (< 2 μm) for the soil samples collected in the depths 0-20, 20-40 and 40-60 cm in different sites of the Amazon region. The terms are identified as: Gt - geothite; Hm - hematite; Gb - gibbsite; Kt - kaolinite; Qz - quartz; Mc - mica; AM-AR - Aruanã farm in Itacoatiara, state of Amazonas; AM-ANO - Anori, state of Amazonas and RO - Porto Velho, state of Rondônia

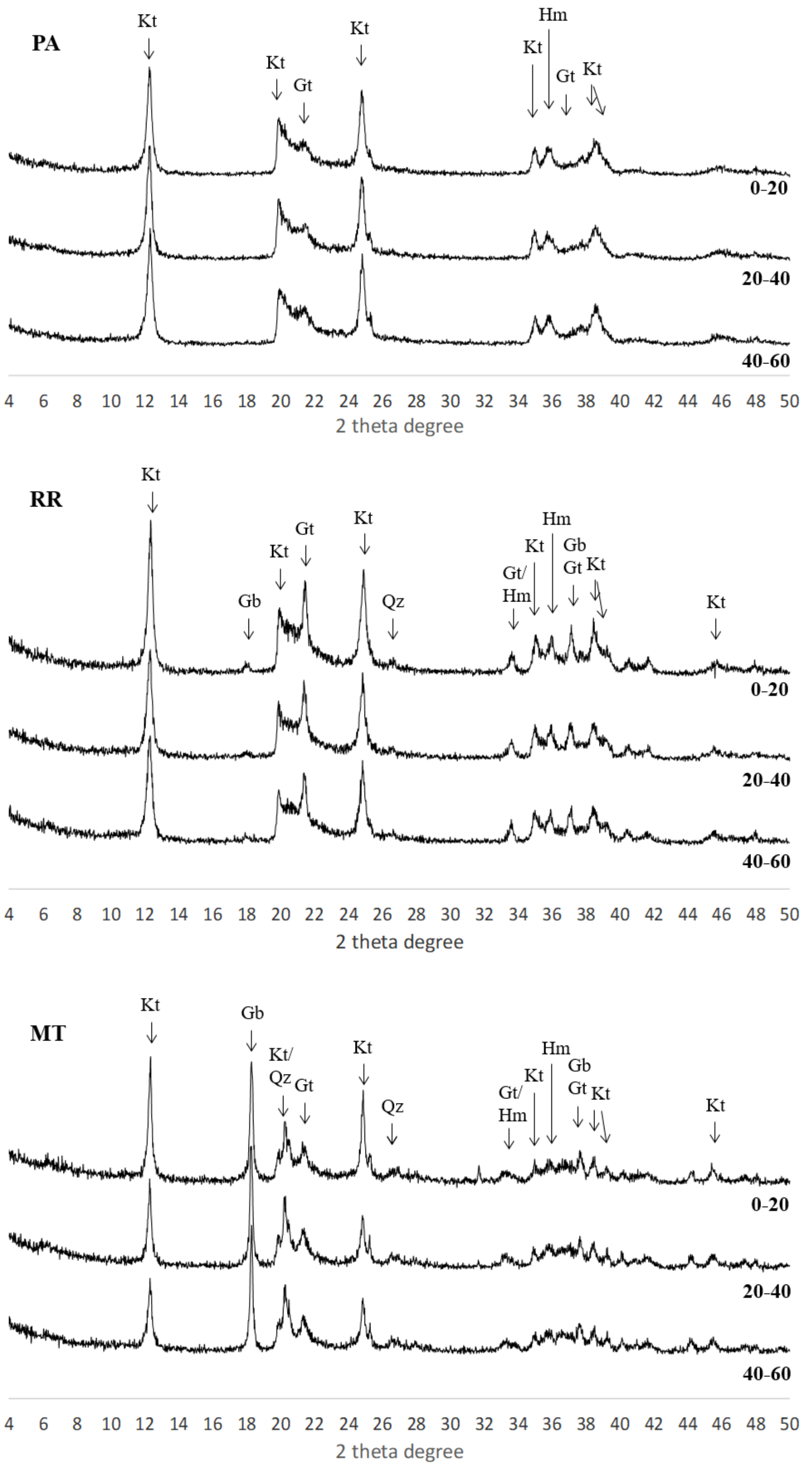

Fig. S4. X-ray diffractometry patterns of the clay size fraction (< 2 µm) for the soil samples collected in the depths 0-20, 20-40 and 40-60 cm in different sites of the Amazon region. The terms are identified as: Gt - geothite; Hm - hematite; Gb - gibbsite; Kt - kaolinite; Qz - quartz; MT - Itaúba, state of Mato Grosso; RR - Caracaraí, state of Roraima and PA - Santarém, state of Pará

Table S2. Descriptive statistics of soil properties for the soil samples collected in different sites of the Amazon region

Properties	Soil layer	Site																			
		ANO *(n = 8)*				AP *(n = 8)*				AR *(n = 8)*				MT *(n = 8)*				PA *(n = 8)*			
		Median	Minimum	Maximum	MAD[a]	Median	Minimum	Maximum	MAD	Median	Minimum	Maximum	MAD	Median	Minimum	Maximum	MAD	Median	Minimum	Maximum	MAD
THg	0-20	106.63	90.55	130.75	14.44	105.03	94.20	141.65	15.85	160.30	138.95	175.05	8.84	38.98	36.30	47.10	3.39	149.13	120.75	165.75	12.47
	20-40	101.45	84.90	154.55	22.70	129.58	90.35	148.60	14.14	158.65	126.85	180.75	16.68	38.05	34.60	40.80	1.75	164.43	135.25	188.70	12.42
	40-60	111.28	85.45	154.10	16.79	135.93	114.30	156.05	11.56	169.05	135.00	189.70	16.35	22.98	21.49	34.15	2.50	177.55	158.65	208.30	12.93
pH (H_2O)	0-20	4.20	3.60	4.50	0.23	5.40	5.00	6.10	0.30	4.20	4.10	4.40	0.07	4.20	4.10	4.30	0.06	4.35	4.20	5.10	0.23
	20-40	4.35	3.40	4.40	0.32	5.45	4.90	6.10	0.38	4.40	4.30	4.80	0.13	4.50	4.30	4.70	0.12	4.40	4.20	4.50	0.07
	40-60	4.10	3.60	4.70	0.25	5.45	5.10	5.70	0.16	4.50	4.40	4.80	0.09	4.75	4.60	5.00	0.13	4.55	4.00	4.80	0.27
SOM (%)	0-20	1.82	1.29	3.84	0.65	1.18	0.75	1.99	0.26	2.55	2.23	3.00	0.19	2.17	1.75	3.14	0.43	2.04	1.56	2.47	0.22
	20-40	1.29	0.34	1.99	0.38	0.70	0.54	1.18	0.16	1.24	0.86	1.64	0.21	1.58	1.29	1.87	0.16	1.07	0.82	1.37	0.12
	40-60	0.92	0.34	1.29	0.28	0.54	0.34	0.97	0.17	0.86	0.44	1.29	0.23	1.29	1.18	1.52	0.09	0.93	0.46	1.45	0.20
CEC (cmol$_c$ dm^3)	0-20	19.60	10.10	42.06	6.51	4.08	3.52	6.05	0.53	7.73	6.05	11.24	1.56	6.63	4.91	11.32	1.48	8.14	6.93	11.79	1.38
	20-40	20.59	17.39	46.84	8.35	3.71	2.60	4.63	0.41	4.61	3.12	8.11	1.47	4.15	3.50	5.32	0.44	6.11	4.71	7.72	0.66
	40-60	24.18	15.65	52.31	10.34	3.17	2.78	4.09	0.44	4.11	2.80	5.87	0.85	3.73	3.16	6.55	0.99	4.86	3.34	8.47	1.14
S (mg dm^3)	0-20	8.85	5.12	25.14	4.42	9.70	7.42	11.23	1.14	17.43	9.06	37.91	6.28	7.82	4.38	8.64	0.98	9.69	6.21	16.21	2.37
	20-40	7.43	5.49	12.14	1.85	9.70	7.03	12.14	1.39	30.47	19.40	42.41	4.52	9.70	5.87	13.08	1.81	13.25	8.02	22.81	3.37
	40-60	8.03	6.25	13.56	2.17	9.91	8.64	11.68	0.97	46.27	30.47	65.42	6.01	9.06	6.25	18.26	3.57	17.59	10.08	29.36	5.66
Fe$_{DCB}$ (g kg^{-1})	0-20	14.36	8.58	18.09	2.33	6.70	6.03	9.32	0.66	6.55	5.53	8.10	0.58	14.04	10.62	16.91	1.90	8.65	5.14	13.81	2.70
	20-40	14.15	12.02	18.30	1.75	8.23	7.03	9.51	0.52	6.52	5.66	7.59	0.44	14.41	10.97	19.63	2.58	8.91	5.15	12.43	2.40
	40-60	14.82	12.51	24.88	3.28	9.53	7.90	9.73	0.69	6.46	5.77	7.26	0.35	14.98	11.75	20.28	2.55	9.67	5.45	14.29	2.72
Fe$_{ox}$ (g kg^{-1})	0-20	3.03	1.90	3.98	0.55	1.08	0.16	1.44	0.26	1.75	1.30	1.98	0.19	1.67	1.34	1.89	0.18	1.14	0.94	1.31	0.08
	20-40	2.28	1.32	3.22	0.54	1.06	0.01	1.46	0.30	1.32	0.85	1.41	0.15	1.52	1.34	1.77	0.13	0.96	0.20	1.23	0.19
	40-60	1.97	1.12	3.18	0.48	0.85	0.12	1.16	0.23	0.88	0.57	1.08	0.11	1.37	1.26	1.49	0.07	0.79	0.64	1.16	0.12
Al$_{DCB}$ (g kg^{-1})	0-20	2.20	1.51	2.95	0.34	0.69	0.60	1.04	0.09	1.79	1.55	1.97	0.11	2.23	1.64	2.47	0.23	1.69	1.00	2.84	0.55
	20-40	2.20	1.89	2.50	0.17	0.81	0.69	1.04	0.10	1.74	1.46	1.99	0.15	2.32	1.76	2.86	0.27	1.81	0.97	2.59	0.52
	40-60	2.34	1.96	2.84	0.25	0.90	0.78	1.09	0.09	1.68	1.42	1.86	0.11	2.19	1.93	2.72	0.19	2.01	1.10	3.04	0.54
Al$_{ox}$ (g kg^{-1})	0-20	1.58	0.93	2.09	0.23	0.40	0.14	0.63	0.11	1.67	1.31	1.96	0.18	1.14	0.87	1.58	0.16	0.85	0.66	1.18	0.12
	20-40	1.51	1.00	1.77	0.20	0.49	0.01	0.66	0.14	1.56	1.26	2.18	0.17	1.20	0.98	1.52	0.14	0.90	0.05	0.98	0.20
	40-60	1.54	1.10	1.84	0.15	0.50	0.01	0.67	0.12	1.46	1.25	1.66	0.12	1.25	0.94	1.33	0.10	0.89	0.74	1.68	0.21

Fe_{ox} / Fe_{DCB}	0-20	0.21	0.16	0.25	0.02	0.15	0.03	0.22	0.04	0.26	0.20	0.32	0.03	0.11	0.11	0.14	0.01	0.12	0.09	0.23	0.05
	20-40	0.15	0.11	0.21	0.04	0.12	0.00	0.17	0.03	0.19	0.15	0.23	0.02	0.10	0.08	0.14	0.01	0.09	0.04	0.24	0.05
	40-60	0.13	0.08	0.16	0.02	0.09	0.01	0.15	0.03	0.13	0.10	0.17	0.02	0.09	0.07	0.12	0.01	0.07	0.05	0.20	0.05
Al_{ox} / Al_{DCB}	0-20	0.69	0.53	0.82	0.09	0.60	0.18	0.81	0.11	0.93	0.81	1.14	0.07	0.53	0.47	0.70	0.04	0.52	0.41	0.73	0.11
	20-40	0.69	0.47	0.82	0.09	0.59	0.01	0.67	0.13	0.87	0.81	1.10	0.07	0.52	0.44	0.66	0.06	0.44	0.04	0.79	0.18
	40-60	0.63	0.47	0.79	0.07	0.55	0.01	0.62	0.13	0.88	0.80	0.95	0.03	0.54	0.43	0.65	0.06	0.44	0.37	1.30	0.23
MS	0-20	1.06	0.85	1.15	0.11	1.75	1.40	2.60	0.26	0.70	0.55	1.08	0.11	19.30	17.30	26.00	2.29	0.79	0.42	1.12	0.24
	20-40	1.07	0.98	1.32	0.10	2.30	2.00	2.90	0.30	0.83	0.63	0.94	0.11	19.70	16.90	25.60	2.31	0.74	0.36	1.11	0.22
	40-60	1.13	0.92	1.73	0.16	2.75	2.00	3.50	0.40	0.67	0.58	0.76	0.05	19.40	17.70	26.40	2.39	0.72	0.39	1.22	0.21
Clay (%)	0-20	29.50	18.00	37.00	4.53	19.00	15.00	25.00	2.25	79.00	68.00	85.00	3.09	19.00	17.00	24.00	1.47	53.00			
	20-40	32.00	26.00	45.00	5.13	23.50	22.00	30.00	2.06	79.50	77.00	88.00	2.44	23.50	18.00	26.00	1.91	62.00			
	40-60	36.00	25.00	50.00	6.75	27.50	22.00	32.00	2.47	84.50	81.00	88.00	1.88	25.50	23.00	26.00	1.16	70.00			
Silt (%)	0-20	59.00	49.00	65.00	5.75	4.50	2.00	7.00	1.38	9.00	6.00	13.00	2.00	3.50	1.00	7.00	2.00	7.00			
	20-40	52.50	44.00	60.00	4.50	4.00	2.00	10.00	1.63	9.50	5.00	16.00	3.00	4.00	2.00	7.00	1.16	6.00			
	40-60	51.50	45.00	57.00	3.50	5.00	2.00	16.00	2.56	7.00	4.00	12.00	2.00	3.00	2.00	6.00	1.13	5.00			
Sand (%)	0-20	12.50	4.00	33.00	9.63	76.50	69.00	80.00	2.91	12.00	9.00	19.00	2.53	75.50	73.00	81.00	2.53	40.00			
	20-40	13.50	3.00	26.00	9.25	71.00	66.00	76.00	2.75	9.00	7.00	13.00	1.69	73.50	70.00	75.00	1.75	32.00			
	40-60	13.00	3.00	25.00	8.75	68.50	52.00	74.00	4.06	8.00	6.00	12.00	1.72	72.00	68.00	75.00	2.13	25.00			
Ca^{2+} ($cmol_c$ dm^3)	0-20	0.10	0.10	0.10	0.00	1.10	0.80	3.00	0.64	0.10	0.10	0.30	0.08	0.15	0.10	0.20	0.05	0.71	0.24	1.25	0.29
	20-40	0.10	0.10	0.10	0.00	0.85	0.30	2.40	0.55	0.10	0.10	0.30	0.04	0.10	0.10	0.20	0.02	0.25	0.10	0.55	0.13
	40-60	0.10	0.10	0.10	0.00	0.80	0.40	1.70	0.36	0.10	0.10	0.20	0.04	0.10	0.10	0.20	0.02	0.20	0.10	0.44	0.10
Mg^{2+} ($cmol_c$ dm^3)	0-20	0.10	0.10	0.20	0.05	0.40	0.30	0.90	0.14	0.10	0.10	0.10	0.00	0.10	0.10	0.20	0.02	0.36	0.22	0.56	0.09
	20-40	0.10	0.10	0.20	0.02	0.30	0.20	0.70	0.14	0.10	0.10	0.10	0.00	0.10	0.10	0.10	0.00	0.16	0.10	0.30	0.06
	40-60	0.10	0.10	0.10	0.00	0.30	0.20	0.50	0.10	0.10	0.10	0.10	0.00	0.10	0.10	0.10	0.00	0.12	0.10	0.27	0.05
Al^{3+} ($cmol_c$ dm^3)	0-20	6.20	4.10	9.30	1.23	0.15	0.00	0.30	0.09	1.60	1.30	1.80	0.10	1.35	1.10	1.80	0.18	1.04	0.52	1.64	0.30
	20-40	7.55	5.40	9.60	1.07	0.15	0.00	0.40	0.11	1.25	1.10	1.40	0.08	0.90	0.80	1.10	0.05	1.32	1.14	1.59	0.10
	40-60	8.05	5.90	9.80	1.03	0.20	0.10	0.40	0.09	1.15	1.00	1.50	0.11	0.75	0.70	0.90	0.08	1.30	0.98	1.49	0.13
K (mg dm^3)	0-20	32.00	26.00	46.00	5.25	27.00	16.00	34.00	3.75	20.00	4.00	36.00	6.38	36.00	32.00	56.00	7.13	25.15	18.80	31.50	2.65
	20-40	22.00	14.00	26.00	2.31	14.00	10.00	16.00	1.38	10.00	4.00	16.00	3.75	24.00	24.00	30.00	1.88	12.45	10.34	16.69	1.59
	40-60	23.00	14.00	48.00	6.38	10.00	8.00	28.00	4.25	6.00	2.00	12.00	2.63	20.00	18.00	26.00	2.00	9.28	6.11	23.03	3.97
P (mg dm^3)	0-20	2.61	1.71	4.81	0.77	2.15	1.42	3.84	0.60	2.45	2.30	4.16	0.50	1.28	0.84	2.00	0.33	1.99	1.60	2.73	0.34

	20-40	1.13	0.84	2.91	0.58	1.71	1.42	2.60	0.33	1.13	1.13	2.00	0.23	0.84	0.56	1.42	0.23	1.63	1.30	1.81	0.15
	40-60	1.13	0.84	2.00	0.27	1.28	0.84	1.71	0.25	0.84	0.84	1.13	0.11	0.70	0.56	1.13	0.18	1.23	0.92	1.69	0.20
Zn (mg dm^{3})	0-20	0.93	0.62	1.48	0.20	1.05	0.41	4.87	1.03	0.48	0.33	0.65	0.09	0.22	0.12	0.37	0.07	0.36	0.10	0.61	0.12
	20-40	0.72	0.39	1.74	0.23	0.65	0.35	1.26	0.25	0.14	0.06	0.33	0.08	0.17	0.09	0.30	0.07	0.21	0.12	0.27	0.04
	40-60	0.70	0.38	0.84	0.13	0.63	0.40	1.12	0.20	0.14	0.01	0.25	0.05	0.15	0.06	0.18	0.03	0.31	0.10	0.40	0.07
Fe (mg dm^{3})	0-20	415.08	343.19	634.89	67.21	56.82	33.24	110.62	23.35	188.11	128.02	258.52	36.17	273.53	214.27	417.29	56.01	274.72	193.17	380.01	48.82
	20-40	229.40	187.39	434.29	83.28	56.74	35.46	65.62	8.51	127.66	80.39	180.63	34.04	278.26	213.88	443.98	71.64	211.93	124.64	367.55	54.20
	40-60	190.43	120.14	290.51	48.18	41.71	33.09	67.30	8.42	109.78	57.08	123.99	17.38	268.37	204.07	370.03	48.08	171.81	105.00	238.24	41.57
Mn (mg dm^{3})	0-20	2.89	1.92	4.44	0.74	116.08	79.21	152.31	23.34	1.71	1.13	3.43	0.63	2.57	1.25	3.53	0.61	8.26	2.72	19.45	5.00
	20-40	1.92	1.01	3.25	0.75	83.01	52.96	173.06	36.27	1.17	0.47	2.21	0.36	3.29	1.18	7.51	1.53	3.53	1.45	4.01	0.79
	40-60	1.64	0.79	2.67	0.56	83.02	45.91	127.54	19.18	0.89	0.48	1.90	0.29	5.25	2.87	8.07	1.59	1.97	1.68	4.68	1.18
Cu (mg dm^{3})	0-20	1.10	0.44	1.64	0.30	6.39	2.66	106.18	24.10	0.16	0.14	0.25	0.03	0.68	0.43	1.18	0.20	0.57	0.17	1.06	0.24
	20-40	0.87	0.24	1.37	0.22	3.79	2.44	104.22	33.28	0.09	0.08	0.20	0.03	0.74	0.51	1.30	0.20	0.33	0.10	0.95	0.27
	40-60	0.63	0.27	0.97	0.20	7.58	2.54	94.41	25.22	0.10	0.07	0.16	0.02	0.52	0.43	0.88	0.08	0.43	0.10	0.94	0.23
B (mg dm^{3})	0-20	0.13	0.08	0.58	0.10	0.35	0.21	0.45	0.05	0.09	0.04	0.17	0.04	0.17	0.10	0.24	0.05	0.08	0.06	0.10	0.01
	20-40	0.07	0.04	0.33	0.07	0.31	0.19	0.43	0.05	0.07	0.02	0.21	0.05	0.12	0.06	0.78	0.15	0.08	0.06	0.11	0.02
	40-60	0.13	0.04	0.21	0.05	0.20	0.17	0.33	0.06	0.07	0.04	0.15	0.04	0.13	0.08	0.26	0.05	0.09	0.08	0.11	0.01

MAD - mean absolute deviation;
Texture (clay, silt and sand contents) in PA was derived from one single analysis performed by a composite sample resulted of subsamples from 5 spots in the site;
The sites are identified as: ANO - Anori, state of Amazonas; AP - Laranjal do Jari, state of Amapá; AR - Aruanã farm in Itacoatiara, state of Amazonas; MT - Itaúba, state of Mato Grosso; PA - Santarém, state of Pará; RO - Porto Velho, state of Rondônia; RR - Caracaraí, state of Roraima; SM - Sena Madureira, state of Acre and XP - Xapuri, state of Acre;
P, K, Fe, Zn, Mn and Cu were extracted by Mehlich-1 (Mehlich, 1953); Ca^{2+}, Mg^{2+} and Al^{3+} exchangeable were obtained by 1 mol L^{-1} KCl extractant; P-Rem - P remaining (Alvarez et al., 2000); B was extracted by curcumin method (Tedesco et al., 1995); P and B were determined colorimetrically, K by flame emission photometry, S by turbidimetry, and Ca, Mg, Zn, Fe, Mn, and Cu were determined by atomic absorption spectrometry; effective cation exchange capacity (t) and aluminum saturation (m) were calculated with the results of the chemical analyzes.

Table S2. (Continued).

Properties	Soil layer	Site															
		RO *(n = 8)*				RR *(n = 8)*				SM *(n = 8)*				XP *(n = 8)*			
		Median	Minimum	Maximum	MAD	Median	Minimum	Maximum	MAD	Median	Minimum	Maximum	MAD	Median	Minimum	Maximum	MAD
THg	0-20	129.18	104.00	159.75	13.68	82.68	70.55	90.70	6.08	72.95	54.60	115.30	11.42	70.85	48.65	102.75	13.70
	20-40	125.98	101.70	156.65	11.20	82.00	69.85	110.60	8.78	72.73	58.85	151.15	20.45	80.08	62.15	117.15	12.48
	40-60	120.15	98.35	141.60	9.88	90.13	72.70	128.80	11.49	89.65	50.35	151.10	22.74	87.18	67.20	103.90	13.98
pH (H_2O)	0-20	3.75	3.50	4.10	0.18	4.45	4.30	4.90	0.15	4.50	4.30	5.50	0.30	4.50	4.10	5.20	0.24
	20-40	4.10	3.70	4.30	0.16	4.75	4.40	4.90	0.13	4.60	4.40	5.20	0.18	4.60	4.30	5.20	0.25
	40-60	4.25	3.90	4.60	0.16	4.90	4.50	5.00	0.12	4.65	4.50	5.00	0.13	4.85	4.60	5.00	0.13
SOM (%)	0-20	2.21	1.98	2.98	0.31	2.61	1.99	3.41	0.29	1.47	0.97	1.99	0.27	1.52	0.75	2.48	0.51
	20-40	1.49	1.08	2.03	0.26	1.29	0.97	1.41	0.12	0.65	0.44	0.97	0.16	1.02	0.54	1.29	0.26
	40-60	0.94	0.77	1.36	0.13	0.92	0.75	0.97	0.07	0.54	0.34	0.54	0.06	0.60	0.24	1.07	0.20
CEC (cmol$_c$ dm^3)	0-20	11.17	7.73	15.11	2.54	5.50	4.43	7.44	0.57	6.29	4.32	7.46	0.88	6.04	4.16	9.63	1.40
	20-40	7.69	4.73	12.32	2.52	3.54	3.14	5.30	0.46	5.33	4.77	7.30	0.82	5.32	4.02	12.76	2.18
	40-60	5.63	4.18	14.14	2.22	2.97	2.55	3.47	0.28	6.56	3.86	8.22	0.93	5.47	4.27	7.96	1.19
S (mg dm^3)	0-20	17.02	6.57	34.36	7.70	9.70	7.03	13.08	1.79	4.94	3.32	7.82	0.98	5.50	3.67	12.61	2.32
	20-40	25.39	8.00	50.88	10.68	7.82	5.87	13.56	1.93	6.83	5.49	13.56	1.53	4.94	2.97	11.68	1.86
	40-60	34.14	6.87	59.65	14.18	13.40	6.25	26.57	5.34	9.27	5.12	20.59	3.94	6.06	1.95	11.23	2.45
Fe$_{DCB}$ (g kg^{-1})	0-20	42.26	5.52	56.52	16.15	34.35	13.94	57.03	8.37	12.54	6.10	27.20	5.81	11.86	4.65	15.24	2.63
	20-40	47.51	15.81	64.92	13.26	43.48	32.55	55.86	6.21	11.50	7.04	35.59	8.80	13.88	11.05	69.75	12.04
	40-60	45.38	16.54	76.75	15.04	47.16	30.48	57.95	5.28	16.33	8.37	40.35	9.82	19.69	11.96	27.25	3.74
Fe$_{ox}$ (g kg^{-1})	0-20	2.36	1.88	3.78	0.41	1.02	0.81	1.29	0.13	1.06	0.75	1.57	0.20	1.07	0.37	1.45	0.20
	20-40	2.18	1.73	3.91	0.47	0.70	0.51	1.46	0.25	0.87	0.55	1.38	0.18	0.92	0.50	1.52	0.20
	40-60	2.03	1.45	2.96	0.31	0.48	0.29	0.67	0.10	0.76	0.55	1.21	0.13	0.72	0.51	0.90	0.11
Al$_{DCB}$ (g kg^{-1})	0-20	6.96	4.39	8.80	1.19	4.68	2.01	6.51	0.87	1.12	0.65	1.77	0.38	1.29	0.97	2.17	0.36
	20-40	7.08	4.29	8.63	1.05	5.35	4.70	6.25	0.38	0.98	0.74	2.58	0.58	1.41	0.87	2.90	0.59
	40-60	7.43	4.25	10.05	1.31	5.82	4.03	7.10	0.60	1.44	0.85	3.07	0.62	2.26	1.40	3.37	0.50
Al$_{ox}$ (g kg^{-1})	0-20	1.74	1.39	2.32	0.23	0.73	0.48	0.96	0.13	0.43	0.35	0.58	0.06	0.52	0.27	0.76	0.12
	20-40	1.94	1.53	2.62	0.28	0.81	0.68	0.94	0.08	0.48	0.42	0.66	0.07	0.49	0.39	0.91	0.16
	40-60	1.91	1.62	2.79	0.29	0.75	0.68	0.85	0.03	0.58	0.47	0.63	0.05	0.59	0.49	0.90	0.13

Fe_{ox} / Fe_{DCB}	0-20	0.05	0.05	0.44	0.10	0.03	0.01	0.07	0.01	0.12	0.03	0.18	0.04	0.08	0.05	0.31	0.05
	20-40	0.05	0.04	0.25	0.05	0.01	0.01	0.03	0.01	0.08	0.02	0.13	0.03	0.06	0.02	0.07	0.01
	40-60	0.04	0.03	0.18	0.03	0.01	0.01	0.02	0.00	0.05	0.01	0.07	0.02	0.04	0.03	0.05	0.01
Al_{ox} / Al_{DCB}	0-20	0.25	0.21	0.47	0.06	0.17	0.11	0.24	0.03	0.45	0.22	0.71	0.13	0.35	0.25	0.78	0.10
	20-40	0.28	0.22	0.50	0.06	0.15	0.13	0.18	0.01	0.49	0.21	0.64	0.14	0.32	0.22	1.05	0.16
	40-60	0.28	0.17	0.48	0.06	0.12	0.11	0.19	0.02	0.40	0.20	0.55	0.10	0.29	0.19	0.35	0.04
MS	0-20	19.05	1.00	38.90	13.23	3.80	3.10	4.90	0.65	2.35	1.40	26.20	5.21	3.95	2.50	10.30	2.23
	20-40	18.90	1.20	36.40	11.86	6.80	3.20	8.50	1.44	4.20	1.60	38.20	7.58	6.00	3.20	10.10	2.13
	40-60	17.45	1.60	37.60	10.88	7.20	5.50	10.10	0.91	4.55	1.90	42.10	8.31	6.05	3.60	10.60	1.76
Clay (%)	0-20	55.00	41.00	70.00	7.88	43.50	39.00	45.00	2.06	18.50	15.00	28.00	3.75	18.00	12.00	33.00	4.00
	20-40	59.00	41.00	75.00	9.63	57.00	52.00	61.00	2.25	22.50	20.00	34.00	4.53	21.00	18.00	26.00	3.00
	40-60	61.50	44.00	77.00	10.25	62.00	57.00	67.00	1.91	26.50	22.00	37.00	3.16	25.00	20.00	36.00	3.63
Silt (%)	0-20	22.00	15.00	41.00	5.25	7.50	5.00	18.00	3.22	22.00	19.00	24.00	1.63	32.50	7.00	39.00	9.75
	20-40	20.50	12.00	41.00	5.66	6.00	3.00	10.00	1.25	22.00	19.00	26.00	2.13	33.00	11.00	40.00	8.75
	40-60	17.50	10.00	41.00	6.44	5.00	2.00	9.00	1.72	23.00	20.00	28.00	2.38	32.00	12.00	37.00	7.56
Sand (%)	0-20	18.50	15.00	36.00	6.41	47.50	43.00	53.00	3.38	59.00	51.00	63.00	3.63	48.50	44.00	81.00	7.75
	20-40	16.50	13.00	34.00	5.88	37.50	35.00	39.00	1.25	54.50	46.00	60.00	3.94	44.00	41.00	71.00	8.75
	40-60	16.00	13.00	34.00	5.81	33.00	29.00	34.00	1.25	50.50	43.00	58.00	4.25	42.00	39.00	64.00	6.75
Ca^{2+} ($cmol_c$ dm^3)	0-20	0.11	0.08	0.67	0.12	0.10	0.10	0.90	0.26	0.20	0.10	2.60	0.58	0.10	0.10	1.20	0.26
	20-40	0.10	0.06	0.26	0.04	0.10	0.10	0.20	0.02	0.15	0.10	1.60	0.38	0.10	0.10	0.90	0.17
	40-60	0.09	0.05	0.15	0.03	0.10	0.10	0.10	0.00	0.15	0.10	1.00	0.27	0.10	0.10	0.60	0.11
Mg^{2+} ($cmol_c$ dm^3)	0-20	0.16	0.10	0.46	0.07	0.20	0.20	0.50	0.11	0.10	0.10	1.30	0.26	0.50	0.20	0.70	0.13
	20-40	0.10	0.08	0.38	0.06	0.10	0.10	0.20	0.04	0.10	0.10	1.00	0.20	0.30	0.20	0.60	0.15
	40-60	0.10	0.05	0.26	0.04	0.10	0.10	0.20	0.02	0.10	0.10	0.80	0.15	0.35	0.10	0.70	0.21
Al^{3+} ($cmol_c$ dm^3)	0-20	1.45	0.90	2.70	0.60	0.95	0.50	1.10	0.18	2.20	0.90	3.90	0.60	1.90	0.60	2.60	0.43
	20-40	1.10	0.70	2.40	0.53	0.75	0.60	0.90	0.10	2.25	1.40	3.00	0.33	2.35	0.50	2.90	0.63
	40-60	0.95	0.50	2.40	0.49	0.55	0.40	0.90	0.13	2.75	2.40	3.40	0.27	2.60	1.10	3.20	0.48
K (mg dm^3)	0-20	38.37	28.33	50.62	5.29	37.00	32.00	52.00	4.00	39.00	24.00	114.00	17.13	79.00	70.00	114.00	9.63
	20-40	21.64	14.95	37.25	6.27	16.00	12.00	22.00	2.44	21.00	16.00	46.00	5.75	50.00	32.00	70.00	12.00
	40-60	11.61	8.26	37.25	7.67	11.00	8.00	20.00	2.50	17.00	14.00	24.00	2.25	31.00	22.00	66.00	11.00
P (mg dm^3)	0-20	2.11	1.36	2.32	0.24	2.45	2.30	2.60	0.15	3.37	1.71	4.48	0.62	2.91	1.71	3.84	0.50

	20-40	1.43	1.02	1.84	0.24	0.99	0.56	1.13	0.18	1.42	1.13	2.30	0.33	1.71	0.84	2.60	0.41
	40-60	0.86	0.61	0.97	0.09	0.56	0.28	0.84	0.21	1.13	0.84	1.42	0.13	1.13	0.56	1.71	0.29
Zn (mg dm^3)	0-20	0.50	0.13	0.77	0.15	0.43	0.30	0.64	0.07	0.61	0.46	6.70	1.32	1.56	1.16	5.34	0.86
	20-40	0.14	0.06	0.52	0.13	0.21	0.09	0.32	0.06	0.55	0.30	1.33	0.25	1.02	0.77	7.16	1.34
	40-60	0.10	0.07	0.48	0.08	0.12	0.01	0.24	0.07	0.55	0.25	0.90	0.17	1.12	0.32	4.97	0.87
Fe (mg dm^3)	0-20	146.78	123.08	257.83	34.14	163.34	110.66	298.41	42.41	200.74	13.56	248.75	68.29	192.78	27.81	391.11	79.31
	20-40	124.51	75.70	299.61	57.42	92.49	65.50	191.47	27.10	83.44	14.58	100.22	26.71	108.37	80.45	334.60	51.58
	40-60	104.54	27.56	174.40	29.13	36.51	28.65	89.59	15.86	34.68	15.74	57.72	9.22	55.88	29.58	96.27	19.62
Mn (mg dm^3)	0-20	1.51	0.10	3.77	1.17	4.95	2.32	35.29	10.53	20.34	3.60	111.30	29.87	22.48	4.71	46.52	10.77
	20-40	1.24	0.42	3.14	0.78	3.48	1.18	25.00	6.88	21.77	9.04	51.57	13.16	17.66	2.20	45.90	12.04
	40-60	2.09	0.60	5.04	1.22	2.27	0.92	26.84	5.83	13.25	6.46	30.90	7.72	14.80	1.64	27.41	8.54
Cu (mg dm^3)	0-20	0.38	0.22	1.15	0.31	1.98	1.33	2.40	0.30	1.23	0.59	1.72	0.24	1.54	0.67	2.35	0.48
	20-40	0.35	0.15	1.42	0.30	1.56	0.99	1.89	0.25	1.01	0.57	1.32	0.15	1.37	0.82	2.26	0.40
	40-60	0.19	0.03	1.26	0.37	1.29	0.82	1.58	0.21	1.02	0.54	1.26	0.18	1.28	0.84	1.50	0.17
B (mg dm^3)	0-20	0.01	0.01	0.01	0.00	0.04	0.02	0.08	0.02	0.17	0.15	0.21	0.01	0.13	0.10	0.38	0.07
	20-40	0.01	0.01	0.01	0.00	0.04	0.02	0.08	0.02	0.13	0.10	0.26	0.03	0.14	0.08	0.26	0.05
	40-60	0.01	0.01	0.01	0.00	0.03	0.02	0.04	0.01	0.14	0.10	0.21	0.03	0.10	0.08	0.24	0.05

Table S3. Descriptive statistics of soil properties for the soil samples collected in different sites of the Amazon region. Elements determined by portable X-ray fluorescence

		Site																			
Properties	Soil layer	ANO *(n = 8)*				AP *(n = 8)*				AR *(n = 8)*				MT *(n = 8)*				PA *(n = 8)*			
		Median	Minimum	Maximum	MAD	Median	Minimum	Maximum	MAD	Median	Minimum	Maximum	MAD	Median	Minimum	Maximum	MAD	Median	Minimum	Maximum	MAD
Al_2O_3 (g kg^{-1})	0-20	84.34	70.08	97.54	5.81	140.46	118.34	166.27	8.87	197.48	187.83	214.14	7.20	133.77	129.58	156.52	6.85	197.00	187.94	203.16	3.89
	20-40	91.37	84.98	107.39	7.76	159.50	151.06	174.03	6.06	206.68	195.85	217.48	5.40	157.95	142.21	167.84	6.23	206.10	195.47	215.67	5.82
	40-60	101.38	94.96	118.26	5.93	159.02	130.96	176.05	8.35	209.07	194.69	215.34	5.97	172.68	155.80	183.27	8.47	208.24	189.80	227.39	7.64
Fe_2O_3 (g kg^{-1})	0-20	34.51	21.49	45.36	5.05	26.67	23.05	31.08	1.80	38.95	30.83	42.71	3.70	40.26	29.31	51.30	6.22	32.46	23.26	41.31	5.08
	20-40	39.00	31.83	49.67	5.34	28.97	24.75	32.88	2.15	40.37	32.48	42.74	3.37	44.32	32.46	59.48	7.82	33.87	23.93	42.33	5.37
	40-60	41.86	34.27	69.68	7.46	30.79	24.97	32.95	1.78	40.71	32.76	43.32	3.23	42.22	34.42	59.99	8.08	37.06	24.73	42.55	5.82
SiO_2 (g kg^{-1})	0-20	432.67	366.88	483.66	23.53	330.94	297.97	353.96	15.08	228.94	220.78	257.58	12.84	287.08	264.77	326.96	14.80	276.33	261.75	283.42	5.52
	20-40	398.10	371.68	436.06	16.56	311.76	291.97	359.83	22.01	236.19	223.79	251.26	6.31	258.60	229.70	300.18	20.76	271.78	253.90	275.69	5.24
	40-60	402.55	345.14	429.26	21.01	298.41	280.88	314.31	9.66	239.02	216.12	248.24	9.72	269.24	222.96	296.55	21.13	269.17	237.28	284.71	10.37
MnO (g kg^{-1})	0-20	0.12	0.11	0.14	0.01	2.54	1.69	6.47	0.95	0.04	0.00	0.05	0.02	0.07	0.00	0.10	0.02	0.05	0.00	0.13	0.02
	20-40	0.12	0.10	0.13	0.01	2.15	1.66	4.11	0.58	0.03	0.00	0.06	0.02	0.07	0.03	0.11	0.02	0.03	0.00	0.05	0.01
	40-60	0.12	0.10	0.13	0.01	2.03	1.35	2.73	0.32	0.03	0.00	0.06	0.02	0.08	0.03	0.11	0.02	0.03	0.00	0.05	0.02
CaO (g kg^{-1})	0-20	0.02	0.02	0.21	0.04	1.04	0.44	2.59	0.65	0.02	0.02	0.02	0.00	0.09	0.02	0.82	0.16	0.18	0.02	0.53	0.15
	20-40	0.02	0.02	0.10	0.03	0.47	0.02	0.99	0.27	0.02	0.02	0.02	0.00	0.02	0.02	0.08	0.02	0.02	0.02	0.02	0.00
	40-60	0.02	0.02	0.10	0.02	0.33	0.02	0.76	0.22	0.02	0.02	0.02	0.00	0.02	0.02	0.07	0.01	0.02	0.02	0.02	0.00
TiO_2 (g kg^{-1})	0-20	5.26	4.40	6.54	0.66	3.09	2.29	3.75	0.33	6.77	6.15	7.45	0.38	3.43	3.28	3.94	0.20	5.80	5.50	6.00	0.15
	20-40	5.16	4.39	6.06	0.49	3.26	2.49	3.87	0.34	6.93	6.07	7.55	0.44	3.85	3.51	4.01	0.12	5.79	5.27	6.11	0.18
	40-60	5.18	4.49	5.92	0.47	3.51	2.46	3.76	0.37	6.93	5.93	7.53	0.41	4.08	3.44	4.50	0.25	5.89	5.48	6.24	0.23
P_2O_5 (g kg^{-1})	0-20	0.11	0.06	0.25	0.07	0.24	0.06	0.48	0.10	0.06	0.06	0.06	0.00	0.27	0.06	0.43	0.08	0.06	0.06	0.06	0.00
	20-40	0.06	0.06	0.06	0.00	0.06	0.06	0.21	0.07	0.06	0.06	0.06	0.00	0.13	0.06	0.27	0.10	0.06	0.06	0.06	0.00
	40-60	0.06	0.06	0.06	0.00	0.06	0.06	0.16	0.02	0.06	0.06	0.06	0.00	0.06	0.06	0.21	0.06	0.06	0.06	0.06	0.00
K_2O (g kg^{-1})	0-20	6.53	4.45	8.02	0.90	0.09	0.02	0.16	0.05	0.02	0.02	0.02	0.00	0.28	0.02	0.66	0.19	0.02	0.02	0.02	0.00
	20-40	6.86	6.02	8.96	0.99	0.02	0.02	0.02	0.00	0.02	0.02	0.02	0.00	0.25	0.02	0.73	0.22	0.02	0.02	0.02	0.00
	40-60	7.73	6.53	9.02	0.86	0.02	0.02	0.07	0.01	0.02	0.02	0.02	0.00	0.28	0.02	0.66	0.20	0.02	0.02	0.02	0.00
Cu (mg kg^{-1})	0-20	16.50	8.00	22.00	4.38	36.00	27.00	46.00	5.03	8.00	2.50	13.00	2.63	11.00	2.50	16.00	3.94	10.00	2.50	12.00	2.02
	20-40	16.50	10.00	26.00	3.66	35.00	24.00	49.00	7.63	8.50	2.50	12.00	1.81	11.50	8.00	23.00	3.03	7.00	2.50	9.00	2.48
	40-60	16.00	8.00	23.00	3.63	37.00	27.00	50.00	6.38	11.00	10.00	16.00	1.59	11.50	2.50	16.00	3.31	7.00	2.50	9.00	2.39

Zn (mg kg^{-1})	0-20	24.50	15.00	32.00	4.88	24.50	15.00	36.00	6.25	7.50	2.50	10.00	1.69	8.00	2.50	9.00	2.47	8.50	7.00	11.00	1.13
	20-40	25.00	17.00	38.00	5.56	24.00	21.00	33.00	4.25	6.00	6.00	8.00	0.63	7.00	2.50	13.00	2.17	8.00	6.00	10.00	1.00
	40-60	29.50	21.00	47.00	5.63	24.50	19.00	37.00	4.00	8.00	6.00	11.00	1.00	8.00	5.00	11.00	1.22	9.00	7.00	10.00	1.13
Ni (mg kg^{-1})	0-20	14.00	2.50	21.00	4.81	23.50	18.00	43.00	6.50	2.50	2.50	13.00	3.38	2.50	2.50	12.00	3.83	2.50	2.50	11.00	3.52
	20-40	15.50	2.50	19.00	4.09	31.00	25.00	37.00	3.06	2.50	2.50	11.00	1.86	2.50	2.50	14.00	4.30	10.50	2.50	15.00	4.55
	40-60	16.00	10.00	19.00	2.63	30.50	23.00	43.00	5.00	2.50	2.50	10.00	3.36	6.75	2.50	15.00	5.00	9.50	2.50	13.00	3.89
Pb (mg kg^{-1})	0-20	12.00	9.00	18.00	2.50	15.50	10.00	17.00	1.72	8.00	6.00	10.00	1.00	5.50	2.50	7.00	1.25	6.00	2.50	8.00	1.05
	20-40	12.50	9.00	21.00	3.75	15.50	11.00	18.00	1.63	8.00	5.00	10.00	0.88	6.50	5.00	8.00	1.00	7.00	5.00	9.00	0.75
	40-60	14.50	10.00	18.00	2.25	14.50	11.00	20.00	2.25	7.00	6.00	11.00	1.50	6.00	5.00	9.00	0.88	7.00	6.00	8.00	0.50
Cr (mg kg^{-1})	0-20	42.00	5.00	50.00	14.81	49.00	34.00	66.00	11.25	43.00	5.00	53.00	10.38	71.50	45.00	92.00	12.22	38.50	5.00	46.00	7.63
	20-40	43.00	5.00	58.00	11.13	42.50	31.00	83.00	11.31	38.50	5.00	46.00	17.72	90.50	47.00	126.00	16.22	42.50	31.00	51.00	4.72
	40-60	43.50	35.00	65.00	6.81	44.50	36.00	60.00	7.88	40.00	5.00	44.00	8.63	86.50	71.00	101.00	10.13	34.00	5.00	66.00	14.91
Co (mg kg^{-1})	0-20	61.00	2.50	82.00	25.41	2.50	2.50	2.50	0.00	29.25	2.50	69.00	29.63	2.50	2.50	2.50	0.00	2.50	2.50	2.50	0.00
	20-40	54.00	2.50	101.00	31.55	2.50	2.50	2.50	0.00	46.00	2.50	63.00	24.14	2.50	2.50	2.50	0.00	2.50	2.50	2.50	0.00
	40-60	67.00	2.50	93.00	27.88	2.50	2.50	2.50	0.00	53.50	2.50	98.00	15.31	2.50	2.50	2.50	0.00	2.50	2.50	2.50	0.00
As (mg kg^{-1})	0-20	6.00	2.50	8.00	1.03	2.50	2.50	5.00	0.55	9.00	8.00	10.00	0.56	2.50	2.50	5.00	0.55	3.75	2.50	6.00	1.38
	20-40	7.00	5.00	8.00	0.91	2.50	2.50	5.00	0.55	9.50	9.00	11.00	0.63	5.00	2.50	6.00	1.27	3.75	2.50	6.00	1.50
	40-60	7.00	5.00	12.00	1.44	2.50	2.50	2.50	0.00	10.00	8.00	11.00	0.69	3.75	2.50	6.00	1.50	5.00	2.50	8.00	1.25
Ba (mg kg^{-1})	0-20	2.50	2.50	574.00	125.02	66.00	43.00	109.00	17.16	2.50	2.50	2.50	0.00	2.50	2.50	2.50	0.00	2.50	2.50	40.00	8.20
	20-40	2.50	2.50	446.00	164.81	53.00	2.50	84.00	15.14	2.50	2.50	2.50	0.00	2.50	2.50	2.50	0.00	2.50	2.50	42.00	8.64
	40-60	2.50	2.50	2.50	0.00	42.00	2.50	78.00	14.53	2.50	2.50	2.50	0.00	2.50	2.50	2.50	0.00	2.50	2.50	51.00	17.25
Sr (mg kg^{-1})	0-20	43.50	29.00	61.00	10.13	20.00	13.00	33.00	4.69	12.50	12.00	15.00	0.75	8.50	5.00	11.00	1.38	13.00	9.00	19.00	2.47
	20-40	43.50	34.00	68.00	8.88	19.00	12.00	23.00	2.63	13.00	11.00	14.00	0.81	9.50	5.00	11.00	1.63	10.50	8.00	12.00	0.88
	40-60	47.50	35.00	67.00	9.38	17.50	15.00	22.00	2.16	13.00	12.00	14.00	0.44	9.00	6.00	12.00	1.50	10.00	9.00	12.00	0.97
V (mg kg^{-1})	0-20	109.00	12.50	126.00	48.14	12.50	12.50	101.00	34.45	140.50	103.00	185.00	18.50	147.00	98.00	198.00	23.63	101.00	12.50	129.00	25.56
	20-40	106.00	12.50	129.00	37.19	12.50	12.50	107.00	33.19	156.50	90.00	186.00	22.19	160.50	135.00	204.00	15.50	101.50	12.50	136.00	24.73
	40-60	102.00	12.50	200.00	44.19	74.50	12.50	110.00	33.33	149.50	96.00	195.00	26.63	149.00	133.00	186.00	14.94	111.00	12.50	141.00	29.56
Zr (mg kg^{-1})	0-20	607.50	523.00	684.00	37.38	218.50	178.00	243.00	20.13	1657.00	1549.00	2128.00	181.38	298.50	272.00	396.00	36.66	676.50	577.00	712.00	42.44
	20-40	573.50	506.00	642.00	44.50	232.00	179.00	282.00	25.63	1636.00	1433.00	1812.00	106.53	345.00	310.00	461.00	31.31	658.50	622.00	744.00	37.25
	40-60	567.00	452.00	632.00	44.34	262.00	202.00	350.00	35.38	1644.50	1400.00	1787.00	135.25	360.50	313.00	392.00	21.28	682.50	637.00	729.00	30.25
Nb (mg kg^{-1})	0-20	24.50	23.00	39.00	5.03	8.00	5.00	9.00	0.97	47.00	37.00	53.00	3.63	13.50	13.00	15.00	0.88	27.00	27.00	28.00	0.47

20-40	27.50	22.00	36.00	4.13	8.50	6.00	11.00	1.25	48.50	43.00	53.00	2.50	16.00	13.00	18.00	1.50	31.50	30.00	33.00	1.00
40-60	28.00	22.00	33.00	3.50	9.00	8.00	10.00	0.50	47.00	42.00	51.00	3.00	16.00	13.00	17.00	1.13	33.00	31.00	35.00	1.50

MAD - mean absolute deviation;

Elemental contents lower than the limit of detection were considered being LOD/2.

The sites are identified as: ANO - Anori, state of Amazonas; AP - Laranjal do Jari, state of Amapá; AR - Aruanã farm in Itacoatiara, state of Amazonas; MT - Itaúba, state of Mato Grosso; PA - Santarém, state of Pará; RO - Porto Velho, state of Rondônia; RR - Caracaraí, state of Roraima; SM - Sena Madureira, state of Acre and XP - Xapuri, state of Acre;

Table S3. (Continued).

		Site															
Properties	Soil layer	RO *(n = 8)*				RR *(n = 8)*				SM *(n = 8)*				XP *(n = 8)*			
		Median	Minimum	Maximum	MAD	Median	Minimum	Maximum	MAD	Median	Minimum	Maximum	MAD	Median	Minimum	Maximum	MAD
Al_2O_3 (g kg^{-1})	0-20	139.74	106.94	160.52	14.73	139.39	133.65	141.99	2.32	96.67	77.85	138.32	15.88	91.53	73.89	168.96	20.75
	20-40	148.91	113.98	166.18	13.16	154.96	133.07	187.07	9.19	118.90	100.07	158.75	15.94	109.07	96.02	193.92	24.73
	40-60	155.40	118.39	166.57	12.39	159.32	151.46	162.93	2.60	141.92	112.21	178.28	19.52	135.13	96.31	196.95	22.58
Fe_2O_3 (g kg^{-1})	0-20	109.20	37.86	141.83	28.10	78.99	72.52	91.58	6.23	25.62	18.27	67.23	14.98	24.48	21.02	43.22	4.85
	20-40	113.53	38.90	159.99	29.37	93.20	83.20	102.09	5.08	33.27	22.95	83.99	18.21	30.91	26.60	51.18	5.41
	40-60	108.01	39.86	147.97	26.40	99.42	89.62	130.61	8.63	41.81	26.36	95.75	21.03	36.08	25.73	52.38	8.52
SiO_2 (g kg^{-1})	0-20	192.28	173.78	316.16	40.09	232.72	218.11	261.38	10.69	477.94	434.15	592.35	62.88	595.89	407.68	629.94	64.87
	20-40	187.19	173.76	311.74	38.05	221.17	202.41	238.33	6.36	442.48	396.78	583.35	65.70	554.43	388.29	600.49	58.17
	40-60	188.92	168.02	291.70	38.35	208.82	198.71	223.29	5.45	424.24	382.16	551.13	60.60	540.01	399.23	570.69	49.29
MnO (g kg^{-1})	0-20	0.16	0.07	0.26	0.04	0.39	0.37	0.61	0.08	0.23	0.09	1.35	0.33	0.15	0.08	0.60	0.12
	20-40	0.16	0.06	0.25	0.04	0.39	0.33	0.49	0.03	0.34	0.16	1.01	0.20	0.16	0.08	0.42	0.08
	40-60	0.17	0.05	0.23	0.04	0.40	0.33	0.62	0.06	0.38	0.14	0.79	0.16	0.17	0.05	0.29	0.05
CaO (g kg^{-1})	0-20	0.02	0.02	0.12	0.02	0.02	0.02	0.79	0.20	0.13	0.02	1.15	0.24	0.09	0.02	3.74	0.80
	20-40	0.02	0.02	0.02	0.00	0.02	0.02	0.45	0.09	0.02	0.02	0.37	0.08	0.02	0.02	0.40	0.08
	40-60	0.02	0.02	0.02	0.00	0.02	0.02	0.02	0.00	0.02	0.02	0.10	0.02	0.02	0.02	0.20	0.04
TiO_2 (g kg^{-1})	0-20	5.78	5.25	6.59	0.31	6.26	5.79	6.67	0.25	4.04	3.33	4.46	0.28	3.65	3.41	4.39	0.29
	20-40	5.68	5.35	6.80	0.39	5.48	5.03	6.00	0.23	4.32	2.95	4.69	0.32	3.93	3.49	4.57	0.34
	40-60	5.90	5.30	6.93	0.31	5.17	4.38	5.50	0.27	4.07	2.96	4.51	0.32	4.05	3.35	4.74	0.39
P_2O_5 (g kg^{-1})	0-20	0.26	0.19	0.62	0.13	0.23	0.17	0.49	0.07	0.31	0.06	0.68	0.21	0.06	0.06	0.06	0.00
	20-40	0.20	0.06	0.59	0.10	0.06	0.06	0.35	0.08	0.06	0.06	0.35	0.13	0.06	0.06	0.06	0.00

	40-60	0.10	0.06	0.48	0.13	0.06	0.06	0.19	0.05	0.06	0.06	0.35	0.12	0.06	0.06	0.06	0.00
K_2O (g kg^{-1})	0-20	0.30	0.02	4.93	1.11	0.02	0.02	0.02	0.00	6.29	5.80	11.23	1.27	6.81	3.27	7.95	1.40
	20-40	0.27	0.02	5.02	1.15	0.02	0.02	0.02	0.00	7.49	6.60	12.15	1.26	8.00	3.64	9.35	1.78
	40-60	0.22	0.02	5.10	1.18	0.02	0.02	0.02	0.00	8.70	7.46	13.12	1.13	8.35	3.54	10.70	1.97
Cu (mg kg^{-1})	0-20	32.50	12.00	62.00	13.38	43.50	37.00	56.00	7.03	10.45	7.40	19.20	2.91	13.60	9.30	18.60	2.38
	20-40	35.50	13.00	63.00	13.00	48.00	36.00	59.00	5.88	11.30	8.00	19.00	3.11	15.40	9.50	21.80	3.26
	40-60	28.00	20.00	69.00	13.75	50.00	41.00	61.00	5.66	12.50	9.70	15.20	1.84	14.95	11.30	19.00	1.81
Zn (mg kg^{-1})	0-20	29.50	18.00	53.00	6.97	41.00	36.00	46.00	2.63	16.65	13.10	49.50	7.94	16.80	14.40	21.30	2.24
	20-40	30.00	22.00	50.00	6.13	43.00	40.00	48.00	2.38	19.40	17.00	40.50	6.09	21.00	12.80	26.80	3.21
	40-60	29.00	25.00	43.00	4.34	45.00	42.00	51.00	3.00	23.25	17.90	41.80	5.90	19.80	14.00	29.40	4.19
Ni (mg kg^{-1})	0-20	8.25	2.50	20.00	7.00	33.00	24.00	41.00	4.25	9.05	2.50	20.70	5.80	10.50	2.50	18.70	5.71
	20-40	2.50	2.50	29.00	9.61	41.00	30.00	46.00	3.88	6.75	2.50	20.90	6.99	15.55	2.50	19.00	3.50
	40-60	8.75	2.50	25.00	8.63	42.00	34.00	49.00	3.75	12.45	2.50	32.70	6.12	15.05	10.30	21.00	2.40
Pb (mg kg^{-1})	0-20	7.50	2.50	15.00	3.38	5.50	5.00	9.00	1.16	12.35	10.70	21.00	2.54	7.70	5.50	10.50	1.53
	20-40	10.00	5.00	21.00	3.50	6.50	5.00	12.00	1.50	17.75	13.90	25.30	2.91	10.15	5.70	11.40	1.41
	40-60	9.00	2.50	19.00	3.53	7.00	6.00	17.00	2.31	17.75	16.00	24.50	3.19	10.80	7.40	13.40	1.60
Cr (mg kg^{-1})	0-20	53.00	5.00	120.00	30.50	56.00	39.00	129.00	22.25	36.50	5.00	45.90	12.77	39.35	5.00	72.70	19.41
	20-40	49.50	5.00	96.00	31.75	100.00	30.00	221.00	53.50	45.50	33.00	65.30	10.02	49.85	5.00	64.80	12.37
	40-60	58.50	5.00	97.00	30.50	59.50	5.00	242.00	55.69	44.45	28.90	82.10	13.48	43.55	5.00	60.40	17.22
Co (mg kg^{-1})	0-20	112.00	55.00	150.00	28.00	2.50	2.50	2.50	0.00	2.50	2.50	2.50	0.00	2.50	2.50	2.50	0.00
	20-40	154.50	2.50	215.00	49.05	2.50	2.50	2.50	0.00	2.50	2.50	2.50	0.00	2.50	2.50	39.00	7.98
	40-60	130.00	2.50	157.00	43.05	2.50	2.50	112.00	33.19	2.50	2.50	2.50	0.00	2.50	2.50	60.40	12.67
As (mg kg^{-1})	0-20	17.50	9.00	47.00	6.94	2.50	2.50	2.50	0.00	17.25	13.00	28.70	3.32	7.30	5.40	14.80	1.77
	20-40	18.50	10.00	42.00	6.28	2.50	2.50	2.50	0.00	23.25	19.00	37.90	4.32	9.00	7.00	17.10	1.87
	40-60	19.00	10.00	45.00	6.63	2.50	2.50	5.00	0.55	28.35	22.20	44.10	4.88	10.20	7.80	17.00	3.13
Ba (mg kg^{-1})	0-20	58.50	2.50	127.00	23.81	2.50	2.50	54.00	11.27	201.75	2.50	979.40	351.05	666.10	2.50	1440.10	413.65
	20-40	52.00	2.50	132.00	29.94	2.50	2.50	78.00	24.45	2.50	2.50	557.00	244.53	501.60	2.50	918.00	223.84
	40-60	29.25	2.50	144.00	45.00	21.75	2.50	76.00	27.25	2.50	2.50	529.80	224.42	2.50	2.50	511.30	216.53
Sr (mg kg^{-1})	0-20	22.50	12.00	54.00	9.38	20.00	16.00	40.00	5.38	20.50	17.90	38.50	5.18	28.95	21.20	36.80	4.36
	20-40	24.00	13.00	54.00	9.78	19.50	17.00	27.00	3.41	24.50	20.80	42.30	5.33	35.40	17.30	39.40	6.92
	40-60	26.00	14.00	56.00	9.56	21.00	14.00	32.00	4.75	28.70	20.60	49.90	8.06	38.45	17.00	42.30	8.28

V (mg kg^{-1})	0-20	107.00	12.50	211.00	48.39	206.50	169.00	243.00	17.09	12.50	12.50	12.50	0.00	12.50	12.50	12.50	0.00
	20-40	119.00	12.50	215.00	34.70	212.00	173.00	249.00	23.38	12.50	12.50	95.90	30.90	12.50	12.50	94.40	17.92
	40-60	111.00	12.50	227.00	67.31	223.00	162.00	245.00	19.75	47.15	12.50	102.00	37.94	12.50	12.50	114.00	40.77
Zr (mg kg^{-1})	0-20	1167.00	654.00	2287.00	360.81	806.50	684.00	965.00	66.88	375.35	310.50	436.00	31.54	487.20	420.70	642.50	58.44
	20-40	1128.50	638.00	2461.00	406.63	760.50	690.00	854.00	45.16	412.50	286.10	468.30	45.75	551.10	453.90	629.60	42.14
	40-60	1178.00	659.00	2705.00	455.56	699.00	594.00	711.00	42.84	371.55	287.00	436.90	31.01	538.55	442.90	745.50	71.15
Nb (mg kg^{-1})	0-20	48.00	29.00	98.00	18.94	14.50	13.00	18.00	1.25	15.20	13.00	17.90	1.28	15.05	11.60	16.90	1.50
	20-40	48.50	29.00	97.00	19.50	14.50	12.00	18.00	1.75	17.30	14.40	19.00	1.03	16.60	11.30	18.10	1.84
	40-60	47.50	33.00	101.00	19.44	14.00	11.00	16.00	0.72	16.70	12.30	19.00	1.66	16.35	11.70	18.40	2.18

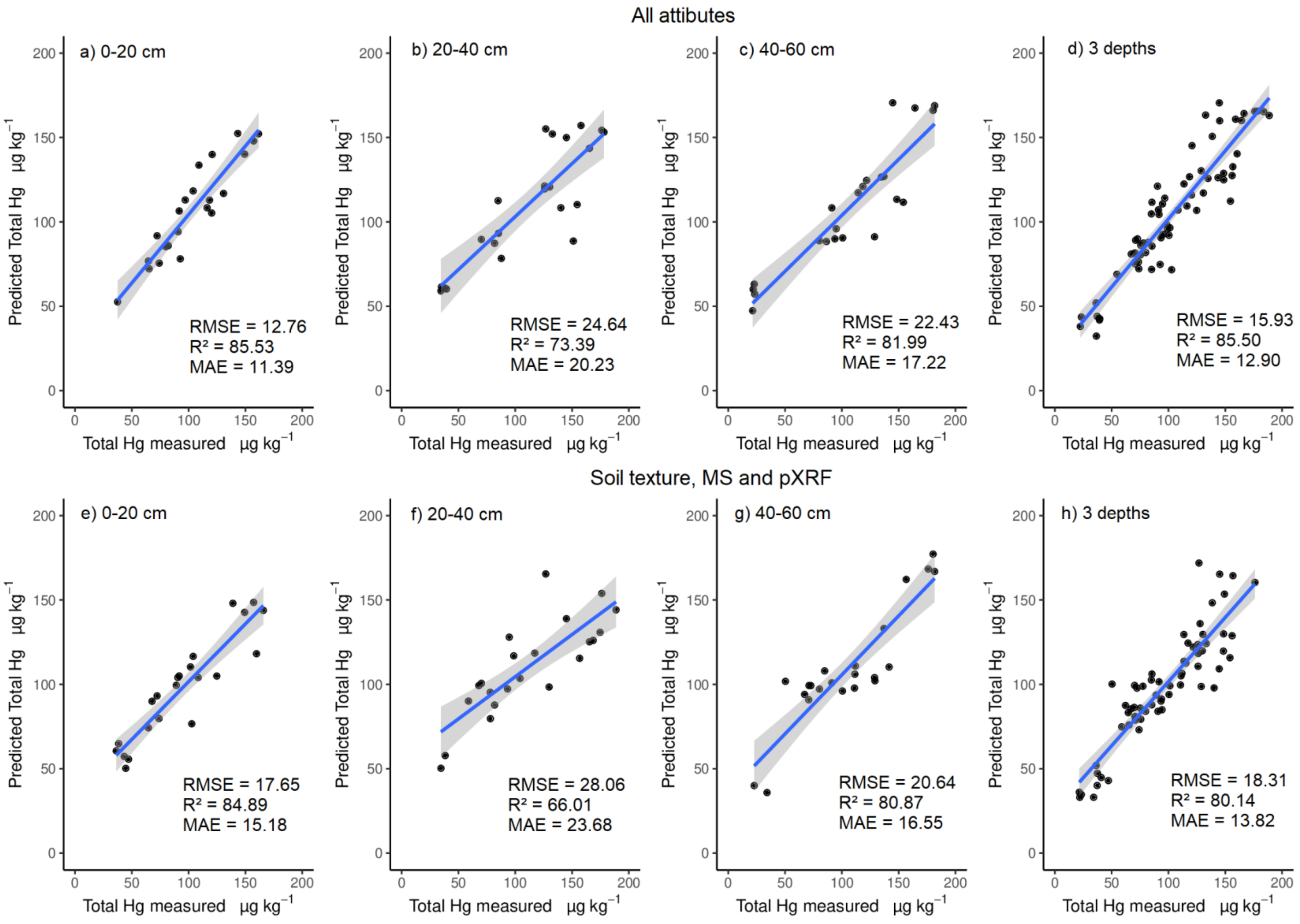

Fig. S5. Plots showing measured soil total Hg vs. soil all physicochemical attributes, soil texture, magnetic susceptibility (MS), portable X-ray fluorescence spectrometry (pXRF) via Random Forest algorithm using 0-20, 20-40 and 40-60 depths data combined obtained from soil samples collected in different sites of the Amazon region. The line is fitted using the geom_smooth command in ggplot2 within R

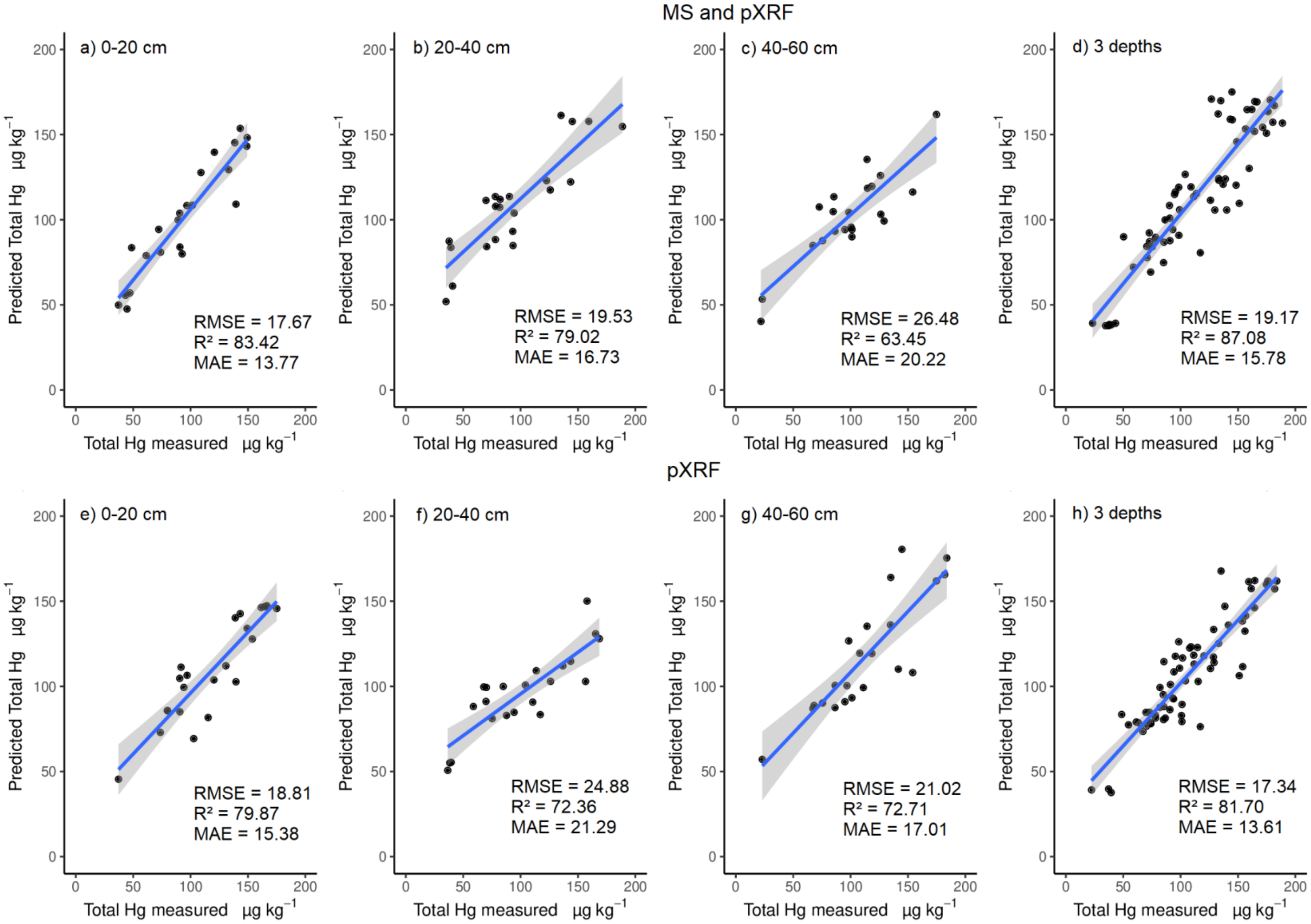

Fig. S6. Plots showing measured soil total Hg vs. magnetic susceptibility (MS) and portable X-ray fluorescence spectrometry (pXRF) via Random Forest algorithm using 0-20, 20-40 and 40-60 depths data combined obtained from soil samples collected in different sites of the Amazon region. The line is fitted using the geom_smooth command in ggplot2 within R

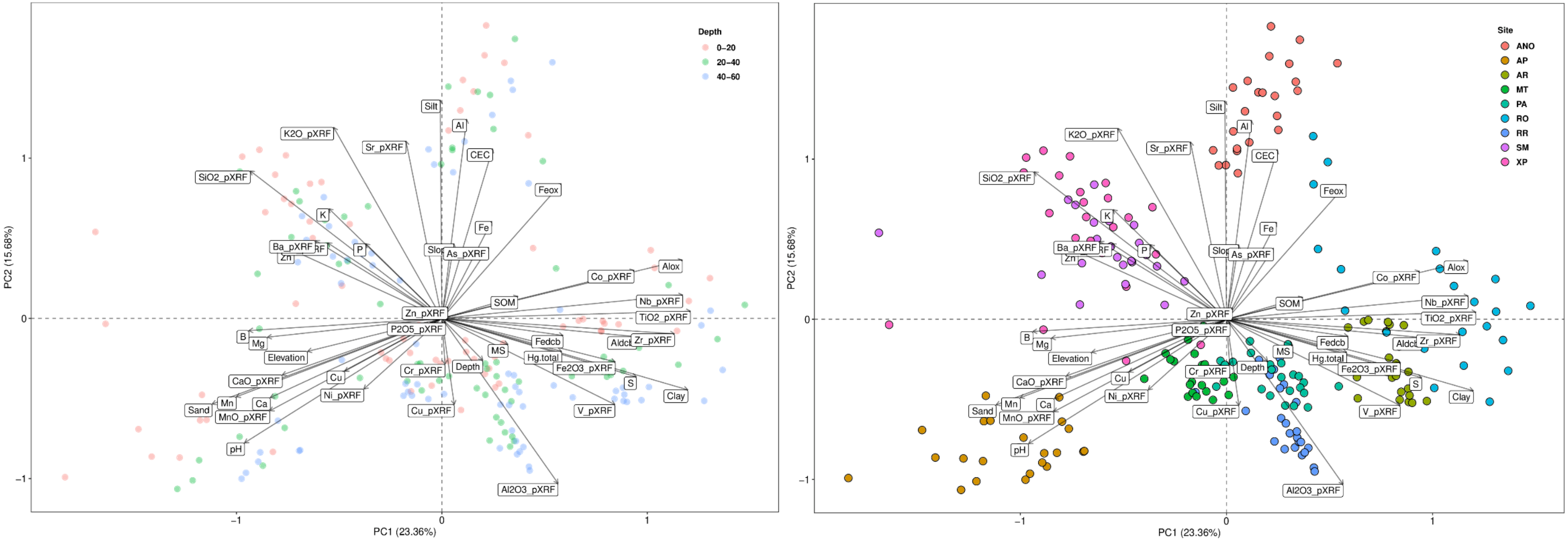

Fig. S7. Principal component analysis between total Hg, elements by portable X-ray fluorescence data, physicochemical properties, elevation and slope for the soil samples collected in the depths 0-20, 20-40 and 40-60 cm in Amazon region. The terms are identified as: ANO - Anori, state of Amazonas; AP - Laranjal do Jari, state of Amapá; AR - Aruanã farm in Itacoatiara, state of Amazonas; MT - Itaúba, state of Mato Grosso; PA - Santarém, state of Pará; RO - Porto Velho, state of Rondônia; RR - Caracaraí, state of Roraima; SM - Sena Madureira, state of Acre and XP - Xapuri, state of Acre; SSA - Specific Surface Área; MS - Magnetic Susceptibility; SOM - Soil Organic Matter; CEC - cation exchange capacity; OX - extracted with ammonium acid oxalate solution and DCB - extracted with sodium dithionite-citrate-bicarbonate solution

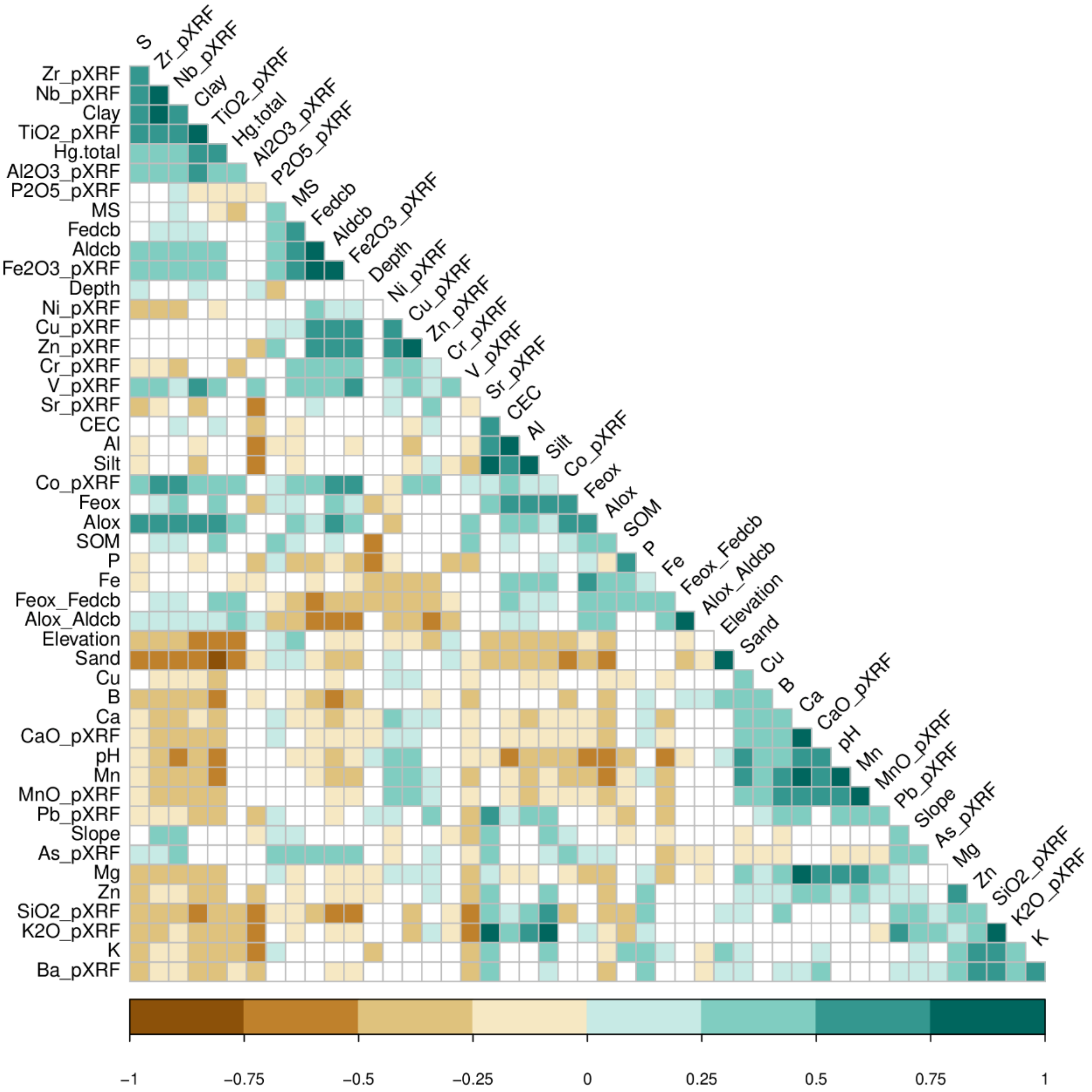

Fig. S8. Pearson's correlation matrix for the total Hg, elements by portable X-ray fluorescence (pXRF), physicochemical properties, elevation and slope for the soil samples collected in the depths 0-20, 20-40 and 40-60 cm in Amazon region. The terms are identified as: MS - Magnetic Susceptibility; SOM - Soil Organic Matter; CEC - cation exchange capacity; OX - extracted with ammonium acid oxalate solution and DCB - extracted with sodium dithionite-citrate-bicarbonate solution. Color indicate statistical significance levels ($P < 0.05$), with green being positively correlated and brown negatively correlated

References

Alvarez, V.H.V., Novais, R.F., Dias, L.E., Oliveira, J.A., 2000. Determinação e uso do fósforo remanescente. Boletim Informativo da Sociedade Brasileira de Ciência do Solo. 25, 27-32.

Mehlich, A., 1953. Determination of P, Ca, Mg, K, Na, and NH_4. North Carolina Soil Test Division. Raleigh, North Carolina.

Tedesco, M.J., Gianello, C., Bissani, C.A., Bohnen, H., Volkweiss, S.J., 1995. Análise de solo, plantas e outros materiais. Boletim Técnico de Solos, 5. Ed. 2. Porto Alegre: UFRGS. 174p.

ARTIGO 2 - Physiological effects of mercury-contaminated Oxisols on common bean and oat

F. R. D. Lima[a], A. P. Barbosa[b], I. C. F. Vasques[c], J. R. Oliveira[a], A. O. Silva[a], G. C. Martins[d], M. M. Engelhardt[a], P. Pereira[a], R. H. C. L. Reis[a], L. R. G. Guilherme[a] & J. J. G. S. M. Marques[a]*

[a] Soil Science Department, Federal University of Lavras, Lavras 37200-900, Minas Gerais State, Brazil

[b] Center for Coastal, Limnological and Marine Studies, Federal University of Rio Grande do Sul, Imbé 95625-000, Rio Grande do Sul State, Brazil

[c] Soils Department, Federal University of Viçosa, Viçosa 36570-000, Minas Gerais State, Brazil

[d] Vale Institute of Technology, Belém 66055-090, Pará State, Brazil

*Corresponding author email: jmarques@ufla.br

Published at Environmental Science and Pollution Research (ISSN: 1614-7499)
https://doi.org/10.1007/s11356-020-11286-x

Abstract

The heavy metal mercury (Hg) is one of the most complex and toxic pollutants. When present in soils, it may impair plant growth, but the intensity of damage depends on physical-chemical properties of the soil such as pH, clay, and organic matter content, which in turn affects Hg sorption and bioavailability. Understanding Hg potential damage to staple food crops is of paramount relevance. Here we evaluated the physiological effects of Hg in *Phaseolus vulgaris* (common bean) and *Avena sativa* (oat) cultivated in two Oxisols with contrasting properties: Rhodic Acudox (RA) and Typic Hapludox (TH). We performed four independent experiments (one per species/soil combination) that lasted 30 days each. Treatments were composed by $HgCl_2$ concentrations in soils (0 to 80 mg kg^{-1} Hg). At the end of the experiment, we determined the impact of Hg on photosynthesis, nutritional status, and oxidative stress. Cultivation in TH contaminated with Hg resulted in oxidative stress in common bean and decreased photosynthesis/P accumulation in oat. No deleterious effects on physiological variables were detected in both species when cultivated in the RA soil. In general, we conclude that the lower Hg sorption in the TH soil resulted in toxicity-like responses, while acclimation-like responses were observed in plants cultivated in RA, reinforcing soil physical-chemical properties as key features driving Hg toxicity in Oxisols.

Keywords: catalase; gas exchange; malonaldehyde; proline; superoxide dismutase; tropical soils.

Highlights

- Common bean and oat physiology is affected by the presence of Hg in Oxisols;
- Cultivation in RA + Hg resulted in *acclimation-like* responses;
- Cultivation in TH + Hg promoted *toxicity-like* responses in both species;
- TH + Hg: oxidative stress in common bean and photosynthesis decrease in oat.

Introduction

Mercury (Hg) pollution poses global risks to human health and the environment. However, there are some gaps in knowledge regarding Hg exposure and its effects to living organisms (Budnik and Casteleyn 2019). In tropical soils, and specifically in mostly Oxisols Hg sorption is affected by soil attributes such as pH and clay content (Soares et al. 2015). Soil organic matter might be positively correlated with Hg content in the soil (He et al. 2019), yet studies have reported low or no correlation between these variables. This could be explained in part by the presence/absence of sulfhydryl groups (-SH) in the organic matter, which is important for establishing strong bindings with Hg (Ravichandran 2004; He et al. 2019). It is known that the natural levels of Hg in tropical soils are very heterogeneous, e.g., in the Brazilian Cerrado soil Hg levels are reported between 15 and 182 μg kg^{-1} (Carvalho et al. 2019), whereas in southern Amazonia Lacerda et al. (2004) identified Hg levels ranging from 15 to 248 μg kg^{-1} in forest soils and from 10 to 74 μg kg^{-1}, in pasture soils. According to Lima et al. (2019a), in Oxisols, the critical concentration of Hg that can be harmful to plants and soil biological attributes, such as microbial biomass carbon, is 36 μg kg^{-1}.

Exposure of plants to Hg can promote oxidative stress, resulting in damage to biomolecules (membrane lipids, nucleic acids, and proteins/enzymes, the main targets), reduced absorption of nutrients and disruption of photosynthesis and chlorophyll biosynthesis (Zhang et al. 2017; Mahbub et al. 2018). The level of damage depends on the intrinsic sensitivity of the species, the concentration/availability of Hg in the soil, and the duration of exposure. The increase in oxidative stress is attributed to the increased generation of reactive oxygen species (ROS), which are reactive forms of normal by-products of aerobic metabolism produced in different cell compartments, such as chloroplasts, mitochondria, peroxisomes, and plasma membrane, being unable to cause damage (Foyer and Noctor 2003; Das and Roychoudhury 2014). However, in the presence of stressors such as Hg, the increased production of ROS can cause extensive damage to plant metabolism (Miller et al. 2010; Das et al. 2015; Zhang et al. 2017; Dutra et al. 2018; Mishra and Sangwan 2019), leading to toxicity responses. The defense mechanism of plants against ROS consists of enzymatic and non-enzymatic components and among the enzymatic ones we can mention superoxide dismutase (SOD), catalase (CAT), and ascorbate peroxidase (APX). The non-enzymatic components involve proline, ascorbic acid, and reduced glutathione, among other compounds that scavenge ROS (Das and Roychoudhury 2014). When antioxidant mechanisms work efficiently, plants may be able to tolerate the stressor, presenting acclimation responses. However, most studies were conducted in hydroponic systems (Cargnelutti et al. 2006; Sahu et al. 2012; Malar et al. 2015; Manikandan et al. 2015; Zhang et al. 2017; Pirzadah et al. 2018; Safari et al. 2019). Besides, no study has been conducted under tropical conditions. Therefore, to the best of our knowledge, this is one of the few studies on this subject carried out in tropical soils.

The phytotoxic potential of heavy metals is accessed by standard environmental protocols (International Organization for Standardization – ISO 11.269-2 and Organization for Economic Co-operation and Development – OECD-208) that use several crops with high productive potential, such as common bean and oat (ISO 2012; OECD 2006). Common bean is an important staple food worldwide, nutritionally rich, with low cost and consumed in several low-income countries (Porch et al. 2013; Rezende et al. 2018). Oat is used mainly as forage, but human consumption as grain (Hareland and Manthey 2003) has increased in recent years, attributed to better knowledge of their health benefits.

Studies based on ISO 11.269-2 (ISO 2012) and OECD-208 (OECD 2006) protocols are relevant for improving our knowledge concerning the environmental risk of a particular pollutant, yet these protocols are based mainly on plant growth variables. Although plant growth endpoints are of upmost relevance for assessing ecological risks of selected pollutants (Martins et al. 2019, 2020), evaluating and understanding the extent of physiological damage in a deeper manner is also very important to access the potential toxicity of a pollutant in crops highly consumed by the human population, since it helps to prevent losses in production due to soil contamination.

For this purpose, we hypothesized that high concentrations of Hg in tropical soils cause toxic effects to the physiological system of common bean and oat. The objective of the study was to evaluate the effects of increasing concentrations of Hg in two tropical soils (Oxisols) on the antioxidant and photosynthetic systems, as well as on the nutritional status of common bean and oat. With that, we hope not only to contribute for better food safety but also to improve risk management of contaminated areas in tropical environments.

Materials and methods

Experimental design and plant cultivation

Soil surface layers (0-0.2 m) of two Oxisols representative for agricultural use in a tropical environment (Gardi et al. 2015) were used in the experiments: a Typic Hapludox (TH) (21º13’30” S and 44º57’38” W) and a Rhodic Acrudox (RA) (21º 09’ 18” S and 45º 05’ 55” W). These soils are classified as Latosols (Santos et al. 2018) and equivalent to Oxisols in USDA (U.S. Department of Agriculture) Soil Taxonomy (Soil Survey Staff 2014). The physical-chemical soil characterization was performed according to Teixeira et al. (2017) on air-dried fine earth fraction (< 2.0 mm), the results are shown in Lima et al. (2019a, b).

Four independent experiments were carried out in a greenhouse to evaluate the ecotoxicological effects of Hg on two important crop species listed as sensitive in ISO 11.269-2 (2012): *Avena sativa* L. cv. São Carlos, (known as “oat”, Poaceae family) and *Phaseolus vulgaris* L. cv. Madrepérola (known as “common bean”, Fabaceae family) in the two abovementioned soils. Considering that, here on we refer to four independent experiments: 1) common bean TH; 2) common bean RA; 3) oat TH; 4) oat RA. Thus, each experiment had seven treatments (Hg concentration) and four biological replicates.

For all experiments, the soil samples were fertilized according to recommendations of Alvarez and Ribeiro (1999) and Malavolta (1981) for plant experiments in pots, and pH was adjusted to ~6.0. We used pots of 500 cm^3 of soil contaminated with the following $HgCl_2$ concentrations: 0, 2.5, 5.0, 10.0, 20.0, 40.0, and 80.0 mg kg^{-1} soil. The experiments were performed in a randomized complete block design, with four biological replicates, followed the regulation ISO 11.269-2 (ISO 2012). Each replicate was composed by one pot and one individual plant. Irrigation considered 70% of field capacity and the experiments lasted 30 days.

Quantification of mercury and nutrients in plant tissue

After the experimental period, Hg concentration in the soil and in the shoot dry matter (SD) of each crop species was determined. The methodology and the results for these analyzes are presented in Lima et al. (2019a, b) and were partially used here for the correlation analyses described below.

The nutrient content of SD was determined according to Malavolta et al. (1997). The digestion of plant material was carried out using 0.5 g of SD, which was dried (70 °C) and ground. Then 4 mL of nitric acid and 2 mL of perchloric acid was added and the suspension was taken to digester blocks (Tecnal®) at 200 °C. An atomic absorption spectrophotometer (AAnalyst 400 by PerkinElmer) was used for determination of total Ca, Mg, Fe, Zn, Cu, and Mn concentrations whereas a flame photometer (DM-62 from Digimed) was used for total K concentration. The determination of the total content of P and S was done according to a colorimetric method using an UV/VIS spectrophotometer (B582 from Micronal®). For B analysis, 0.2 g of the plant material was incinerated in a muffle furnace (Quimis®) at 550 °C and dissolved in 10 mL of 0.1 mol L^{-1} hydrochloric acid solution. Then, the extract was added to a solution of oxalic acid and curcumin and taken to the water bath until evaporation. After cooling, ethyl alcohol was added and the concentration of the element was determined at the UV/VIS spectrophotometer.

Determination of gas exchange variables

The day before the plants were harvested, gas exchanges were analyzed (10:00 AM) using a portable infrared gas analyzer (IRGA, LI-COR Biosciences, model LICOR 6400) with a photosynthetic active radiation of 800 μmol m^{-2} s^{-1} for common bean and 1000 μmol m^{-2} s^{-1} for oat. The following variables were obtained: CO_2 assimilation rate (A: µmol CO_2 m^{-2} s^{-1}), stomatal conductance (g_s: mol H_2O m^{-2} s^{-1}), transpiration (E: mmol H_2O m^{-2} s^{-1}) and internal/external CO_2 concentration ratio (C_i/C_a:µmol CO_2 mol air^{-1}).

Evaluation of lipid peroxidation and hydrogen peroxide

On the end of experimental period, leaves were collected in the morning and stored at -80 °C. Lipid peroxidation and H_2O_2 were quantified from an extract made by adding 0.2 g of leaves macerated in liquid nitrogen to 1.5 mL of trichloroacetic acid (TCA). Then, centrifugation (centrifuge 5415R from Eppendorf®) was carried out at 12,000 g for 15 min at 4 °C (Buege and Aust 1978; Velikova et al. 2000).

For H_2O_2 quantification, aliquots of the supernatant were added to a reaction medium containing 2.5 mmol L^{-1} potassium phosphate buffer (pH 7.0) and 500 mmol L^{-1} potassium iodate (Velikova et al. 2000). Quantification of H_2O_2 was performed based on a standard curve with known concentrations of H_2O_2 levels by measuring the absorbance of the final extract in a ELISA (Enzyme Linked Immuno Sorbent Assay) spectrophotometer at 390 nm, Epoch™ Microplate Spectrophotometer by BioTeK® Instruments (Epoch-BioTek-Elisa).

Lipid peroxidation followed the methodology of Buege and Aust (1978), where its quantification was performed through the quantification of species that reacted with thiobarbituric acid (TBA). The extraction and centrifugation process followed the same methodology as the H_2O_2 quantification. Aliquots of the supernatant were added to a reaction medium containing 0.5% TBA (w/v) and 10% TCA (w/v) and incubated at 95 °C for 30 min. After the period, the reaction was paralyzed by contact on the ice. Lipid peroxidation were expressed in nanomoles of malondialdehyde (MDA) per milligram of fresh biomass after absorbance reading with a spectrophotometer at 535 nm and 600 nm (Epoch-BioTek-Elisa).

Determination of antioxidant enzymes activity

For antioxidant enzymes activity determination, an extract was obtained by macerating 0.2 g of leaves in liquid nitrogen. In that macerate were added an extraction buffer solution containing 0.1 mol L^{-1} potassium phosphate (pH 7.8), 0.1 mmol L^{-1} EDTA (pH 7.0), 0.01 mol L^{-1} ascorbic acid and 22 mg of polyvinylpyrrolidone (Biemelt et al. 1998). The extract was centrifuged (centrifuge 5415R from Eppendorf®) at 13,000 *g* for 10 min at 4 ºC and the supernatant was collected and conserved at -20 ºC in order to evaluate superoxide dismutase (SOD), catalase (CAT) and ascorbate peroxidase (APX).

SOD (EC 1.15.1.1) activity was based on its inhibition of the photoreduction of nitroblue tetrazolium (NBT) (Giannopolitis and Ries 1977), where an aliquot of the supernatant was added to an incubation medium composed of 50 mmol L^{-1} potassium phosphate (pH 7.8), 14 mmol L^{-1} methionine, 0.1 μmol L^{-1} EDTA, 75 μmol L^{-1} NBT and 2 μmol L^{-1} riboflavin. The material (samples and blank control) was illuminated for 7 min with a 20-W fluorescent lamp. Finally, the reading was performed in a spectrophotometer at 560 nm (Epoch-BioTek-Elisa).

CAT (EC 1.11.1.6) activity was quantified according to Havir and McHale (1987). An aliquot of sample was added to an incubation medium containing 100 mmol L^{-1} potassium phosphate (pH 7.0) that was previously incubated at 30 °C. Before placing the samples in the equipment for reading, 12.5 mmol L^{-1} H_2O_2 was added to trigger the reaction. The readings were carried in a spectrophotometer at 240 nm (Epoch-BioTek-Elisa) for 3 min.

APX (EC 1.11.1.11) activity was determined through the oxidation rate of ascorbate (Nakano and Asada 1981). An aliquot of sample was added to an incubation buffer composed of 100 mmol L^{-1} potassium phosphate (pH 7.0) and 0.5 mmol L^{-1} ascorbic acid, which was previously incubated at 30 °C. Before placing the samples in the equipment for reading, 0.1 mmol L^{-1} H_2O_2 was added to the sample. The readings were carried in a spectrophotometer at 290 nm (Epoch-BioTek-Elisa) for 3 min.

Proline quantification

The extraction and quantification of proline was performed according to Bates et al. (1973), with modifications. Leaves (0.2 g) were macerated with 3% sulfosalicylic acid and the extract was stirred for 60 min at room temperature and filtered through a 40-μm filter paper. Then 0.1

mL of the extract was added along with 1.9 mL of water, 2 mL of ninhydrin and 2 mL of acetic acid in test tubes, and finally placed to react for 60 min at 100 °C. After the tubes were placed on ice and the samples were cooled, the readings were performed in a spectrophotometer at 520 nm (Epoch-BioTek-Elisa). Proline quantification was performed using a standard curve with known proline concentrations.

Quality control and quality assurance

All glassware and laboratory supplies used during the experiment were rinsed with 10% HNO_3 and with distilled water in order to ensure no contamination. Only analytical grade reagents were used. To guarantee quality control, in addition to the treatment with no Hg, the quantification of MDA and H_2O_2 was performed in duplicate and with two blank samples on each microplate as normally used for determination at Epoch-BioTek-Elisa. SOD, CAT, APX, and proline were quantified in triplicates and using three blank samples in each microplate.

Statistical analysis

All statistical analyzes were performed in R software version 3.5.3 (R Development Core Team 2019), as follows: the data obtained for each variable were subjected to the variance analysis ($P < 0.05$) and the means were compared using Tukey's HSD test with the emmeans v1.4 package (Length 2019). A Pearson’s correlation matrix was performed with the corrplot v0.84 package (Wei and Simko 2017) for SD, Hg concentration in SD, gas exchanges, concentrations of MDA, activities of SOD, CAT and APX, proline and nutrients in SD for the common bean cultivated in RA, because it was the only experiment that provided SD for analysis of nutrients in all treatments. The objective was to evaluate the correlations among Hg contents and the physiological attributes. The Pearson’s correlations coefficients (r) were classified as strong ($0.75 < r \leq 1.0$), moderate ($0.50 < r \leq 0.75$) or weak ($0.25 < r \leq 0.50$).

Results

High Hg concentrations in soils (generally from 20 mg kg^{-1} Hg on) resulted in reduced shoot growth, leaf chlorosis, and necrosis in leaf margins and tips in both species/soils evaluated. Common bean plants also presented shoot tip rotting when cultivated at 40 and 80 mg kg^{-1} Hg in the TH. The general effects of Hg on plant growth can be seen in Fig. 1. Considering that there were four independent experiments, it is important to highlight that it is not possible to establish comparisons between different plant species and soils. For this reason, the results described below are exclusively related to the effects of Hg concentrations in each species when cultivated in one specific soil.

The effects of Hg on gas exchanges variables are presented in Fig. 2. Oat TH showed a 37% approximate reduction in *A* (17.58 µmol CO_2 m^{-2} s^{-1} without adding Hg and an average of 10.46 µmol CO_2 m^{-2} s^{-1} in 40 and 80 mg kg^{-1} Hg) and *E* (4.16 mmol H_2O m^{-2} s^{-1} without adding Hg and an average of 2.73 mmol H_2O m^{-2} s^{-1} in 40 and 80 mg kg^{-1} Hg) after cultivation in 40 and 80 mg kg^{-1} Hg (Fig. 2b and 2D). In the other hand, a significant increase of *E* (at 40 and 80 mg kg^{-1} Hg) and C_i/C_a (from 10 mg kg^{-1} Hg on) was detected in common bean RA (Fig. 2c and 2e). The g_s data was highly correlated to *E* ($R^2 = 0.99$ in common bean TH/RA and oat TH; $R^2 = 0.67$ in oat RA; $P \leq 0.05$).

Fig. 3 shows the effects of Hg on variables related to oxidative stress, such as lipid peroxidation, antioxidant enzymes activity, and proline concentration in leaves. Lipid peroxidation - estimated through the MDA concentration in leaves - doubled in common bean TH (from 10 mg kg^{-1} Hg on) and showed a 66% approximate reduction in Oat RA (175.48 mmol mg^{-1} FM without adding Hg and 66.03 and 53.61 mmol mg^{-1} FM in 40 and 80 mg kg^{-1} Hg, respectively) (Fig. 3a and 3b). In agreement with MDA data, the activity of the antioxidant enzymes SOD and CAT increased only for common bean (Fig. 3c and 3e). SOD activity increased (0.56 and 0.67 U mg^{-1} FM in 0 and 80 mg kg^{-1} Hg, respectively) only when common bean was grown in RA (Fig. 3c) and for CAT, a significant increase was detected only when it was grown in TH (Fig. 3e). Oat showed no changes in the activity of the enzymes SOD and CAT when cultivated in the both soils TH and RA (Fig. 3d and 3f). Proline concentration was negatively affected in leaves of oat RA where concentrations of 40 and 80 mg kg^{-1} of Hg promoted reductions of 59% (11.38 and 4.67 µg proline mg^{-1} SD in 0 and 40 mg kg^{-1} Hg, respectively) and 66% (11.38 and 3.91 µg proline mg^{-1} SD in 0 and 80 mg kg^{-1} Hg, respectively), respectively (Fig. 3h). No significant differences between control and Hg treatments were found for APX and H_2O_2 content in leaves.

The concentration of macro (P, K, Ca, Mg, S) and micronutrients (Cu, Fe, Mn, Zn, B) was evaluated in leaves of both species and for the both soils. However, due to low production of dry mass, we couldn't perform the analysis for some of the highest Hg concentrations in soil. A significant reduction of nutrient concentration in leaves was found only for oat TH: P was almost 50% lower than control (5.24 g kg^{-1}) at 40 mg kg^{-1} Hg (2.76 g kg^{-1}) and S (8.02 g kg^{-1} for control) was around 32 (5.48 g kg^{-1}) and 47% (4.27 g kg^{-}1) lower after growing at 20 and 40 mg kg^{-1} Hg, respectively. Other changes detected in nutrients concentration were all related to increases: higher P was detected in both oat and common bean cultivated in RA; higher S in common bean cultivated in the both soils; and higher K and Mg in common bean RA. No significant differences were found in micronutrients concentration, except for B, which was quantified only in in common bean and showed a significant increase of 33% after growing in RA (20.02 mg kg^{-1} without adding Hg and 26.60 mg kg^{-1} in 80 mg kg^{-1} Hg).

The results found for common bean RA were submitted to Pearson's correlation (Fig. 4). Shoot dry matter showed a strong negative correlation (-0.75) with Hg, Mg, S, K, and B and a moderate negative correlation (-0.50) with P concentration in dry mass and with *E*. On the other hand, a strong positive correlation (0.75) was found for Hg with S, K, and B concentration in leaves. Several moderate and weak correlations were also found (Fig. 4), being the most meaningful the correlation between Hg and MDA concentration in leaves.

Discussion

Higher clay and organic matter levels in RA resulted in lower Hg bioavailability for common bean and oat, in comparison to TH. When 80 mg kg^{-1} of Hg was added to the soils, common bean presented 84 and 38 mg Hg kg^{-1} SD in TH and RA, respectively. However, in oat plants an average of 27 (±0.47) mg Hg kg^{-1} SD was detected when grown in both soils (Lima et al. 2019a, b). Detailed information concerning soil analyses as well as Hg levels in SDM of both species in RA and TH soils are specified in Lima et al. (2019a, b). As shown in Fig. 1, the effect of Hg on plant growth is clear, especially in common bean cultivated in TH. In this soil, the addition of 20 and 40 mg kg^{-1} Hg was enough to promote visible deleterious effects such as leaf chlorosis, apical/marginal leaf necrosis, and dwarfism in both species.

The higher Hg bioavailability in TH affected plant physiology promoting toxicity-like responses in both species. Common bean showed increased MDA levels and CAT activity even at the lowest Hg concentrations, as observed in other studies (Malar et al. 2015; Manikandan et al. 2015; Zhang et al. 2017). The increased MDA levels is a response most easily attributed to oxidative damage caused mainly by ROS, and it is often used as an indicator of oxidative stress (Cargnelutti et al. 2006). Mitochondria and chloroplasts are O_2-rich microenvironments and the presence of transition metals such as Hg can interfere in oxidation-reductions reactions and increase the conversion levels of O_2 in $O_2^{\bullet-}$. When $O_2^{\bullet-}$ undergoes univalent reduction and protonation (which may occur from the reaction catalyzed by SOD and in a non-enzymatic way), there is formation of H_2O_2 and $OH^{\bullet}$. It is worth mentioning that $OH^{\bullet}$ is one of the most harmful ROS in living systems and therefore the regulation of its precursors, $O_2^{\bullet-}$ and H_2O_2 is the fundamental step to avoid $OH^{\bullet}$ formation. H_2O_2 can be decomposed by CAT and APX when it is produced above baseline levels (Das and Roychoudhury 2014), explaining the great levels of CAT in common bean TH.

Toxicity-like responses were also detected in oat cultivated in the TH soil. However, in this species only the photosynthetic responses were significantly affected, as shown by the reduced A, g_s and E when cultivated under 40 and 80 mg kg^{-1} Hg. In this species, A dropped in response to reduction of stomatal conductance (g_s). Despite the lack of alteration in MDA content in oat TH, it is important to highlight that in some cases the reduced g_s may act a trigger to the oxidative stress process described above for common bean, since it can impair CO_2 input into the leaf tissues, which can negatively affect the photochemical reactions, leading to increased formation of $O_2^{\bullet-}$ in chloroplasts. It is also worth to mention that Hg may negatively impair A due to the inhibition of the activity of the enzyme delta-aminolevulinate dehydratase (δ-ALA- D), an important enzyme in chlorophyll biosynthetic pathway (Morsch et al. 2002; Calgaroto et al. 2011).

In contrast to what was described for plants grown in TH soil, plants cultivated on RA did not present evidences of physiological damage, but showed acclimation-like responses instead. The increased C_i/C_a ratio detected in common bean is a consequence of the higher stomatal conductance, which was accompanied of increased SOD activity. Together, these responses may represent an attempt to increase CO_2 available for photosynthetic reactions, thus keeping ROS under homeostatic level.

The relationship between Hg and plant nutrients is not very clear, but it is known that Hg can compete with K, Mg, and Mn (Doening 2000), Ca (Sahu et al. 2012), as well as N and P (Gupta and Chandra 1998) for protein transporter, promoting deficiency. This explains the reduced P concentration in SD of common bean TH. On the other hand, we detected higher B, K, Mg, P, and S in SD of common bean RA in comparison with the control treatment. The affinity between Hg and S is well known: Hg can be absorbed and transported in plants through complexes between these two elements (Wang et al. 2012). However, Pearson`s correlation showed a significant negative correlation between these five elements and SD, which means that there is a "concentration effect” of elements in tissues. Considering that, increased B, K, Mg, P, and S should be an indirect effect of Hg promoted by SD reduction.

We are aware that the different responses found between common bean and oat after cultivation in two Oxisols resulted from intrinsic biological features of each species, but may also be a consequence of environmental conditions in the greenhouse, since the experiments were conducted in different moments (common bean – January/February and oat – March/April). This is also the reason why we did not compare both species regarding tolerance to Hg. Besides that, it is evident how plants cultivated in TH soil are more negatively affected by the presence of Hg than plants cultivated in RA.

Finally, we highlight that only a few studies regarding Hg phytotoxicity were carried out in soil (Zhou et al. 2014; Sheetal et al. 2016; Smolinska and Szczodrowska 2017; Xun et al. 2017; Pogrzeba et al. 2019). Moreover, there is a shortage of such studies mainly in tropical environments. Considering that, our work represents an important effort in bringing light to the knowledge about the phytotoxic effects of Hg, in a more realistic scenario for tropical environments.

Conclusion

The physiology of common bean and oat is affected by Hg in both soils evaluated. The physical-chemical properties of TH resulted in reduced sorption and increased bioavailability of Hg in soil, which in turn resulted in toxicity-like responses in both species, such as oxidative stress and reduced photosynthesis, suggesting a decrease in the productive potential of these agricultural crops in the presence of Hg. In contrast, plants cultivated in RA, a soil with lower available Hg content showed acclimation-like responses. Considering the accumulative effect of Hg in plant crops tissues, studies focusing on Hg accumulation in grains should be performed to increase food safety.

Compliance with ethical standards

Conflict of interest: The authors declare that they have no conflict of interest.

Ethical approval: This article does not contain any studies with human participants or animals performed by any of the authors.

References

Alvarez VH, Ribeiro AC (1999) Calagem. In: Ribeiro AC, Guimarães PTG, Alvarez VH (eds)

Recomendações para o uso de corretivos e fertilizantes em Minas Gerais: 5ª aproximação. Comissão de Fertilidade do Solo do Estado de Minas Gerais, Viçosa, pp 43–60 (in Portuguese)

Bates LS, Waldren RP, Teare ID (1973) Rapid determination of free proline for water-stress studies. Plant Soil 39:205-207. https://doi.org/10.1007/BF00018060

Biemelt S, Keetman U, Albrecht G (1998) Re-aeration following hypoxia or anoxia leads to activation of the antioxidative defense system in roots of wheat seedlings. Plant Physiol 116:651–658. https://doi.org/10.1104/pp.116.2.651

Budnik LT, Casteleyn L (2019) Mercury pollution in modern times and its socio-medical consequences. Sci Total Environ 654:720-734. https://doi.org/10.1016/j.scitotenv.2018.10.408

Buege JA, Aust SD (1978) Microsomal lipid peroxidation. Methods Enzymol 52:302-310. https://doi.org/10.1016/s0076-6879(78)52032-6

Calgaroto NS, Cargnelutti D, Rossato LV et al (2011) Zinc alleviates mercury-induced oxidative stress in *Pfaffia glomerata* (Spreng.) Pedersen. Biometals 24:959-971 https://doi.org/10.1007/s10534-011-9457-y

Cargnelutti D, Tabaldi LA, Spanevello RM et al (2006) Mercury toxicity induces oxidative stress in growing cucumber seedlings. Chemosphere 65:999-1006. https://doi.org/10.1016/j.chemosphere.2006.03.037

Carvalho GS, Oliveira JR, Curi N et al (2019) Selenium and mercury in Brazilian Cerrado soils and their relationships with physical and chemical soil characteristics. Chemosphere 218:412-415. https://doi.org/10.1016/j.chemosphere.2018

Das K, Roychoudhury A (2014) Reactive oxygen species (ROS) and response of antioxidants as ROS-scavengers during environmental stress in plants. Front Environ Sci 2:53. https://doi.org/10.3389/fenvs.2014.00053

Das P, Nutan KK, Singla-Pareek SL, Pareek A (2015) Oxidative environment and redox homeostasis in plants: dissecting out significant contribution of major cellular organelles. Front Environ Sci 2:70. https://doi.org/10.3389/fenvs.2014.00070

Doening DW (2000) Ecological effects, transport, and fate of mercury: a general review. Chemosphere 40:1335-1351. https://doi.org/10.1016/S0045-6535(99)00283-0

Dutta S, Mitra M, Agarwal P et al (2018) Oxidative and genotoxic damages in plants in response to heavy metal stress and maintenance of genome stability. Plant Signal Behav 13:8. https://doi.org/10.1080/15592324.2018.1460048

Foyer CH, Noctor G (2003) Redox sensing and signaling associated with reactive oxygen in chloroplasts, peroxisomes and mitochondria. Physiol Plant 119:355-364. https://doi.org/10.1034/j.1399-3054.2003.00223.x

Gardi C, Angelini M, Barceló S et al (2015) Soil atlas of Latin America and the Caribbean. European Comission, Publications Office of the European Union, L-2995 Luxembourg

Giannopolitis CN, Ries SK (1977) Superoxide dismutases: I. Occurrence in higher plants. Plant Physiol 59:309-314

Gupta M, Chandra P (1998) Bioaccumulation and toxicity of mercury in rooted-submerged macrophyte *Vallisneria spiralis*. Environ Pollut 103:327-332. https://doi.org/10.1016/s0269-7491(98)00102-x

Hareland GA, Manthey FA (2003) Oat. North Dakota State University, Fargo, ND, USA. Encyclopedia of Food Sciences and Nutrition, 2nd edn. Elsevier Science Ltd., pp 4213-4220. https://doi.org/10.1016/B0-12-227055-X/00849-X

Havir EA, McHale NA (1987) Biochemical and developmental characterization of multiple forms of catalase in tobacco leaves. Plant Physiol 84:450-455. https://doi.org/10.1104/pp.84.2.450

He M, Tian L, Braaten HFV et al (2019) Mercury–Organic Matter Interactions in Soils and Sediments: Angel or Devil? B. Environ Contam Tox 102;621-627. https://doi.org/10.1007/s00128-018-2523-1

International Organizations for Standardization – (ISO) (2012) Soil quality – determination of the effects of pollutants on soil flora – part 2: effects of contaminated soil on the emergence and early growth of higher plants. ISO 11269-2. ISO, Geneva

Lacerda LD, de Souza M, Ribeiro MG (2004) The effects of land use change on mercury distribution in soils of Alta Floresta, Southern Amazon. Environ Pollut 129:247–255. https://doi.org/10.1016/j.envpol.2003.10.013

Length R (2019) emmeans: Estimated marginal means, aka least-squares means. R package version 1.4. https://CRAN.R-project.org/package=emmeans. Accessed 31 July 2019

Lima FRD, Martins GC, Silva AO et al (2019) Critical mercury concentration in tropical soils: Impact on plants and soil biological attributes. Sci Total Environ 666:472-479. https://doi.org/10.1016/j.scitotenv.2019.02.216

Lima FRD, Engelhardt MM, Vasques ICF et al (2019) Evaluation of mercury phytoavailability in Oxisols. Environ Sci Pollut Res 26:483-491. https://doi.org/10.1007/s11356-018-3623-5

Mahbub KR, Bahar MM, Megharaj M, Labbate M (2018) Are the existing guideline values adequate to protect soil health from inorganic mercury contamination? Environ Int 117:10–15. https://doi.org/10.1016/j.envint.2018.04.037

Malar S, Sahi SV, Favas PJC, Venkatachalam P (2015) Assessment of mercury heavy metal toxicity-induced physiochemical and molecular changes in *Sesbania grandiflora* L. Int J Environ Sci Technol 12:3273-3282. https://doi.org/10.1007/s13762-014-0699-4

Malavolta E (1981) Manual de química agrícola: adubos e adubação. Agronômica Ceres, São Paulo (in Portuguese)

Malavolta E, Vitti GC, Oliveira SA (1997) Avaliação do estado nutricional das plantas: princípios e aplicações, 2nd edn. Potafos, Piracicaba (in Portuguese)

Manikandan R, Sahi SV, Venkatachalam P (2015) Impact assessment of mercury accumulation and biochemical and molecular response of *Mentha arvensis*: a potential hyperaccumulator plant. Sci World J 2015:1-10. http://dx.doi.org/10.1155/2015/715217

Martins GC, Oliveira C, Ribeiro PG et al (2019) Assessing the Brazilian prevention value for soil arsenic: Effects on emergence and growth of plant species relevant to tropical agroecosystems. Sci Total Environ 694:133663. https://doi.org/10.1016/j.scitotenv.2019.133663

Martins GC, Oliveira C, Ribeiro PG et al (2020) Assessing the most sensitive and reliable endpoints in plant growth tests to improve arsenic risk assessment. Sci Total Environ 708:134753. https://doi.org/10.1016/j.scitotenv.2019.134753

Miller G, Suzuki N, Ciftci-Yilmaz S, Mittler R (2010) Reactive oxygen species homeostasis and signalling during drought and salinity stresses. Plant Cell Environ 33:453–467. https://doi.org/10.1111/j.1365-3040.2009.02041.x

Mishra B, Sangwan, NS (2019) Amelioration of cadmium stress in *Withania somnifera* by ROS management: active participation of primary and secondary metabolism. Plant Growth Regul 87:403-412. https://doi.org/10.1007/s10725-019-00480-8

Morsch VM, Schetinger MRC, Martins AF, Rocha JBT (2002) Effects of cadmium, lead, mercury and zinc on-aminolevulinic acid dehydratase activity from radish leaves. Biol Plantarum 45:85-89. https://doi.org/10.1023/A:1015196423320

Nakano Y, Asada K (1981) Hydrogen peroxide is scavenged by ascorbate-specific peroxidase in spinach chloroplasts. Plant Cell Physiol 22:867–880. https://doi.org/10.1093/oxfordjournals.pcp.a076232

Organization for Economic Co-operation and Development – OECD (2006) Test no. 208: terrestrial plant test: seedling emergence and seedling growth test, OECD guidelines for the testing of chemicals. OECD Guidelines for the Testing of Chemicals, Section 2. OECD Publishing https://doi.org/10.1787/9789264070066-en

Pirzadah TB, Malik B, Tahir I et al (2018) Characterization of mercury-induced stress biomarkers in *Fagopyrum tataricum* plants. Int J Phytoremediat 20:225-236. https://doi.org/10.1080/15226514.2017.1374332

Pogrzeba M, Rusinowski S, Krzyżak J et al (2019) *Dactylis glomerata* L. cultivation on mercury contaminated soil and its physiological response to granular sulphur aided phytostabilization. Environ Pollut 255: 113271. https://doi.org/10.1016/j.envpol.2019.113271

Porch TG, Beaver JS, Debouck DG (2013) Use of wild relatives and closely related species to adapt common bean to climate change. Agronomy 3:433-461. https://doi.org/10.3390/agronomy3020433

Ravichandran M (2004) Interactions between mercury and dissolved organic matter: a review. Chemosphere 55:319-331. https://doi.org/10.1016/j.chemosphere.2003.11.011

Rezende AA, Pacheco MTB, Silva VSND, Ferreira TAPDC (2018) Nutritional and protein quality of dry Brazilian beans (*Phaseolus vulgaris* L.). Food Sci Technol 38:421-427. http://dx.doi.org/10.1590/1678-457x.05917

R Development Core Team (2019) R: A language and environment for statistical computing. R Foundation for Statistical Computing, Vienna, https://www.r-project.org/. Accessed 31 July 2019

Safari F, Akramian M, Salehi-Arjmand H, Khadivi A (2019) Physiological and molecular mechanisms underlying salicylic acid-mitigated mercury toxicity in lemon balm (*Melissa officinalis* L.). Ecotoxicol Environ Saf 183:109542. https://doi.org/10.1016/j.ecoenv.2019.109542

Sahu GK, Upadhyay S, Sahoo BB (2012) Mercury induced phytotoxicity and oxidative stress in wheat (*Triticum aestivum* L.) plants. Physiol Mol Biol Plants 18:21-31. https://doi.org/10.1007/s12298-011-0090-6

Santos HG, Jacomine PKT, Anjos LHC et al (2018) Sistema Brasileiro de Classificação de Solos. Embrapa Solos, Rio de Janeiro

Sheetal KR, Singh SD, Anand A, Prasad S (2016) Heavy metal accumulation and effects on growth, biomass and physiological processes in mustard. Indian J Plant Physiol 21:219-223. https://doi.org/10.1007/s40502-016-0221-8

Smolinska B, Szczodrowska A (2017) Antioxidative response of *Lepidium sativum* L. during assisted phytoremediation of Hg contaminated soil. N Biotechnol 38:74-83.

https://doi.org/10.1016/j.nbt.2016.07.004

Soares LC, Linhares LA, Egreja Filho FB (2015) Mercúrio em solos da Região Sudeste do Brasil sem influência antropogênica e sua correlação com as características químicas e físicas. Rev Bras Ciênc Solo 39:903–914. https://doi.org/10.1590/01000683rbcs20140411

Soil Survey Staff (2014) Keys to Soil Taxonomy. 12th edn. U.S. Department of Agriculture, Natural Resources Conservation Service, Washington

Teixeira PC, Donagemma GK, Fontana A, Teixeira WG (2017) Manual de métodos de análise de solo, 3rd edn. ed. EMBRAPA, Brasilia, DF (in Portuguese)

U.S. Environmental Protection Agency – USEPA (2007) Method 3051A (SW-846): Microwave Assisted Acid Digestion of Sediments, Sludges, and Oils, Revision. 1. ed. USEPA, Washington

Velikova V, Yordanov I, Edreva A (2000) Oxidative stress and some antioxidant systems in acid rain-treated bean plants. Plant Sci 151:59–66. https://doi.org/10.1016/S0168-9452(99)00197-1

Wang J, Feng X, Anderson CW et al (2012) Implications of mercury speciation in thiosulfate treated plants. Environ Sci Technol 46:5361-5368. https://doi.org/10.1021/es204331a

Wei T, Simko V (2017) Corrplot: Visualization of a Correlation Matrix. R package version 0.84. https://cran.r-project.org/web/packages/corrplot/. Accessed 31 July 2019

Windmöller CC, Silva NC, Andrade PHM et al (2017) Use of a direct mercury analyzer® for mercury speciation in different matrices without sample preparation. Anal Methods 9:2159–2167. https://doi.org/10.1039/c6ay03041f

Xun Y, Feng L, Li Y, Dong H (2017) Mercury accumulation plant *Cyrtomium macrophyllum* and its potential for phytoremediation of mercury polluted sites. Chemosphere 189:161-170. https://doi.org/10.1016/j.chemosphere.2017.09.055

Zhang T, Lu Q, Su C (2017) Mercury induced oxidative stress, DNA damage, and activation of antioxidative system and Hsp 70 induction in duckweed (*Lemna minor*). Ecotoxicol Environ Saf 143:46–56. http://dx.doi.org/10.1016/j.ecoenv.2017.04.058

Zhou J, Liu H, Du B (2015) Influence of soil mercury concentration and fraction on bioaccumulation process of inorganic mercury and methylmercury in rice (Oryza sativa L.). Environ Sci Pollut Res 22:6144-6154. https://doi.org/10.1007/s11356-014-3823-6

Ethics approval and consent to participate: Not applicable.

Consent for publication: Not applicable.

Availability of data and materials: All data generated or analysed during this study are included in this published article and its supplementary information files.

Competing interests: The authors declare that they have no competing interests.

Funding: The authors thank the Coordenação de Aperfeiçoamento de Pessoal de Nível Superior - Brasil (CAPES) - Finance Code 001 for granting the doctorate scholarship for FRDL (Grant no. 88882.349697/2019-01), Conselho Nacional de Desenvolvimento Científico e Tecnológico (CNPq), and Fundação de Amparo à Pesquisa do Estado de Minas Gerais (FAPEMIG) for financial support.

Authors' contributions: All authors contributed to the conceptualization, investigation, data analysis, and writing of the manuscript. **Francielle R. D. Lima**: Conceptualization; Data curation; Methodology; Formal analysis; Writing - original draft and Writing - review & editing. **Alice P. Barbosa**: Writing - original draft and Writing - review & editing. **Isabela C. F. Vasques**: Writing - review & editing. **Jakeline R. Oliveira**: Writing - original draft and Writing - review & editing. **Aline O. Silva**: Writing - original draft and Writing - review & editing. **Gabriel C. Martins**: Writing - original draft and Writing - review & editing. **Mateus M. Engelhardt**: Methodology. **Polyana Pereira**: Methodology. **Rayner H. C. L. Reis**: Methodology. **Luiz R. G. Guilherme**: Funding acquisition and Writing - review & editing. **João J. G. S. M. Marques**: Conceptualization; Funding acquisition; Supervision; Writing - review & editing and Methodology.

Acknowledgements: The authors would like to thank Coordenação de Aperfeiçoamento de Pessoal de Nível Superior - Brasil (CAPES) - Finance Code 001, Conselho Nacional de Desenvolvimento Científico e Tecnológico (CNPq), and Fundação de Amparo à Pesquisa do Estado de Minas Gerais (FAPEMIG) for financial support and especially CAPES for granting the doctorate scholarship for FRDL (Grant no. 88882.349697/2019-01). The support on the experiment provided by Kamila Rezende Dázio de Souza and Lissa Vasconcellos Vilas Boas is also acknowledged.

List of Figures

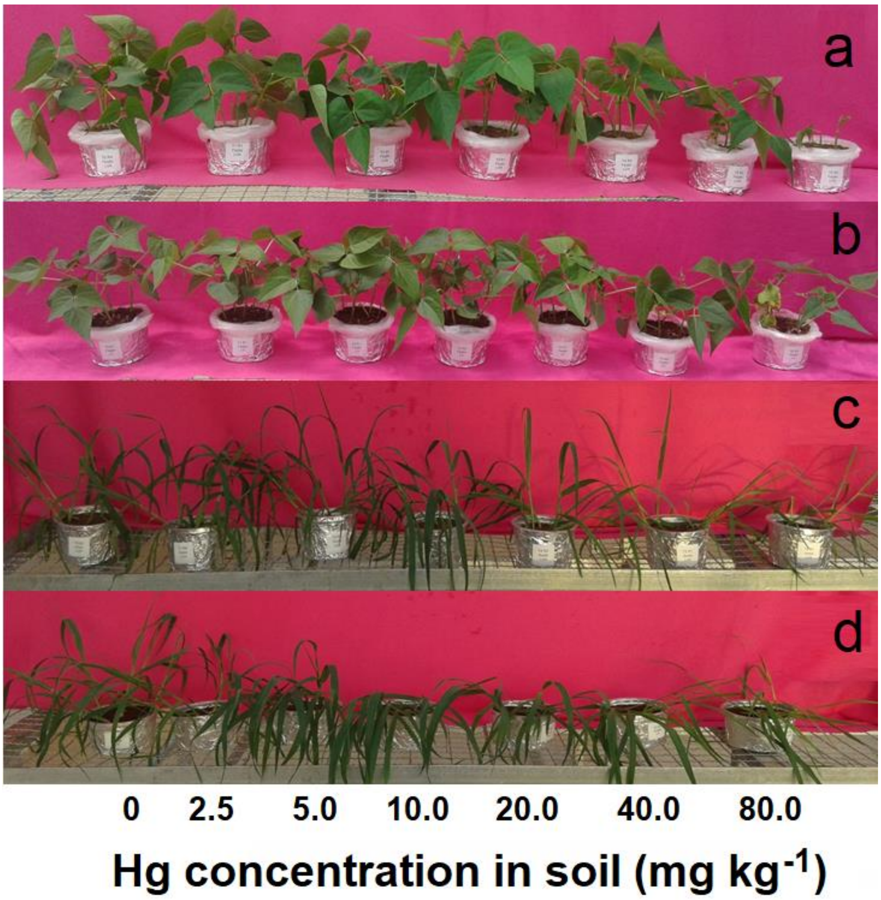

Fig.1 Common bean in Typic Hapludox (TH) (a) and Rhodic Acrudox (RA) (b) and oat in TH (c) and RA (d) after cultivation with increasing concentrations of mercury (0 to 80 mg kg^{-1}) for 30 days.

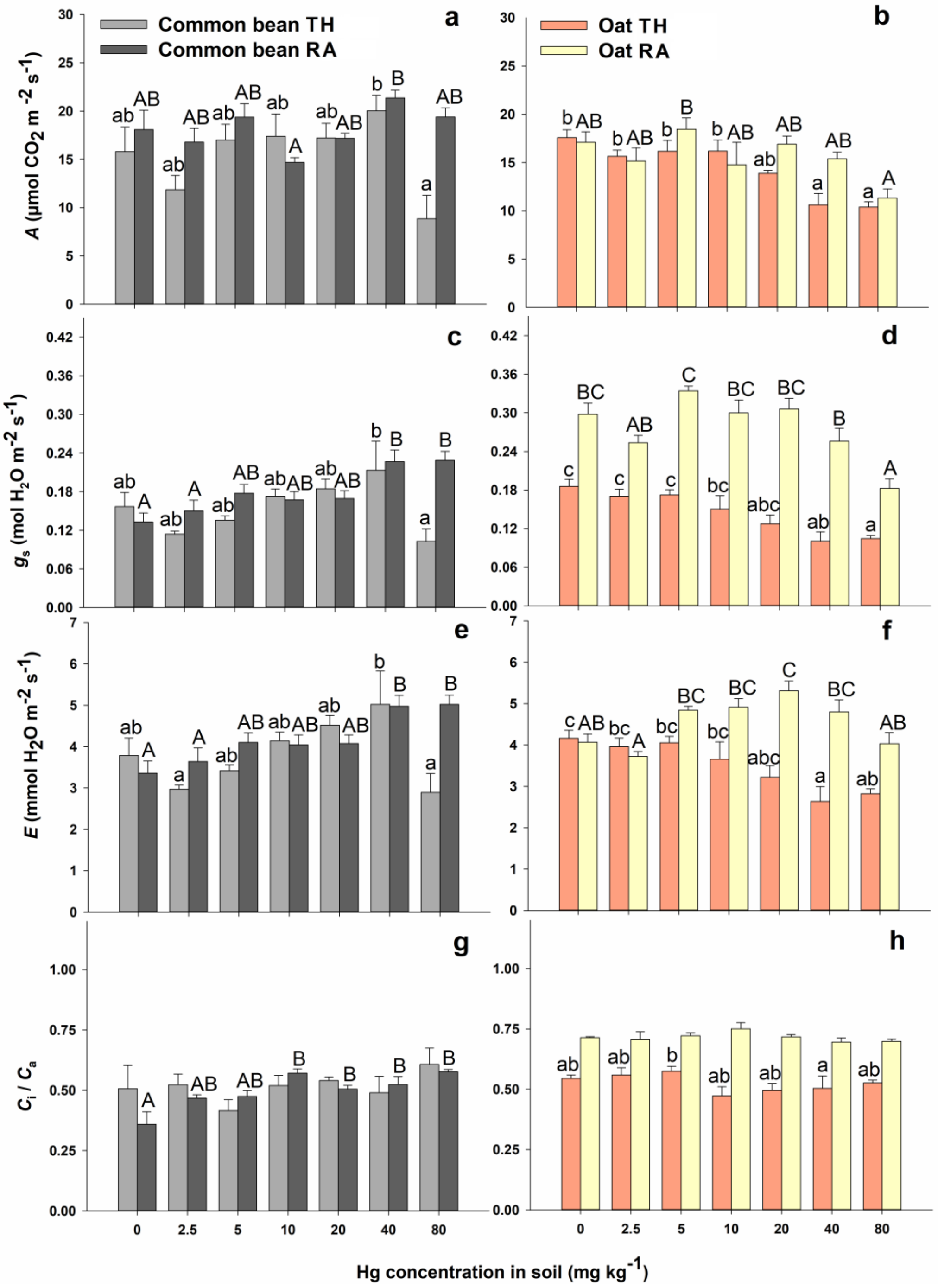

Fig.2 Gas exchange variables (CO$_2$ assimilation rate – A, stomatal conductance – g_s, transpiration – E and internal/external CO$_2$ concentration ratio – C_i/C_a) in effect of Hg on contents in common bean and oat after cultivation with increasing concentrations of mercury (0 to 80 mg kg^{-1} Hg) in Typic Hapludox (TH) and Rhodic Acrudox (RA) soils for 30 days. Results from the ANOVA and Tukey's test ($P < 0.05$), means follow a decreasing order: c > b > a. Different letters corresponds to significant differences across Hg concentrations within one species and one soil. Error bars represent the standard errors of the means (n = 4).

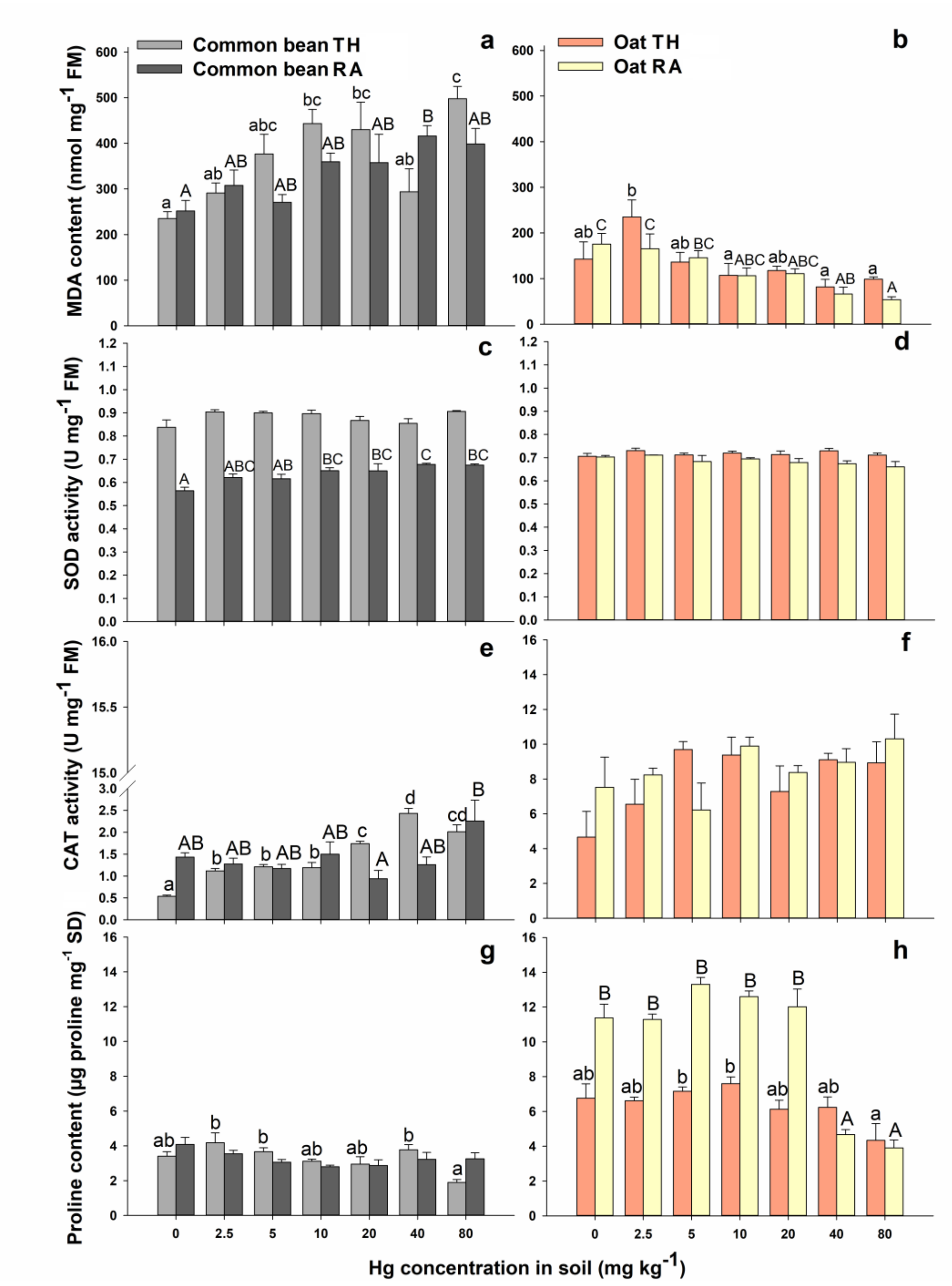

Fig.3 Concentrations of malonaldehyde (MDA), activities of superoxide dismutase (SOD), catalase (CAT) and proline content in leaves of common bean and oat after cultivation with increasing concentrations of mercury (0 to 80 mg kg^{-1} Hg) in Typic Hapludox (TH) and Rhodic Acrudox (RA) soils for 30 days. Results from the ANOVA and Tukey's test (*P* < 0.05), means follow a decreasing order: c > b > a. Different letters corresponds to significant differences across Hg concentrations within one species and one soil. Error bars represent the standard errors of the means (n = 4).

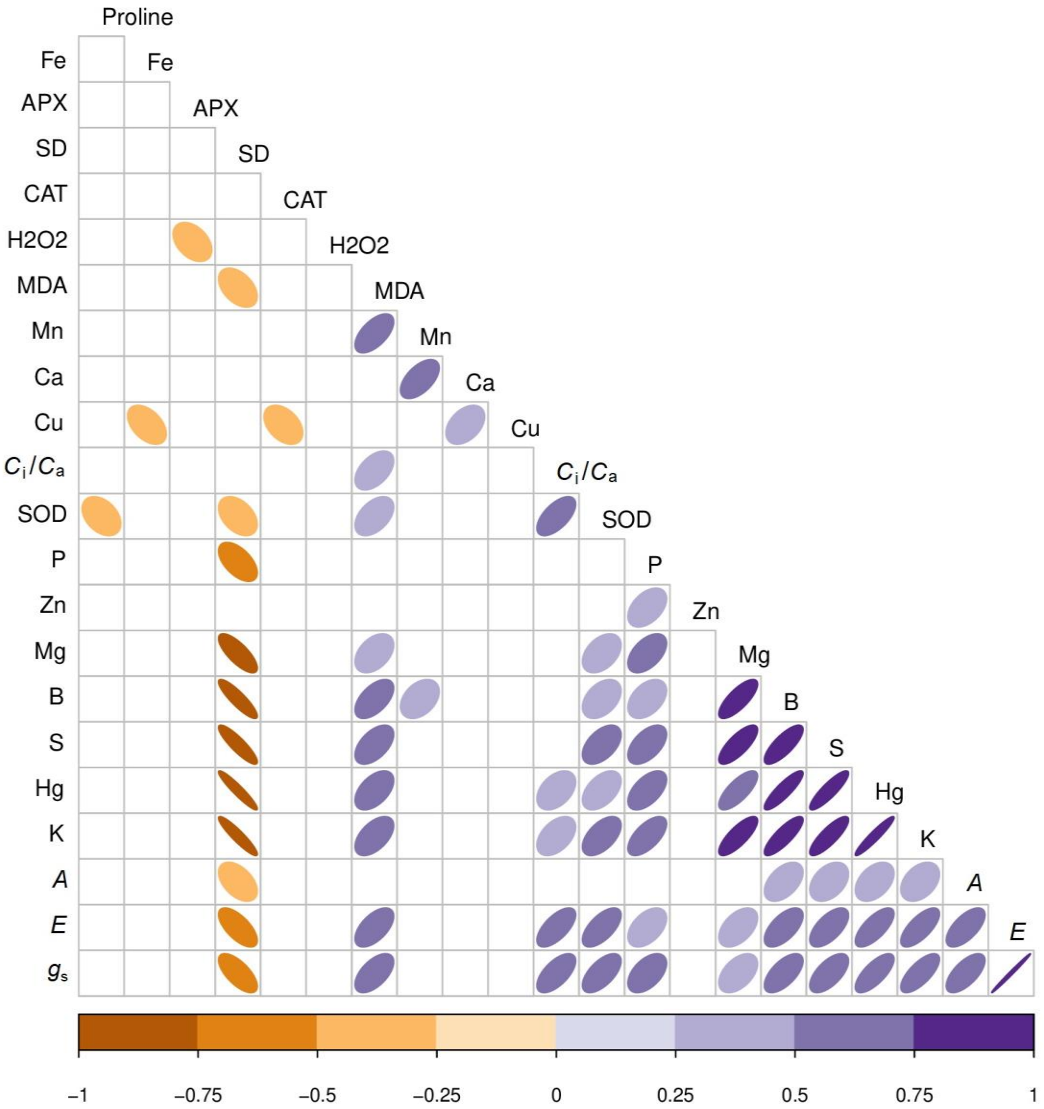

Fig.4 Pearson's correlation matrix for the shoot dry matter (SD), concentrations of the nutrients and Hg in SD, content of proline, malonaldehyde (MDA), superoxide dismutase (SOD), catalase (CAT), ascorbate peroxidase (APX), hydrogen peroxide (H_2O_2) and gas exchange variables (CO_2 assimilation rate – A, stomatal conductance – g_s, transpiration – E and internal/external CO_2 concentration ratio – C_i/C_a) for the common bean cultivated in Rhodic Acrudox. Colour ellipses indicate statistical significance levels ($P < 0.05$), with purple being positively correlated and brown, negatively correlated

Supplementary material

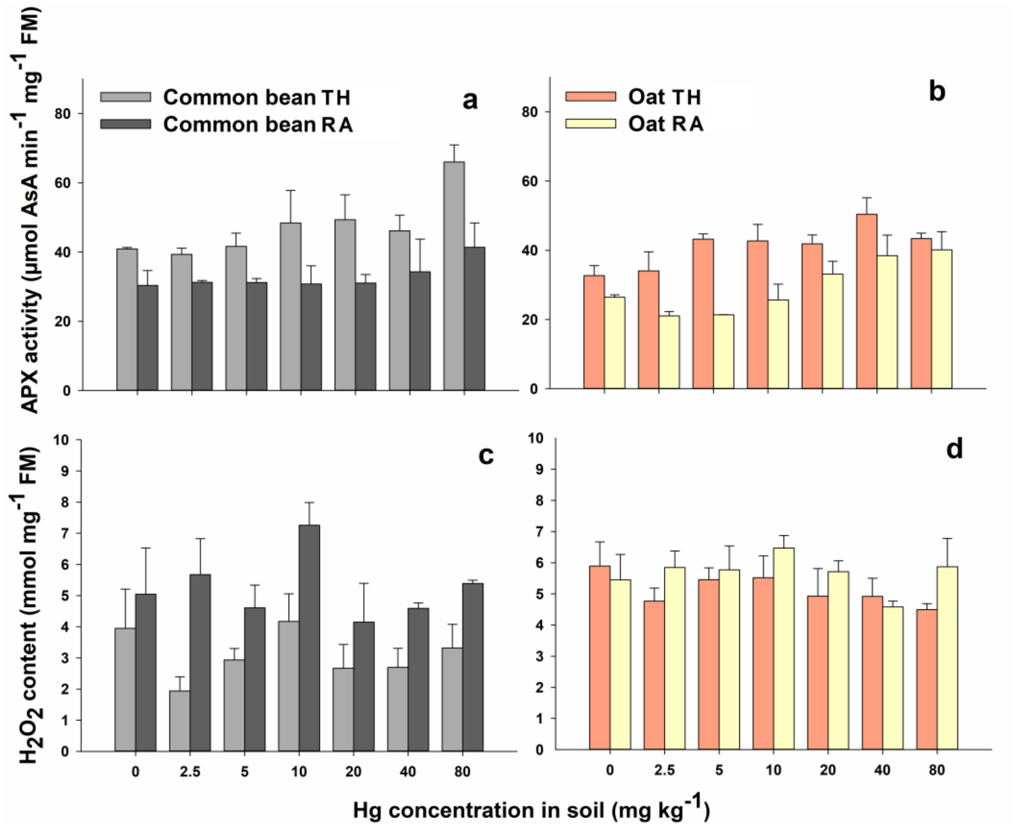

Fig. S1. Activities of ascorbate peroxidase (APX) and hydrogen peroxide (H_2O_2) content in leaves of common bean and oat after cultivation with increasing concentrations of mercury (0 to 80 mg kg^{-1} Hg) in Typic Hapludox (TH) and Rhodic Acrudox (RA) soils for 30 days. Results from the ANOVA test ($P < 0.05$). Error bars represent the standard errors of the means (n = 4)

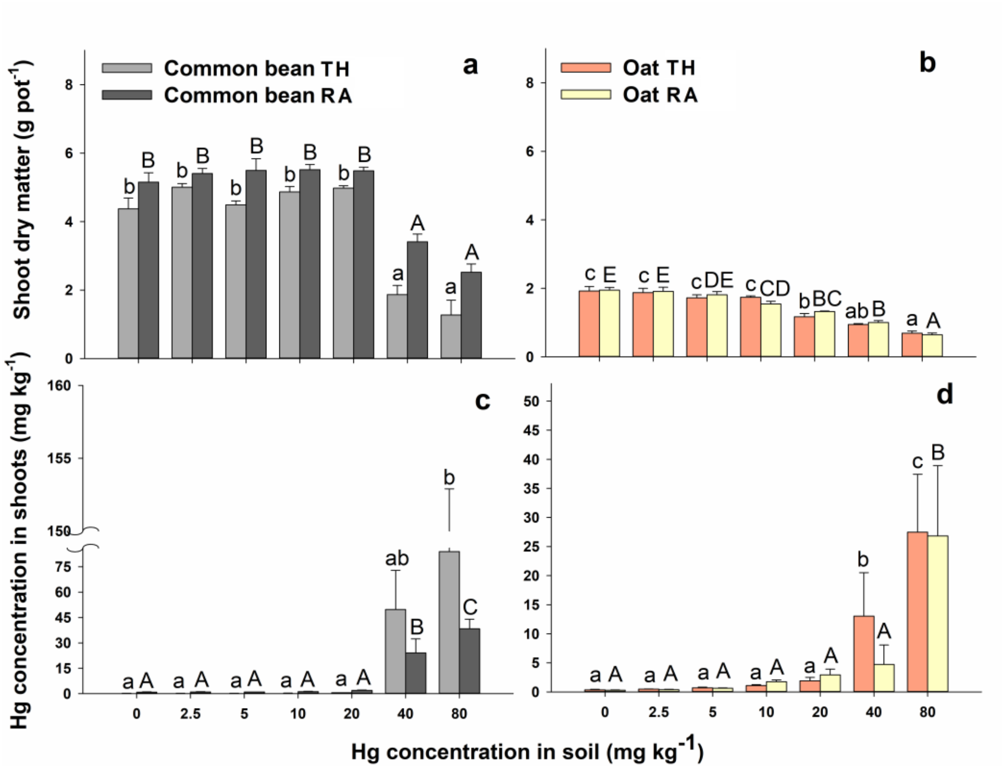

Fig. S2. Shoot dry matter and mercury (Hg) concentration in shoots of common bean and oat after cultivation with increasing concentrations of mercury (0 to 80 mg kg^{-1} Hg) in Typic Hapludox (TH) and Rhodic Acrudox (RA) soils for 30 days. Results from the ANOVA and Tukey’s test (*P* < 0.05), means follow a decreasing order: c > b > a. Different letters corresponds to significant differences across Hg concentrations within one species and one soil. Error bars represent the standard errors of the means (n = 4)

Table S1 Concentration of macronutrients in leaves of common bean and oat after cultivation with increasing concentrations of mercury (0 to 80 mg kg^{-1} Hg) in Typic Hapludox (TH) and Rhodic Acrudox (RA) soils for 30 days. Results from the ANOVA test (*P* < 0.05). Error bars represent the standard errors of the means (n = 4)

Hg concentration (mg kg^{-1})	P	K	Ca	Mg	S
	-- g kg^{-1} --				
			Oat - TH		
0	5.24 ± 0.26 b	29.13 ± 2.02 ab	2.41 ± 0.12	1.80 ± 0.09	8.02 ± 0.26 c
2.5	3.80 ± 0.28 ab	27.89 ± 0.76 a	1.85 ± 0.24	1.37 ± 0.18	7.03 ± 0.31 bc
5	5.68 ± 0.28 b	31.28 ± 1.70 abc	1.76 ± 0.36	1.35 ± 0.26	7.51 ± 0.23 bc
10	5.56 ± 0.49 b	32.86 ± 2.95 abc	1.90 ± 0.30	1.48 ± 0.13	6.75 ± 0.71 abc
20	5.25 ± 0.38 b	41.69 ± 2.26 c	1.22 ± 0.11	1.39 ± 0.06	5.48 ± 0.37 ab
40	2.76 ± 0.86 a	40.38 ± 2.76 bc	1.24 ± 0.14	1.42 ± 0.07	4.27 ± 0.05 a
80	-	-	-	-	-
ANOVA	*	*	ns	ns	*
			Oat - RA		
0	3.23 ± 0.05 a	25.27 ± 0.81 a	1.40 ± 0.09	1.56 ± 0.04	3.94 ± 0.32
2.5	3.24 ± 0.15 a	24.63 ± 1.95 a	1.53 ± 0.13	1.51 ± 0.09	4.86 ± 0.61
5	3.63 ± 0.11 ab	28.64 ± 0.91 ab	1.33 ± 0.18	1.52 ± 0.05	4.79 ± 0.52
10	3.73 ± 0.35 ab	34.19 ± 1.71 b	2.29 ± 0.54	1.36 ± 0.13	5.04 ± 0.28
20	4.52 ± 0.42 b	30.21 ± 2.40 ab	1.81 ± 0.29	1.38 ± 0.21	3.91 ± 0.77
40	-	-	-	-	-
80	-	-	-	-	-
ANOVA	*	*	ns	ns	ns
			Common bean - TH		
0	3,33 ± 0.33 a	19.55 ± 2.54 a	7.80 ± 0.87	3.26 ± 0.25	1.62 ± 0.69 a
2.5	3,67 ± 0.14 ab	25.57 ± 2.22 ab	8.38 ± 0.11	3.23 ± 0.15	2.64 ± 0.18 a
5	3,58 ± 0.22 ab	27.42 ± 2.92 ab	7.76 ± 0.71	3.52 ± 0.33	3.77 ± 0.43 a
10	3,17 ± 0.34 a	21.31 ± 1.75 a	7.72 ± 0.15	3.25 ± 0.07	1.49 ± 0.18 a
20	4,03 ± 0.49 ab	28.79 ± 6.86 ab	7.88 ± 0.80	3.86 ± 0.37	3.08 ± 0.71 a
40	5,30 ± 0.23 b	49.46 ± 5.79 b	6.91 ± 0.27	4.64 ± 0.05	8.40 ± 0.66 b
80	4,42 ± 0.57 ab	31.37 ± 5.79 ab	4.75 ± 1.46	3.16 ± 0.77	-
ANOVA	*	*	ns	ns	*
			Common bean - RA		
0	2,06 ± 0.11 a	11.36 ± 0.26 a	8.26 ± 0.35	3.22 ± 0.04 ab	1.31 ± 0.15 a
2.5	2,22 ± 0.22 ab	11.23 ± 0.49 a	8.31 ± 0.42	3.29 ± 0.14 ab	1.44 ± 0.07 a
5	2,71 ± 0.25 ab	11.33 ± 0.62 a	7.49 ± 0.85	2.85 ± 0.26 a	1.19 ± 0.14 a
10	2,20 ± 0.14 a	12.64 ± 0.68 a	8.34 ± 0.16	3.31 ± 0.12 ab	1.26 ± 0.07 a

20	2,37 ± 0.13 ab	12.58 ± 0.19 a	8.58 ± 0.54	3.39 ± 0.04 abc	2.02 ± 0.09 a
40	2,72 ± 0.15 ab	17.91 ± 0.80 b	9.29 ± 0.38	3.90 ± 0.28 bc	3.10 ± 0.48 b
80	3,11 ± 0.31 b	22.52 ± 0.60 c	6.68 ± 0.75	4.12 ± 0.04 c	3.51 ± 0.22 b
ANOVA	*	*	ns	*	*

- missing data due to low production of shoot dry matter.
* significant (*P* < 0.05); ns, non-significant.

Table S2 Concentration of micronutrients in leaves of common bean and oat after cultivation with increasing concentrations of mercury (0 to 80 mg kg^{-1} Hg) in Typic Hapludox (TH) and Rhodic Acrudox (RA) soils for 30 days. Results from the ANOVA test (*P* < 0.05). Error bars represent the standard errors of the means (n = 4)

Hg concentration (mg kg^{-1})	Cu	Fe	Mn	Zn	B
	-------------------------------------		mg kg^{-1}	----------------------------------	
			Oat - TH		
0	11.49 ± 3.23	321.8 ± 148	53.93 ± 8.2	54.62 ± 11.4	-
2.5	11.27 ± 2.17	289.3 ± 16	61.24 ± 1.6	39.32 ± 1.8	-
5	10.22 ± 1.39	395.1 ± 104	59.26 ± 1.1	51.75 ± 7.3	-
10	8.99 ± 0.34	428.4 ± 150	60.82 ± 4.5	38.38 ± 3.1	-
20	9.98 ± 1.37	344.9 ± 115	65.33 ± 10.8	44.59 ± 4.1	-
40	-	467.4 ± 104	-	39.92 ± 3.2	-
80	-	-	-	-	-
ANOVA	ns	ns	ns	ns	-
			Oat - RA		
0	5.93 ± 0.10	336.4 ± 55	35.23 ± 1.4 a	34.24 ± 0.7	-
2.5	9.30 ± 1.10	301.5 ± 35	37.6 ± 3.3 a	40.50 ± 2.5	-
5	6.70 ± 0.67	365.9 ± 52	45.19 ± 1.2 ab	34.11 ± 0.8	-
10	7.77 ± 1.26	420.7 ± 224	50.48 ± 3.2 b	37.44 ± 0.9	-
20	5.67 ± 1.06	150.0 ± 11	41.53 ± 3.2 ab	36.29 ± 3.4	-
40	-	-	-	-	-
80	-	-	-	-	-
ANOVA	ns	ns	*	ns	-
			Common bean - TH		
0	4.00 ± 0.56 a	147.1 ± 27 a	90.7 ± 16.6 a	22.24 ± 3.1 a	21.46 ± 1.3
2.5	4.01 ± 0.22 a	135.7 ± 26 a	99.89 ± 3.1 ab	28.69 ± 2.8 ab	22.27 ± 1.2
5	4.04 ± 0.49 a	107.2 ± 3 a	107.26 ± 6.8 ab	29.92 ± 2.9 ab	23.37 ± 0.5
10	4.62 ± 0.49 a	116.0 ± 11 a	107.5 ± 8.1 ab	38.29 ± 0.7 bc	22.70 ± 1.1
20	5.38 ± 0.72 ab	142.9 ± 38 a	162.34 ± 34.7 bc	38.17 ± 2.8 bc	23.37 ± 0.6
40	7.12 ± 0.37 b	240.3 ± 97 ab	271.34 ± 9.6 c	49.03 ± 2.5 c	-

80	5.53 ± 0.29 ab	317.0 ± 5 b	222.17 ± 1.2 c	39.41 ± 2.5 bc	-
ANOVA	*	*	*	*	ns
			Common bean - RA		
0	3.52 ± 0.02 ab	308.6 ± 171	50.21 ± 2.8	21.51 ± 0.6	20.02 ± 0.3 a
2.5	3.53 ± 0.10 ab	103.9 ± 5	54.26 ± 3.6	22.89 ± 1.0	18.78 ± 0.5 a
5	3.26 ± 0.25 ab	195.0 ± 77	49.37 ± 2.6	21.82 ± 2.4	16.59 ± 1.0 a
10	2.98 ± 0.08 a	153.2 ± 72	52.36 ± 0.9	18.98 ± 1.2	17.93 ± 0.9 a
20	3.10 ± 0.23 a	109.2 ± 11	54.13 ± 3.8	21.42 ± 1.3	18.79 ± 0.7 a
40	4.03 ± 0.04 b	171.1 ± 56	67.30 ± 4.8	23.94 ± 3.0	27.26 ± 1.5 b
80	3.96 ± 0.20 b	128.7 ± 31	50.78 ± 5.2	22.15 ± 1.9	26.60 ± 1.2 b
ANOVA	*	ns	ns	ns	*

- missing data due to low production of shoot dry matter.

* significant (*P* < 0.05); ns, non-significant.